ผลของตำรับยาเบญจอำมฤตต่อการรักษามะเร็งตับในหนู

EFFECT OF BENJA-

UMMARIT DISPENSATORY FOR TREATMENT OF HEPATOCELLULAR CARCINOMA IN

RAT

NATTPAWIT KAEWNOONUAL

GRADUATE SCHOOL Srinakharinwirot University

2018

ผลของตำรับยาเบญจอำมฤตต่อการรักษามะเร็งตับในหนู

ณัฏฐ์ปวิตร แก้วหนูนวล

ปริญญานิพนธ์นี้เป็นส่วนหนึ่งของการศึกษาตามหลักสูตร
ปรัชญาดุษฎีบัณฑิต สาขาวิชาชีวภาพการแพทย์
คณะแพทยศาสตร์ มหาวิทยาลัยศรีนครินทรวิโรฒ
ปีการศึกษา 2561
ลิขสิทธิ์ของมหาวิทยาลัยศรีนครินทรวิโรฒ

EFFECT OF BENJA-

UMMARIT DISPENSATORY FOR TREATMENT OF HEPATOCELLULAR CARCI

NOMA IN RAT

NATTPAWIT KAEWNOONUAL

A Dissertation Submitted in partial Fulfillment of Requirements

for DOCTOR OF PHILOSOPHY (Biomedical Sciences)

Faculty of Medicine Srinakharinwirot University

2018

THE DISSERTATION TITLED

EFFECT OF BENJA-

UMMARIT DISPENSATORY FOR TREATMENT OF HEPATOCELLULAR CARCINOMA IN RAT

BY

NATTPAWIT KAEWNOONUAL

HAS BEEN APPROVED BY THE GRADUATE SCHOOL IN PARTIAL FULFILLMENT OF THE

REQUIREMENTS FOR THE DOCTOR OF PHILOSOPHY IN BIOMEDICAL SCIENCES

AT SRINAKHARINWIROT UNIVERSITY

.... Dean of Graduate School

(Asst. Prof. Dr. Chatchai Ekpanyaskul, MD.)

....

ORAL DEFENSE COMMITTEE

.... Major-advisor

(Assoc. Prof. Dr.Wisuit Pradidarcheep, Ph.D.)

.... Chair

(Asst. Prof. Dr.Wanlaya Tanechpongtamb, Ph.D.)

.... Co-advisor

(Assoc. Prof. Dr.Arunporn Itharat, Ph.D.)

.... Committee

(Dr.Srisombat Puttikamonkul, Ph.D.)

.... Committee

(Assoc. Prof. Dr.Treetip Ratanavalachai, Ph.D.)

Title   EFFECT OF BENJA-

                         UMMARIT DISPENSATORY FOR TREATMENT OF HEPATOCELLU

                         LAR CARCINOMA IN RAT

Author   NATTPAWIT KAEWNOONUAL

Degree   DOCTOR OF PHILOSOPHY

Academic Year   2018

Thesis Advisor   Associate Professor Dr. Wisuit Pradidarcheep , Ph.D.

There has yet to be a standard no curative treatment of hepatocellular carcinoma (HCC). Therefore, the alternative treatment of HCC with medical herbs was considerably helpful. The Benja-ummarit (BU) extract has been proven to show cytotoxic activity against HepG2 liver cancer cells, but its efficacy has not yet been studied *in vivo*. Thus, the present study aimed to determine the efficacy of different doses of BU extract for the treatment of HCC in Wistar rats. The rats were divided into eight groups: (1) control rats that did not receive any treatment or (2) control rats that received the solvent propylene glycol; and HCC- bearing rats received no any treatment (3), or were treated with (4) propylene glycol, (5) thirty mg/kg of Sorafenib, (6) one mg/kg of BU, (7) ten mg/kg of BU, or (8) fifty mg/kg of BU. All of the rats were sacrificed after two months of treatment and the reduction of cancer in the livers was studied in term of gross pathology and histopathology. The expressions of angiogenesis marker (*Vegfa*), and two cell proliferation markers (*Ctnnb1*, *Ccnd1*) by real-time quantitative PCR, Western blot analysis and immunohistochemistry (VEGF only) were investigated. The blood samples were collected to determine liver function, including AST, ALT, ALP, and albumin. The comparison of the respective groups showed that the size and number of cancer area and nodules were reduced significantly in all HCC groups treated with BU. However, the reduction of cancer area was larger in the Sorafenib group. The ALT and albumin levels were higher and lower, respectively, in the HCC group treated with Sorafenib in comparison to BU-treated groups, implying that BU caused milder liver injuries than Sorafenib. The liver weight/body weight ratio was lowest in the HCC group treated with Sorafenib than in groups treated with BU, irrespective of the dose. Both Sorafenib and BU reduced the expression of *Vegfa*, *Ctnnb1*, and *Ccnd1*. Both Sorafenib and BU also reduced the liver VEGF protein content. The degree of its reduction after BU treatment was dose-dependent (1<10<50 mg/kg). Overall, the present study indicated that the BU inhibited cancer cell proliferation and angiogenesis in HCC-bearing rats. Therefore, BU, a medical herb, may be a promising candidate for supportive treatment of HCC.

ACKNOWLEDGEMENTS

TABLE OF CONTENTS

Page

LIST OF TABLES

LIST OF FIGURES

CHAPTER 1

INTRODUCTION

Hepatocellular carcinoma (HCC), the most common type of primary liver cancer, is the world's third leading cause of cancer-related death[1]. It is the fifth most common cause of male cancer (7.9% of all cancers) and the seventh most common female cancer (6.5% of all cancers). The incidence of HCC varies considerably, with most cases occurring in developing countries. In Southeast Asia and Sub-Saharan Africa, more than 75% of HCC occurs, with incidence rates exceeding 20 per 100,000 people. Southern European countries have intermediate incidence rates, whereas North America, South America, and Northern Europe have the lowest incidence rates (< 5 per 100,000 individuals)[2].

Recent reports suggest that the incidence of HCC in areas of high and intermediate incidence may stabilize or decrease. This is associated with more widespread vaccination programs for hepatitis B virus (HBV) and higher HBV treatment rates in China and Taiwan[3]. The decrease in HCC incidence in Japan and Southern Europe may be associated with an aging cohort of patients with hepatitis C (HCV) infection[4]. In contrast, there is a rapid increase in the incidence of HCC in low - incidence areas, such as the United States. HCC had the largest increase in incidence among all solid tumors in the United States over the 10-year period from 1995 to 2004[5]. There are several factors associated with the rising incidence of HCC in the United States, but the two most importance are growing populations of patients with advanced HCV infection and non - alcoholic steatohepatitis (NASH)[2]. HCC also has one of the fastest - growing death rates among solid tumors in parallel with its rising incidence rate. While the prognosis for most solid cancers improved from 1994 to 2003, the mortality rate for HCC was almost double[6]. In HCC, several molecular changes were observed. Many signaling pathways were thought to play a role in the development of HCC, specifically those involving the angiogenesis-mediated vascular endothelial growth

factor (VEGF) and the Wnt/β-catenin pathway that may result in the expression of cyclin D1, which regulates cell proliferation in cancer[7, 8].

There is currently no effective HCC treatment. Using of medicinal herbs now become very helpful as an alternative treatment. At U-thong hospital in Thailand, Benja-ummarit (BU) was used as a cancer dispensatory for cancer treatment, particularly hepatocellular carcinoma. BU is a Thai traditional medicine dispensatory from Thai scripture called Tadbunjob. It consists of 8 herbs as follow: aloe (*Aloe barbadensis*; Yadum), red physic nut (*Baliospermum montanum*; Thongtak), kaffir lime (*Citrus hystrix*; Makrut), asafoetida (*Ferula assafoetida*; Mahahing), gamboge resin (*Garcinia hanburyi*; Rongthong), Javanese long pepper (*Piper retrofractum* / *Piper Chaba*; Deeplee), black pepper (*Piper nigrum*; Prikthaidum), ginger (*Zingiber officinale*; Khing), and 1 chemical is epsom salt (Magnesium sulphate; Deegleuafarang). Moreover, it was also used to treat patients who have these following symptoms: asthma, coughing, short breath, liver abscess, and also anorexia. In Thai traditional medicine theory, all of those symptoms assessed as malignant tumor. In addition, BU was used as detoxification in Thai traditional medicine. Evidence has shown that BU could improve physical health of cancer patients and prolong their lives (Tamra Phaetsart Songkroh).

Seven cancer cell lines including the liver (HepG2), colon (LS174 T, SW480 and CaCO-2), lung (COR-L23), cervical (Hela) and prostate (PC3) have been tested for cytotoxic activity by Sulforhodamine B (SRB) assay of all extracts. The Benja-ummarit dispensatory's 95 percent ethanol extract showed strong toxicity to all cancer cell lines, particularly liver and colon cancers[9].

Studies have shown that a chemical component of rong thong - gambogic acid has an inhibitory effect on the proliferation of many types of cancer cells, such as HepG2[10] cells and SMMC-7221 cells[11]. In addition, evidence suggests that when gambogic acid is co-administered with docetaxel, a chemotherapy drug used to treat a number of cancer types, an increased inhibitory effect is observed against the proliferation of gastrointestinal cell lines[12]. It has also been shown that gambogic derivatives inhibit HepG2 and A549 cancer cell line proliferation[13]. Furthermore,

gambogic acid has been found to have an anti-angiogenic effect in many cancer types[14-18], exhibit anti-inflammatory activity[19-21], and anti-invasion of A549 human lung cancer cell[22] and osteosarcoma cell line[23]. Morever, when being used against human breast carcinoma MCF-7 cells and human chronic myelogenous leukemia K562 cells, the cells are found to be arrested at G2/M[24] and G0/G1 cell cycle[25], respectively. It has also been found that decreased adhesion of human cancer cells is an effect of gambogic acid[26]. From the above - mentioned anti-angiogenesis and anti-cancer effects of gambogic acid, a chemical component of rong thong in Benja-ummarit, this study expected that BU could inhibit the proliferation of cancer cells by suppressing β-catenin activation and could also exert anti - angiogenesis by reducing the expression of VEGF. Benja-ummarit will therefore, be a good candidate of medicinal herbs for being used as an alternative medicine in treatment of HCC.

This study aims to determine whether Benja-ummarit dispensatory has a medicinal effect on hepatocellular carcinoma rats in the following aspects:

1. Gross structure of the liver

- To examine the changes of external morphology of the liver.

2. Liver enzymes

- To assess liver functions by measuring the levels of liver enzymes and proteins including aspartate aminotransferase (AST), alanine aminotransferase (ALT), alkaline phosphatase (ALP), gamma-glutamyltransferase (GGT), total protein, albumin, direct bilirubin and total bilirubin.

3. Histomorphology of the liver

- To examine the histomorphological changes in liver tissues by hematoxylin and eosin staining.

4. Lipid peroxidation

- To examine the changes of lipid peroxidation by measuring malondialdehyde (MDA) level by thiobarbituric acid (TBA) method.

5. Protein markers

- To examine the changes and expression of vascular endothelial growth factor (VEGF), β-catenin, and cyclin D1 by Western blot analysis and immunohistochemical technique.

6. Real time PCR

- To examine the expression of angiogenesis and cell proliferation in hepatocellular carcinoma by study the pattern of VEGF, β-catenin and cyclin D1 of liver rat.

Hypothesis

To induce hepatocellular carcinoma, diethylnitrosamine will be employed as an initiator which causes DNA damage while thioacetamide will be employed as a promotor to induce inflammation so as to achieve the state of HCC. In the pathogenesis of HCC, excessive cell proliferation will eventually lead to formation of tumor and also formation of blood vessels to supply the tumor. In this study, we hypothesized that the Benja-ummarit dispensatory possesses anti-proliferative property of cancer cells by interfering with the Wnt/β-catenin signaling pathway and also anti-angiogenesis property by interfering with the VEGF signaling pathway as shown in the Figure 1[27].
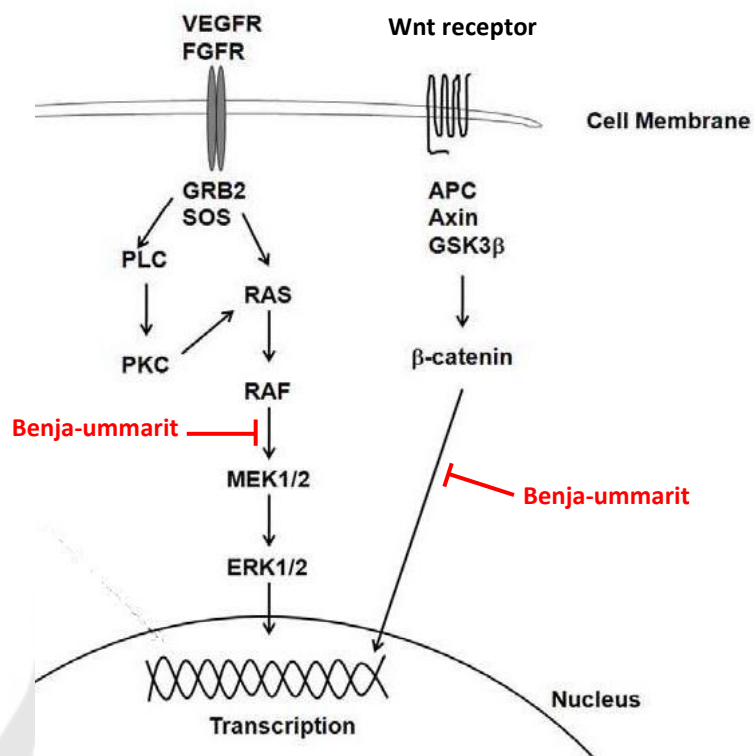
Figure 1 Conceptual framework

Modified from Wu X and Li Y, 2012

VEGFR = Vascular endothelial growth factor receptor	FGFR = Fibroblast growth factor receptor
GRB2 = Growth factor receptor bound protein 2	SOS = son of sevenless
PLC = Phospholipase C	PKC = protein kinase C
RAF = Rapidly accelerated fibrosarcoma	MEK1/2 = Mitogen-activated protein kinase kinase 1 and 2
APC = Adenomatous polyposis coli	GSK3β = Glycogen synthase kinase 3 beta
ERK1/2 = Extracellular signal-regulated protein kinases 1 and 2 (ERK1/2)	

CHAPTER 2
REVIEW LITERATURE

1 The liver

The liver is the body's biggest gland. The hepatic portal vein carries the nutrients absorbed from the gastrointestinal tract to the liver, which takes nutrients and vitamins up, stores and distributes them. The liver plays an important role in maintaining blood glucose levels. It also regulates the circulating blood lipids by the amount of very low density lipoproteins (VLDLs) secreted. Many of the circulating plasma proteins are synthesized by the liver. Moreover, from the portal circulation, the liver absorbs numerous toxic compounds and drugs. The liver also serves as an excretory organ for bile pigments, cholesterol, and drugs. Finally, it performs important endocrine functions[28].

1.1 Gross anatomy of human liver

In the right upper quadrant of the abdomen, the liver is a reddish brown color and triangular shaped organ (Figure 2). The normal liver lies on the right side deep to ribs seven to eleven, crossing the midline to the left nipple and extending over the edge of the stomach to the left side of the body. Most of the mass of the liver is located on the body's right side where it falls inferior to the right kidney. The liver's diaphragm surface is smooth and dome-shaped, where it is associated with the concavity of the diaphragm's lower surface. The diaphragm surface of the liver is covered with visceral peritoneum, except in the bare area of the liver, where it contacts the diaphragm directly. The visceral surface of the liver is covered with peritoneum, with the exception of the fossa for the gallbladder and the porta hepatis (a transverse fissure in which the vessels, the hepatic nerve plexus and the hepatic ducts enter and leave the liver). Moreover, the gall bladder and its ducts are just below the liver's right side. The liver consists of very soft, pink-brown tissues encapsulated by a capsule of the connective tissue. The peritoneum of the abdominal cavity, which protects the liver and holds it in place within the abdomen, further covers and strengthens this capsule. This capsule is

called the capsule of Glisson that consists of collagen, fibroblasts and small blood vessels including lymphatic venules. It invaginates in liver hilum, becomes continuous with intrahepatic portal connective tissue, and encloses branches of hepatic artery, portal vein and bile duct and lymphatic channels, also known as portal triads or portal tracts. In four locations, the peritoneum connects the liver, including the coronary ligament, the triangular ligaments left and right, and the falciform ligament.
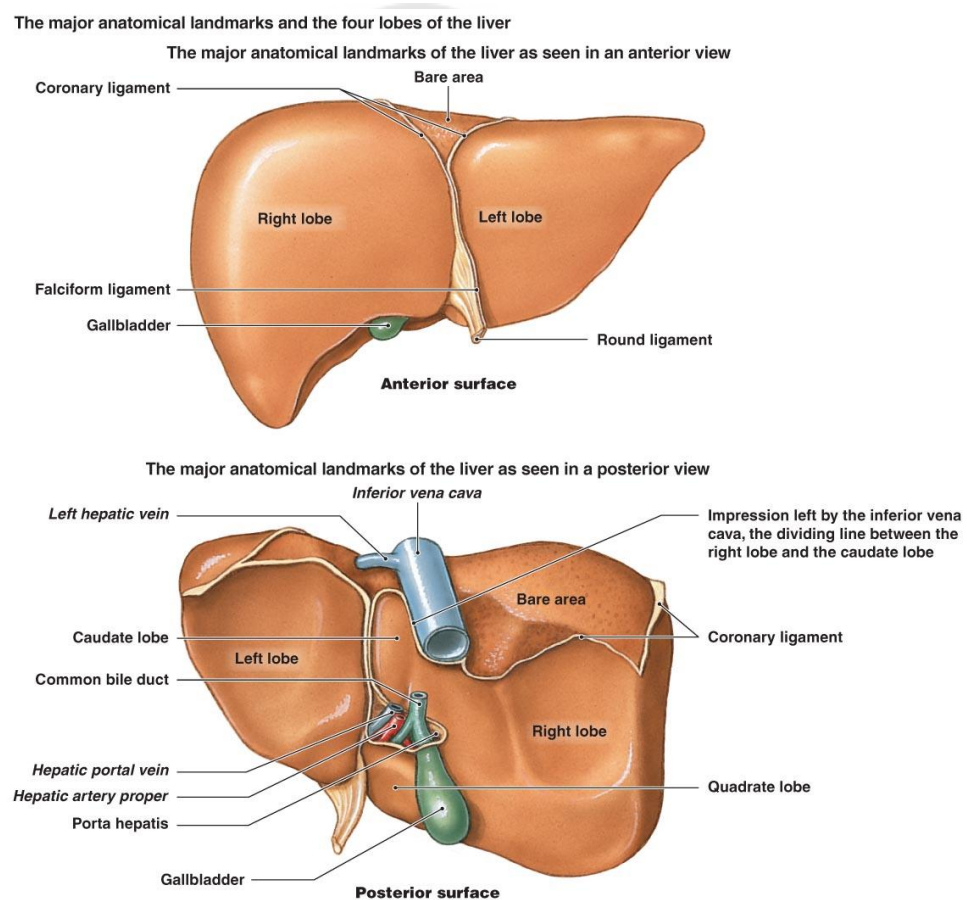
Figure 2 Gross anatomy of the human liver.

Source:http://www2.highlands.edu/academics/divisions/scipe/biology/faculty/harnden/2122/images/liver.jpg

In the front view, the liver is divided into a larger right lobe and a smaller left lobe by the falciform ligament. The coronary ligament of the liver is located at the junction of the triangular and falciform ligaments in the posterior view of the liver. It consists of two layers separated by a space equal to the breath of bare area. The rear view of the liver right lobe is divided into caudate lobe and quadrate lobe[29].

1.2 Rat liver

Because of many factors, Rats are the most widely used experimental model in research. They are particularly easy to handle and cheap. Rats are by far the most used model in hepatic regeneration, liver metastasis, immunology for transplantation, and hepatic disease studies. Like other mammals, the rat liver is multilobulated. In rats, the liver mass is about 5% of the total body weight, whereas in adults it is about 2.5%. The mean weight of the liver in rats weighing between 250 and 300 g is 13.6 g and the diameter of the liver transverse is 7.5-8.0 cm. The diameter superior-inferior is 3.8-4.2 cm, while the diameter anterior-posterior ranged from 2.2-2.5 cm (Figure 3)[30].

Figure 3 Gross anatomy of the rat liver.

1.2.1 Surface anatomy of the rat liver

The rat liver has basically three surfaces when the rat is in the decubitus position: superior, inferior and posterior. A sharp, well-defined margin separates the lower from the upper surface. The other margins are also sharp, unlike the human liver. Despite lobulating the rat liver, it has somewhat uniform surfaces as lobes are flat against each other. The only exception to this is the posterior lobe of caudate (CL), separated by the stomach from the rest of the liver. The upper (parietal) surface consists of a part of the lateral and medial lobes on the left and is convex as a whole and fits under the diaphragm's vault. The peritoneum completely covers it, except along the falciform ligament attachment line. The falciform ligament attachment line divides the liver into two parts, called the right and left lobes. Unlike human livers, where the right lobe is much larger than the left lobe, the left and right rats have about the same volume. The lower (visceral) surface is uneven and concave with respect to the stomach, duodenum, right colic flexure, the upper part of the pancreas, right kidney and suprarenal gland. The lower surface of the rat liver has no fossae in the form of letter H as in humans. The peritoneum invests this surface almost entirely. The portal vein, the hepatic artery and nerves, the hepatic duct and lymphatics pass through the porta (transverse fissure). The impressions of the liver (colic, renal, duodenal and suprarenal) are not as obvious as those of human livers. The posterior surface is not covered by the peritoneum and is in direct contact with the diaphragm over a certain part of its extent. It stretches obliquely between the CL and the liver's bare area. The lower vena cava is totally intrahepatic[30, 31].

1.2.2 Liver lobes

Like the human liver, the rat liver lobes are named after the portal branches providing them, as the portal system is the most constant anatomical reference among mammals. The largest middle or median lobe (ML) is about 38 percent of the liver weight. It has a trapezoidal form and is fixed by the falciform ligament in the diaphragm and abdominal wall. It is in continuity with the left lateral lobe (LLL) and is divided into a large right medial lobe (RML) by a vertical fissure (main fissure or

umbilical fissure) (2/3 of the medial lobe volume) and a smaller medial lobe (LML; 1/3 of the volume). The hepatic vascular components of the RML are both left and right. The right lobe (RL) is located on the right side of the vena cava and later in the right hypochondrium and is covered almost entirely by the medial lobe. It comprises about 22% of the liver weight and is divided into two pyramidal lobules by a horizontal fissure: the upper lobules (SRL, also known as the right rear lobe) and the lower lobules (the lower right lobe, IRL, also known as the right anterior lobe). The rhomboid shape of the left lateral lobe (LLL) is flattened and located above the anterior aspect of the stomach in the epigastric and left hypochondriac regions. Its medial portion is covered by the medial lobe's left portion. Its upper surface on the diaphragm is slightly convex. It doesn't have any cracks. The CL is located at the back of the LLL and at the left of the vena porta and lower cava vein. It comprises 8–10% of the liver weight and is divided into two parts: the paracaval portion (caudate process), which represents 2-3% of the liver mass, encircles the lower vena cava and bridges the CLs and the right lateral lobe. The other is the Spiegel lobe, which has an anterior (superior) and a subsequent (inferior) disk-shaped portion, each representing 4% of the liver mass. The anterior part of the CL is located in front of the esophagus and stomach and its pedicle is higher, while the back is located behind these structures and its pedicle is lower. Both are covered with a very thin peritoneum layer, hepatoduodenal and hepatogastric ligaments (Figure 4)[30, 32, 33].
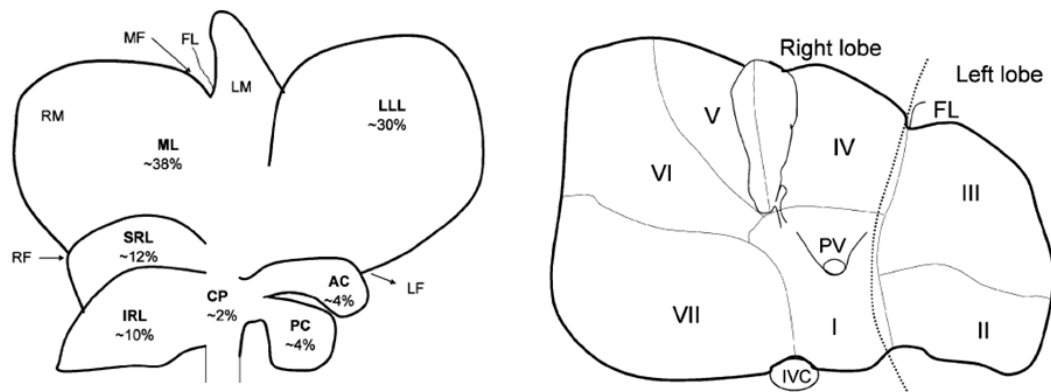
Figure 4 Visceral rat liver surface and human liver.

Source: Martins PN and Neuhaus P. (2007) Surgical anatomy of the liver, hepatic vasculature and bile ducts in the rat.

Visceral rat liver surface showing lobes and their relative mean weight. The liver mass of the rat's lobe is quite constant. The caudate lobe (CL) consists of CP, AC and PC, SRL and IRL form the right liver lobe and LM and RM form the medial lobe. A human liver's visceral surface showing a segment of the liver. Segment VIII is superior to Segment V and in this figure can not be seen. In rats, CL, LLL, LML, RML, (IRL1SRL) represent segments I and IX, segment II, segments III, IV, V and VIII, respectively, as well as segments VI and VII. The left hemi-liver in the rat is the LLL, CL, and LML, while the right hemi-liver is the RL (SRL1IRL) and the RML. CP, caudate process; AC, anterior caudate lobe: PC, posterior caudate lobe; SRL, upper right lateral lobe; IRL, lower right lateral lobe; ML, median lobe; RML, right portion of the medial lobe; LML, left portion of the medial lobe; LLL, left lateral lobe; MF, median fissure; LF, left fissure; RF, right fissure and FL, falciform ligament; PV, portal vein and IVC, inferior vena cava[30].

1.2.3 Liver vasculature

The origin and course of the major vessels are similar to those of humans, and no variability in vessel origin was identified in rats.

1.2.3.1 Hepatic artery

The liver is provided with the proper hepatic artery originating from the common hepatic artery. The celiac trunk, which in humans is relatively longer than that, originates from the anterior or right side of the abdominal aorta just below the pillars of the diaphragm, ascends for 5-7 mm near the aorta and branches into the common hepatic, left gastric and splenic arteries. The common hepatic artery runs into the proper hepatic artery and gastroduodenal artery within the pancreas and bifurcates at portal vein level. The proper hepatic artery is between 0.2 and 0.5 mm in diameter and between 4 and 5 mm in length. The proper hepatic artery runs at the back of the portal vein, dividing it into the right and left branches at the liver hilus. The arterial branches run on the portal vein's anterior surface and behind the bile ducts, pass behind the major hepatic ducts and follow a parallel course with the portal vein branches as they divide into their main lobar branches. Sometimes, a single lobar portal vein is accompanied by two lobar arteries. For the upper right lateral, lower right lateral and medial lobes, the most visible branches are. In addition to the four branches to the main hepatic lobes, the proper hepatic artery gives off a branch called the hepato-esophageal artery. This branch arises on the hepatic pedicle of 10-12 mm in length and 0.1 mm in diameter between the caudate and left lobes and supplies the lower two-thirds of the esophagus. It is also possible to find an accessory left hepatic artery from the left gastric artery that supplies the dorso-medial part of the LLL. It was not found in the description of the arterial branches intrahepatic[30, 32, 33].

1.2.3.2 Portal vein

Posterior and lateral to the hepatic artery and common bile duct (CBD) is the extrahepatic portal vein. It consists of the higher mesenteric vein, the gastrosplenic vein, and the gastroduodenal vein. The higher mesenteric vein drains the pancreaticoduodenal vein and lower mesenteric vein. The portal vein's diameter and length range was 2-4 and 4-7 mm, respectively, in this series. The rat liver has three main portal branches that identify the following fissures: fissure of the left portal, fissure of the right portal and fissure of the main portal. The left portal fissure separates the RLL

from the ML, the main fissure separates the RML from the LML and the left fissure that separates the CL from the LLL (corresponding to the fossa for the ductus venosus in the human liver). The common portal vein at the porta hepatis first gives branches to the right lobe (RL), then to the CL, then to ML, and finally to the LLL. The left, right, and CLs have one primary branch of portal, while the middle lobe has two branches of portal. The right portal vein divides immediately into two branches: one for the right superior lobule and the right lobule inferior. The branch of the portal to the CL is very short and branches into two main veins: one for the anterior and one for the lobe of Spiegel afterwards. The paracaval portion (caudate process) is supplied by other very small veins, originating directly from the main portal vein and its left and right branches (Figure 5 B)[30, 32, 33].

1.2.3.3 Hepatic veins

In most cases, the IRL and the SRL drain by one branch each into the lower vena cava, but each can be drained by two veins. They correspond to the right hepatic and lower right hepatic vein in humans, the latter representing a normal anatomy variation. There are two or three large hepatic veins in the middle lobe (median veins right, middle and left). The center lobe's right and left portions are drained by one vein each. Like in humans, the vein draining the left portion of the middle lobe (left medial vein) may enter the vena cava separately or join the LLL (left hepatic vein) draining vein to form a common trunk before joining the suprahepatic cava vein. In most cases, the left and CLs are drained by two large hepatic veins (left and right) opening separately into the vena cava, but in some cases they may be joined together by a common trunk. The caudate process drains through multiple branches into the intrahepatic vena cava (Figure 5 A)[30, 32, 33].

1.2.3.4 Biliary tract

The rat has no gallbladder. The rat's extrahepatic biliary ducts are formed by branches of the first order of each liver lobe and lay superficially on the branches of the arteries and portals. For superior and inferior CLs, right middle lobe and caudate process, second-order branches exist. There are many anatomical variations in

the rat biliary tract. Most commonly, their own bile ducts drain each lobe. The LLL is most commonly drained by two biliary branches (in 62.5 percent of cases). Branches from the right middle lobe (1-4 branches) and the LML drain the middle lobe. Each CL has one branch in 57.5 percent of cases that unites to form a common branch before draining into the CBD. The upper part of the caudate process drains into branches of the right lateral lobe or the main biliary trunk, while the lower part drains into the caudate process branches or into the right lateral lobe branch. The CBD is formed by the main hepatic duct junction. On the caudate process, the main hepatic ducts join together. The CBD ranged from 12 to 16 mm in length and 0.6 to 1 mm in diameter in this series, but it can be as long as 45 mm. The CBD descends on the surface of the caudate process and portal vein to the left of the hepatic artery and portal vein, and then along the lower omentum's right border, keeping some distance from them. A long extent of the CBD is fully embedded in the pancreas, having a diffuse and lobulated appearance. The CBD opens slightly below its middle and about 10–22 mm from the pylorus on the medial side of the downward portion of the duodenum. The rat's extrahepatic biliary system also has small branches of intercommunication (Figure 5 C)[30, 33].
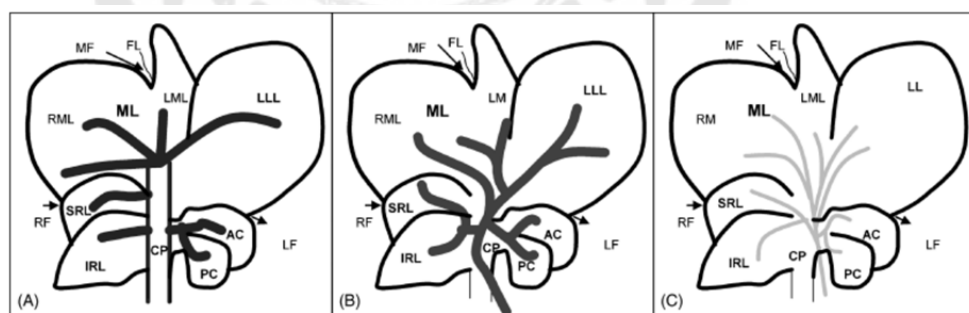
Figure 5 Diagram showing most common anatomy of the hepatic veins (A), portal vein (B) and biliary system (C) of the rat.

Source: Martins PN and Neuhaus P. (2007) Surgical anatomy of the liver, hepatic vasculature and bile ducts in the rat.

1.3 Liver microanatomy

The liver is a complex three-dimensional structure consisting of epithelial and mesenchymal elements arranged in microscopic repetitive units. Such structural and functional organization makes it possible for small representative biopsy specimens to evaluate diffuse disease processes. The microscopic structure is conceptualized in several ways, with the hepatic lobule, portal lobule and hepatic acinus being the three most common (Figure 6)[34].
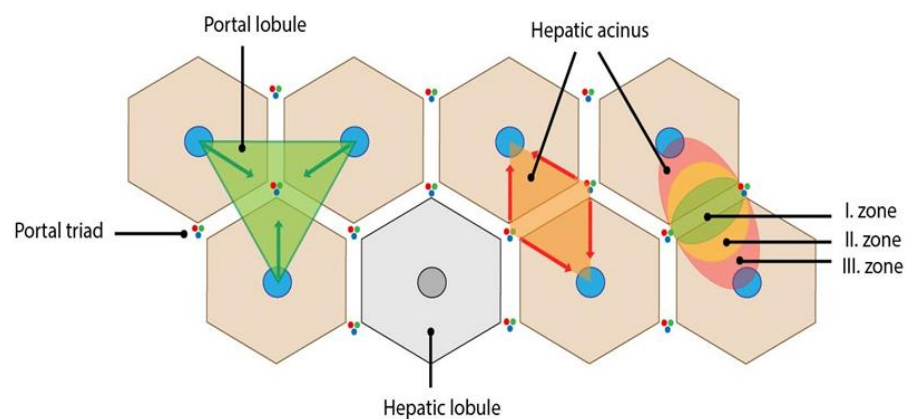
Figure 6 Hepatic functional units – hepatic lobule, portal lobule and hepatic acinus.
.

Source:http://fblt.cz/wp-content/uploads/2013/12/jaterni-acinus-a-portalni-lalucek-ENG-01.jpg

1.3.1 Hepatic lobule

Hepatic lobule is a polyhedral (hexagonal) prism with hepatocyte cords based on blood flow direction. The center of the lobule is the central vein, a terminal hepatic venula, surrounded by portal triads at the hexagonal corners, consisting of portal vein branches, hepatic artery branches and bile ductile branches[34, 35]. Periportal hepatocytes are the first to receive blood, the last to undergo necrosis, a group of hepatocytes around the portal vein. The first areas to regenerate when hepatocytes

receive low oxygenated blood and toxins are hepatocytes between portal tracts and central veins. Centrilobular hepatocytes are the most susceptible to ischemic insults and contain drug metabolizing enzymes (Figure 7)[36].
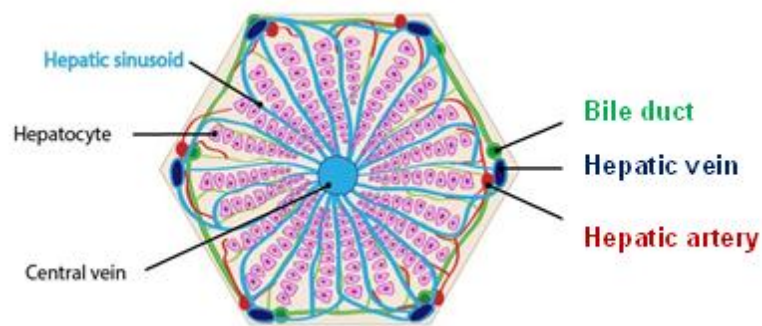
Figure 7 Diagram showing hepatic lobule

Source: http://fblt.cz/wp-content/uploads/2013/12/jatra-lobulus-ENG-01.jpg

1.3.2 Portal lobule

Portal lobule is a triangular region at the center of which is a portal triad and a central vein at each corner peripherally. It includes portions of three adjacent classic liver lobules all draining bile into one portal channel. This lobule is the portion of the hepatic parenchyma that secretes bile and drains into the portal triad bile duct in the portal lobule center (Figure 8)[36].
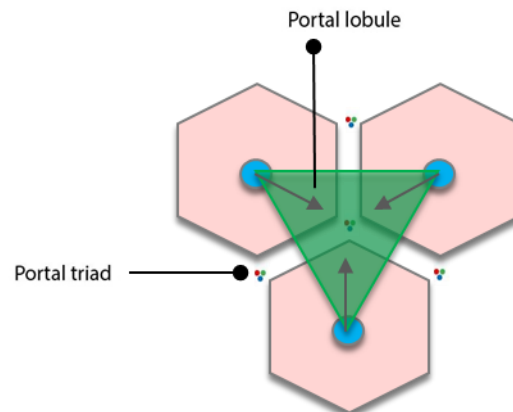
Figure 8 Diagram showing portal lobule

Source:http://fblt.cz/wp-content/uploads/2013/12/jaterni-acinus-a-portalni-lalucek-ENG-01.jpg

1.3.3 Hepatic acinus

Hepatic acinus is the structure in the form of an ellipse. By connecting line between adjacent portal triads, the short axis of the acinus is defined and the long axis is defined by connecting line between two adjacent central veins. It remotely resembles two triangles with central veins in vertices attached to each other by their bases. The circumlobular vein and artery that supplies the liver acinus sinusoids are located between their bases. Hepatic acinus is the smallest functional unit and is divided into zone 1, zone 2 and zone 3, where zone 1 surrounds the portal tract and zone 3 surrounds the hepatic venula. Hepatic acinus provides the best correlation between blood perfusion, metabolic activity, and liver pathology. Because blood flows through these zones from the portal tract to the venula with a declining oxygen and nutrient gradient (Figure 9)[34].
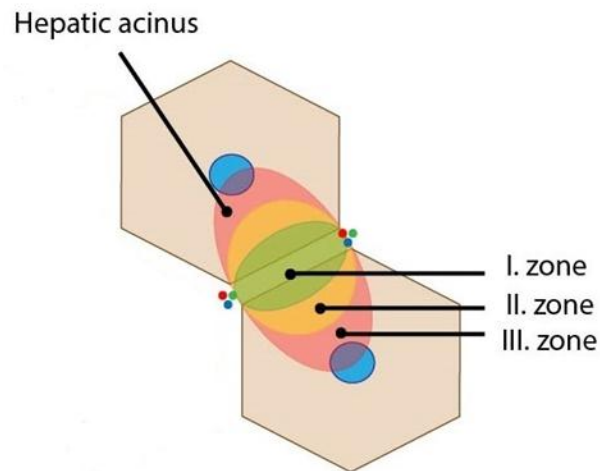
Figure 9 Diagram showing the hepatic acinus

Source: http://fblt.cz/wp-content/uploads/2013/12/Acinus-zony-ENG1.jpg

Zone I – represents the portion of parenchyma closest to the circumlobular vein and artery. It is the first zone to receive oxygen and nutrients. The oxidative metabolism predominates here e.g. gluconeogenesis.

Zone II – lies between zone I and zone III – receives less oxygenated blood.

Zone III – lies farthest from circumlobular vein and artery (closest to the central veins). It is the least oxygen gradient. The reduction processes are predominant in this location e.g. detoxification.

This classification is also important for description of pathological conditions to selective damage of hepatocytes[34].

1.3.4 Cell type and sinusoids

The liver's principal parenchymal cell is the hepatocyte. The sinusoidal endothelial cells, Kupffer cells, hepatic stellate (Ito) cells and so-called pit cells (large granulated lymphocytes) are among these cells[37].

1.3.4.1 Hepatocytes

Hepatocytes are the lobules ' main cells and epithelial cells. They are usually arranged in cords that are separated by sinusoids, one or two cells thick. A sheath-like layer called the limiting plate forms hepatocytes bordering portal tracts.[38] Hepatocytes are large polyhedral cells (diameter 20-40 μm) with an abundance of eosinophilic cytoplasm and a central nucleus. The nucleus is in round or oval shape. There are three important surfaces for hepatocytes: 1) Sinusoidal surfaces are separated by space of Disse from the sinusoidal vessel. They are covered with short microvilli protruding into space of Disse. The sinusoidal surface is the site where the sinusoids and the hepatocyte transfer material. 2) Canalicular surfaces are the surfaces through which bile drains into the canaliculi from the hepatocytes. 3) The intercellular surfaces are the surfaces of adjacent hepatocytes not in contact with sinusoids or canalicules[37].
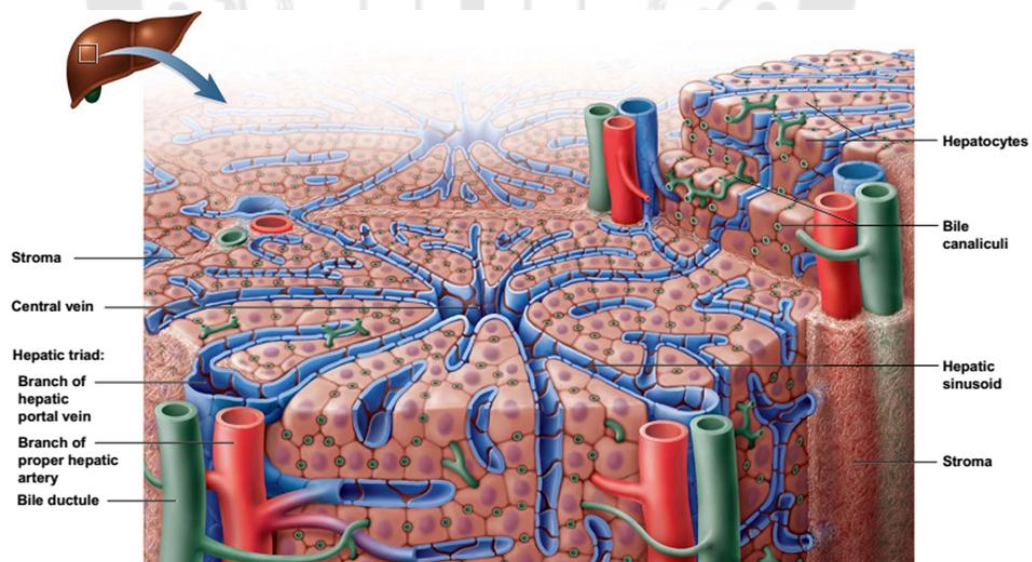
Figure 10 Diagram showing the area of the portal and the central vein.

Source: Dancygier H. (2010) Gross anatomy: Clinical Hepatology

Portal area is located at each lobule's corner and consists of branches of the hepatic portal vein, hepatic artery, and bile duct. The central vein is a blood vessel in the center of each lobule that receives blood through the sinusoids from the hepatic portal vein and hepatic artery and drains blood into the hepatic vein[37].

Hepatocytes usually have one round, central nucleus; some of them are binucleated (25 %). Nuclei are sometimes polyploid (more than one set of chromosomes). The hepatocyte cytoplasm is typically fairly acidophilic with basophilia areas (many mitochondria and some SER). The hepatocytes are unusual because in the same cells they have abundant RER (rough endoplasmic reticulum) and SER (smooth endoplasmic reticulum). Protein synthesis like: albumin, fibrinogen, globulin, prothrombin is associated with the RER. The SER is associated with steroid metabolism and is also responsible for the oxidation, methylation and conjugation processes required to inactivate or detoxify different substances prior to their body excretion. The conjugation of water-insoluble toxic bilirubin by glucuronyl-transferase to form a water-soluble non-toxic bilirubin glucuronide is one of the main processes occurring in the SER. Hepatocytes excrete this conjugate into the bile. If bilirubin or bilirubin glucuronide is not excreted, it may result in various jaundice-characterized diseases. There are about 2,000 mitochondria in each hepatocyte. There are also numerous golgi complexes up to 50 per cell. The functions of this organelle include lysosome formation and plasma protein secretion (e.g. albumin, complement system proteins), glycoproteins (e.g. transferrin), and lipoproteins (e.g. lipoproteins of very low density). Hepatocytes have lysosomes that are important in intracellular organelle turnover and degradation. Peroxisomes are plentiful and are involved in a variety of metabolic reactions, including lipid metabolism and chemical detoxification. Depending on the functional state of the cells, lipid droplet and glycogen are found in different amounts. The glycogen appears as coarse, electron-dense granules in the electron microscope that often collect near the SER. Perhaps the most versatile cell in the body is the hepatocyte. It is a cell with functions that are both endocrine and exocrine. Endocrine secretion involves several plasma proteins being produced and released. Unlike other

body protein synthesizing and secreting cells, hepatocytes are unusual because they lack granules for protein storage. The production and release of bile involve exocrine secretion. Located at different distances from the portal triads, hepatocytes show differences in structural, histochemical and biochemical properties. This fact then leads to the concept of the hepatocytes called " metabolic zonation "[39]. There are numerous microvilli of hepatocytes on the sinusoidal surface that increase the surface area available to exchange and absorb substances from the blood portal[37]. The cell membrane faces the sinusoids in part, forms the biliary canaliculus with the adjacent hepatocyte, and has a portion adjacent to the canaliculus with specialized junctions attached to the adjacent hepatocyte. There is abundant endoplasmic reticulum and glycogen in the cytoplasm (Figure 11)[34].
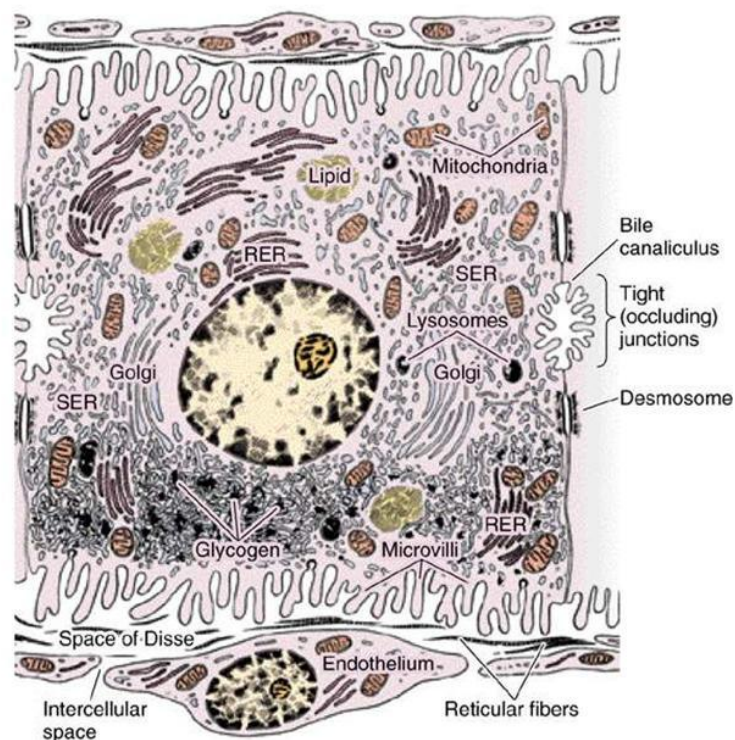
Figure 11 Hepatocyte and its organelles.

Source:http://intranet.tdmu.edu.ua/data/kafedra/internal/histolog/classes_stud/en/med/lik/ptn/2/18%20Large%20glands%20of%20digestive%20system.htm

On two sides of the cell and intracellular organelles, the endothelial-lined sinusoids are shown. The extracellular fluid space of Disse is shown between the microvilli of the hepatocyte plasma membrane and the sinusoids. The opposing cells form bile canaliculi along the lateral intercellular plasma membrane, where microvilli extends into the canaliculus. The bile canaliculi form a ring around each hepatocyte by imaging the cell in three dimensions.

1.3.4.2 Sinusoids

Sinusoids are the channels formed by hepatocyte plates. In the portal areas, they receive blood and nutrients from the vessels and deliver them to the central vein. They are about 8-10 μm in diameter, more irregular in shape. The sinusoid lining consists of a discontinuous layer of fenestrated endothelium and also includes endothelial Kupffer cells. The basal lamina is missing (Figure 12).
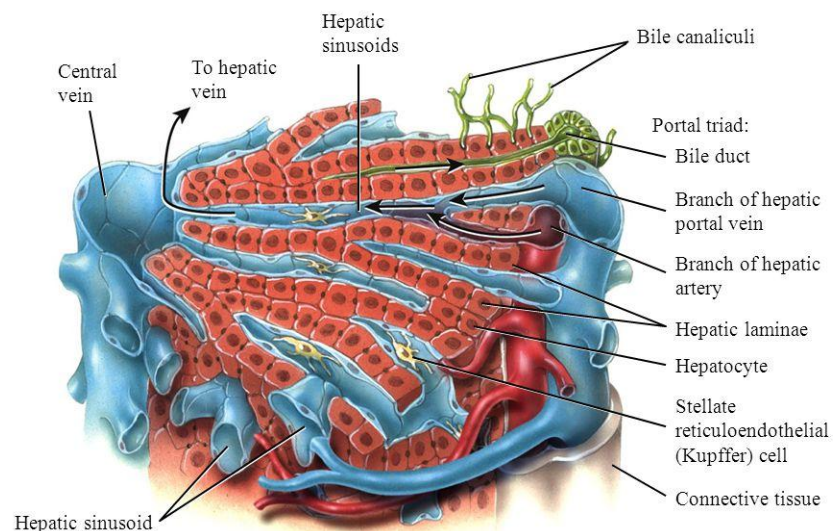
Figure 12 Illustration of hepatic sinusoids.

Source: http://slideplayer.com/slide/5258442/

Hepatic sinusoids pass between and through hepatic plates as they carry blood from the hepatic artery and portal venule to the central vein[34].

1.3.4.3 Kupffer cells

Kupffer cells are the cells of the monocyte or macrophage arise from bone marrow. Kupffer cells are irregular, with cytoplasmic extensions making their phagocytic function easier. Kupffer cells are in the lumen of the sinusoids of the liver. They are polymorphic cells with membranous folds, microvilli plumps and cytoplasmic processes similar to stars. They adhere to the sinusoidal endothelial cells with the help of these pseudopodia. They are not evenly distributed throughout the liver, but in different areas of the hepatic acinus. They show differences in population density, cytological characteristics and physiological functions. In periportal zone 1, 32% in zone 2, and 25% in perivenous zone 3, 43% of Kupffer cells are found [39]. They are relatively rich in lysosomes compared with hepatocytes. Kupffer cells in zone 1 contain more lysosomes per cell than Kupffer cells that are centrilobular. Kupffer's most important cell function is the uptake, processing, and antigenic material presentation. Kupffer cells are capable of producing phagocytosis of foreign material, cytokines, and tumor cells that are similar to macrophage function. They affect the function of hepatocytes, sinusoidal endothelial cells and hepatic stellate cells through assumed paracrine effects. These functions are adapted to their shape and topographical distribution within the lobule. The numerous cellular pseudopodial processes confer a large area of contact and their numerical predominance in the periportal zone corresponds to the region of the most intense initial antigen wealth. While Kupffer periportal cells are more active phagocytes, relatively more cytokines are secreted by their perivenous counterparts. Bacteria derived from gut, microbial debris, and bacterial endotoxin are constantly exposed to kupffer cells. They clear about 90% of the bacteria transported by the sinusoidal blood in the normal liver. Kupffer cells proliferate significantly during acute viral hepatitis. Kupffer cells use a receptor-independent mechanism to absorb endotoxins and may transfer them for further degradation to hepatocytes. Kupffer cells release various products upon activation, including cytokines, prostanoids, nitric oxide and species of

reactive oxygen, and may acquire cytotoxic characteristics. Morphological evidence of this activation is an increase in size and an increase in membrane folds associated with an increase in cytoplasmic process extension. Kupffer cells are closely involved in the response of the liver to infection, toxins, ischemia, resection, and other stresses. Kupffer cells play an important role in the activation of innate and acquired immunity and endotoxin-mediated Kupffer cells as well as cytotoxic mechanisms induced by Kupffer cells seem to be key mechanisms in the pathogenesis of different liver diseases. Kupffer cells are supposed to exert paracrine effects on hepatocytes, sinusoidal endothelial cells, and stellate cells by secreting eicosanoids, growth factors, and cytokines in addition to their phagocytic and endocytic abilities. 65 percent of hepatic eicosanoid production is responsible for kupffer cells. Kupffer cells ' production of hepatocyte growth factor suggests they may affect hepatocyte growth and proliferation, e.g. following liver injury or hepatic resection. They perform a variety of functions, including immune complex phagocytosis, activated platelet aggregates, and polymerized blood coagulation proteins[34, 37, 40].

1.3.4.4 Fenestrated endothelium

Fenestrated endothelium is the endothelial cells that contain large holes that facilitate the easy exchange of blood and hepatocytes through space of Disse. Endothelial cells also contain numerous pinocytotic vesicles which actively transport substances into the hepatocytes from the portal blood[34].

1.3.4.5 Space of Disse

Space of Disse is the perisinusoidal space located between hepatocytes and the endothelium of hepatic sinusoids (Figure 13). It contains hepatocyte microvilli, plasma, reticular fibers, and cells that store fat (Ito cells or hepatic stellate cells). Blood plasma enters this space through openings that are too small for blood cells to pass between the endothelial cells. Therefore, blood-borne substances directly contact the hepatocyte microvilli. These cells are absorbing nutrients, oxygen, and toxins from these spaces and releasing endocrine secretions into them. It works in

the exchange of material between the bloodstream and hepatocytes that do not contact the bloodstream directly. The cells that present in the space of Disse include[28].

a) Hepatic stellate cells (HSCs) (Ito cells, fat storing cells, lipocytes, pericytes) is the primary cell type in the liver responsible for excess collagen synthesis during hepatic fibrosis[41]. These cells store Vitamin A and manufacture and secrete a number of important hepatic growth factors and matrix components (collagens) and therefore play role in liver regeneration and in the development of liver fibrosis. Furthermore, HSCs have an impact on growth and proliferation of hepatocytes, and participate in the inflammatory reaction and in the immune function of the liver. In every acute and chronic liver injury HSC are activated. The activation process is characterized by phenotypic changes. The cell transforms from a resting, vitamin A storing HSCs to an active, proliferating, myofibroblast-like, contractile, mobile and fibrogenic cell. HSCs increase in size, their vitamin A content diminishes and the protein secretory apparatus becomes prominent. Cytoskeletal markers of smooth muscle and fibroblasts are expressed. The most intense activation and proliferation takes place in the regions of maximal liver injury[42, 43].

b) Pit cells also known as large granular lymphocytes, natural killer cells or NK that are a primitive cellular immune host defense mechanism, active against viruses, and tumor cells.

c) T and B lymphocytes[37].
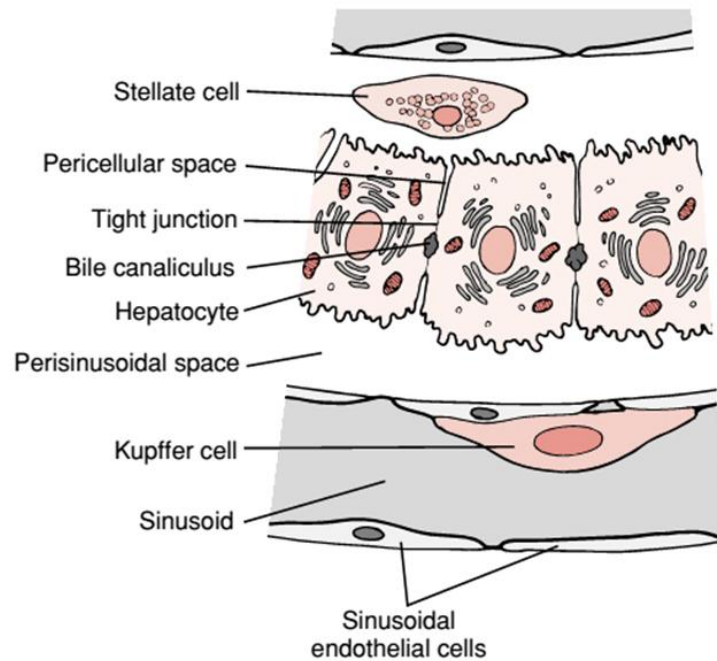
Figure 13 The relationship between hepatocytes.

Source: Tso P and McGill J. (2004) The Physiology of the Liver.

The perisinusoidal space and the sinusoid. The space between hepatocytes is the perisinusoidal space. A layer of sinusoidal endothelial cells separates it from the sinusoid. The hepatic sinusoids are also lined with kupffer cells. These are resident macrophages of the fixed monocyte-macrophage system that play a crucial role in removing unwanted material from circulation. Some perisinusoidal cells in the cytoplasm contain separate lipid droplets. These stellate cells or Ito cells are called these fat storage cells. Vitamin A is found in the lipid droplets. Stellate cells are transformed into myofibroblasts through complex and typically inflammatory processes, which then become capable of both secreting collagen into space of Disse and regulating sinusoidal portal pressure through contraction or relaxation. Pathological fibrosis of the liver may involve stellate cells[28].

1.4 Liver function

The liver is responsible for some 500 bodily functions. It plays a role in digestion, sugar and fat metabolism, and the body's immune defense. It processes almost everything a person eats, breathes, or absorbs through the skin. About 90% of the nutrients of the body pass from the intestines through the liver. The liver transforms food into energy, stores nutrients and produces proteins in the blood. The liver also acts as a filter for blood removal of harmful substances. Blood cells are produced in the liver in the developing fetus[44].

1.4.1 Digestion

In the digestion and processing of food, liver plays an important role. Liver cells produce bile, a greenish-yellow fluid that helps fat digestion and fat-soluble nutrient absorption. Bile is delivered through the bile duct to the small intestine; when no food is to be digested, extra bile is stored in a small organ called the gallbladder below the liver. By-products from the breakdown of liver-processed drugs and toxic substances are transported in the bile and excreted from the body. The production and flow of bile may be impaired by a person with a damaged liver. The body may not be able to absorb nutrients properly when this happens. Liver cells also convert heme (a hemoglobin component released when broken down red blood cells) into bilirubin. Bilirubin can build up in the blood when the liver is damaged, causing jaundice. The intestine supplies the majority of water-soluble nutrients to the liver and water-soluble vitamins and minerals absorbed from the small intestine are transported to the liver through the portal blood. Amino acids, monosaccharides and fatty acids (predominantly short-and medium-chain forms) are the nutrients transported in portal blood. Short-chain fatty acids are largely derived from the colon bacteria fermenting dietary fibers. Some dietary fibers, such as pectin, are almost entirely digested to form short-chain fatty acids (or volatile fatty acids), while the bacteria do not digest cellulose well. Only a small amount of long-chain fatty acids, bound to albumin, are transported through the blood portal; most are transported as triglyceride-rich lipoproteins (chylomicrons) in the intestinal lymph[28, 44].

1.4.2 Metabolism

The liver is pivotal in regulating the metabolism of carbohydrates, lipids, and proteins. It also helps to maintain a constant blood glucose concentration by converting other substances, such as amino acids, into glucose[28]. The liver performs a lot of metabolic functions, giving the body the energy it needs. It regulates sugar, fats, and cholesterol production, storage, and release. The liver converts glucose (blood sugar) into glycogen when food is eaten, which is stored for subsequent use. When energy is needed, in a process called gluconeogenesis, the liver converts glycogen back into glucose. The liver regulates fat storage by converting amino acids from digested foods into fatty acids such as triglycerides; when the body has insufficient sugar, the liver converts fatty acids into ketones that can be used for fuel. The liver also controls cholesterol production, metabolism and excretion, an important component of cell membranes and certain hormones[28, 37, 44].

1.4.3 Protein synthesis

The liver synthesizes a number of important proteins, including enzymes, hormones, factors of clotting and immune factors. Liver enzymes known as aminotransferases or transaminases (ALT and AST) break down amino acids from digested food and reconstruct them into new proteins that the body needs. These enzymes can leak out and build up to high blood levels when liver cells are inflamed or damaged; these enzymes can be measured by a simple blood test. For proper blood functioning, several of the proteins synthesized by the liver are needed. These include various binding proteins (which bind and carry substances such as vitamins, minerals, hormones, and fats) and albumin (a protein that helps to maintain the proper volume of blood). Hepatic coagulation factors include fibrinogen, prothrombin (Factor II) and a protein in the process of coagulation cascade (Factor VII). These allow the blood to clot after an injury; low levels may result in prolonged bleeding and easy bruising. Alkaline phosphatase, gamma-glutamyl transferase (GGT), and insulin-like growth factor (IGF-1) are other proteins synthesized by the liver[28].

1.4.4 Storage

The liver stores several nutrients, including vitamins A, D, B9 (folate), and B12. It also stores iron and plays a role in converting iron into heme, a component of hemoglobin (the oxygen-carrying molecule in red blood cells)[44].

1.4.5 Detoxification

The liver plays a crucial role in detoxifying body harmful substances, including alcohol, drugs, solvents, pesticides, and heavy metals. The liver may get overwhelmed when a person is exposed to high levels of these chemicals. The portal vein delivers toxins to the liver. These chemicals are processed by the liver and excreted in the bile. The liver also processes and excretes toxic by-products of normal metabolism (such as ammonia) and excess hormones (such as sex hormones like estrogen in particular). Many drugs including common over-the-counter drugs such as acetaminophen (Tylenol), most anti-HIV drugs, and some herbal remedies— are processed through the liver and can cause damage to the liver. The combination of alcohol, multiple drugs and/or herbs should be particularly careful for people. If the liver is damaged, it may not be able to break down and effectively excrete drugs, potentially leading to dangerously high blood levels and intensified side effects[28].

1.4.6 Immunity

The liver functions as an immune system organ through the function of the sinusoids-line Kupffer cells. Kupffer cells are a type of fixed macrophage that together with macrophages in spleen and lymph nodes form part of the mononuclear phagocyte system. Kupffer cells play an important role in bacteria, fungi, parasites, worn-out blood cells, and cellular debris being captured and digested. The large blood volume that passes through the hepatic portal system and the liver enables Kupffer cells to clean large blood volumes very quickly[44].

2 Hepatocellular carcinoma (HCC)

2.1 Pathogenesis

Hepatocellular carcinoma (HCC) is one of the most lethal and prevalent cancers worldwide [45]. The prognosis of patients with HCC is dismal and the mortality rates are almost the same as the incidence rates (Figure 14).
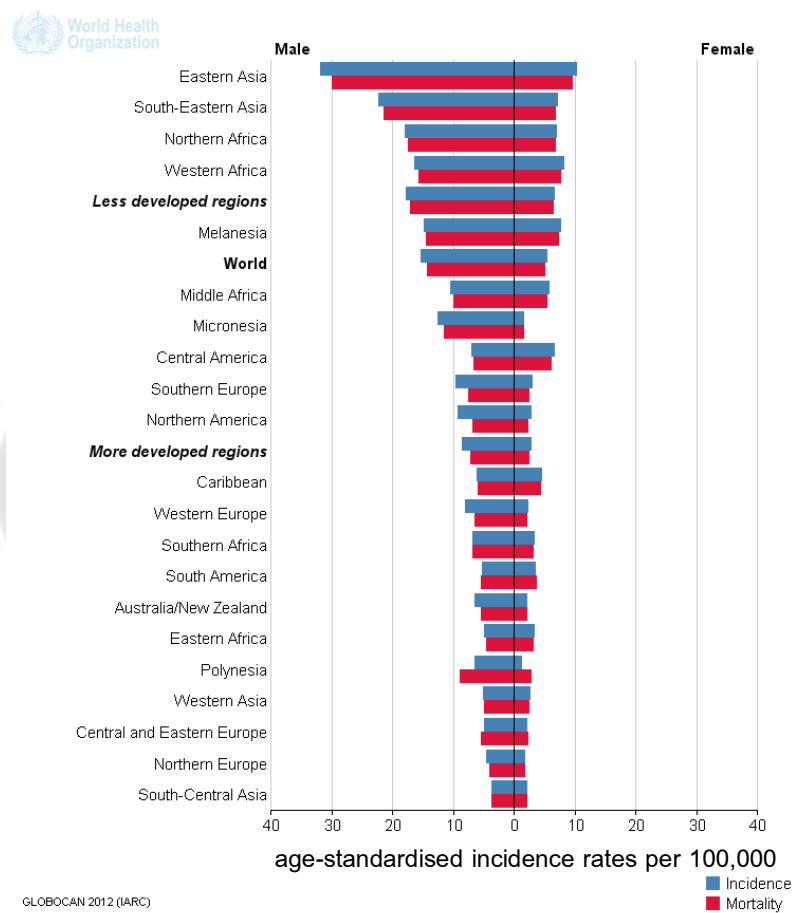
Figure 14 Incidence and mortality of HCC worldwide.

Source: Ferlay J, Soerjomataram I, Ervik M, Dikshit R, Eser S, Mathers C, Rebelo M, Parkin DM, Forman D, Bray, F. (2012) Cancer Incidence and Mortality Worldwide

The Sorafenib multikinase inhibitor remains the only approved agent for advanced disease patients. HCC affects the entire world population, although the prevalence of HCC and the underlying etiological factors vary considerably in regional, ethnic and gender dependence[46]. HCC develops in patients with advanced liver cirrhosis in more than 70% of cases. Overall, these patients have up to 30% cumulative five-year cancer risk. In the vast majority of patients, the underlying risk factors for HCC can be identified. HCC is most commonly caused by viral hepatitis worldwide (almost 75 %). It is possible to attribute 54% of all HCC to hepatitis B virus (HBV) and 31% to hepatitis C virus (HCV). It is associated less frequently with chronic toxins or hereditary liver diseases[45]. Moreover, nonalcoholic fatty liver disease (NAFLD) is an emerging risk factor gaining increasing prevalence nowadays (Table 1)[47].

Table 1 Distribution of risk factors by geographic region for HCC worldwide

Region	M/F	Risk factors (%)			
		HCV	HBV	alcohol	other
Europe	6.7/2.3	60-70	10-15	20	10
North america	4.1/2.3	50-60	20	20	10 (NASH)
Asia and Africa		20	70	10	10 (aflatoxin)
Asia	21.6/8.2				
China	23/9.6				
Japan	20.6/7.8	70	10-20	10	10
Africa	1.6/5.3				
world	16/6	31	54	15	

Source: European association for the study of the liver and European organisation for research and treatment of cancer. (2012) EASL-EORTC clinical practice guidelines: management of hepatocellular carcinoma.

Pathogenesis is considered primarily a sequence of hepatic injury, regeneration, fibrosis, cirrhosis, dysplasia, and malignancy. Most of the time, a drastic alteration of the hepatic matrix and microenvironment, including phenotypically altered hepatocytes, results in dysplastic hepatocytes forming nodules and finally in the appearance of HCC[48]. Recently, genomic approaches such as transcriptome and whole-genome or -exome analysis have been applied for molecular and prognostic classifications[49].

2.1.1 Hepatitis B virus infection

Approximately 50% of all HCCs worldwide are due to HBV infection. Countries with a high incidence of HBV infections have already significantly reduced new diagnosis rates and HCC through routine newborn vaccination[50]. The infection may resolve spontaneously in up to 90% of cases. Of all chronically infected individuals, about 25% will eventually develop HCC[51]. HCC occurs in high viraemic patients not only in cirrhotic livers, but also in non-cirrhotic livers. Overall, 5-to 100-fold increases the risk of developing HCC in HBV-infected patients. High viraemia (> 2,000 IU / ml), high aminotransferases, positive HBeAg and HBV genotype C infection are the main risk factors[52, 53]. Risk factors related to patients, male gender, over 40 years of age, positive family history of HCC, hyperendemic migration background, co-infection with hepatitis D virus, HIV or HCV, and alcohol or aflatoxin exposure were identified[2, 54].

Treatment options are nucleoside / nucleotide analogs or interferon-α for HBV-infected patients. Sustained suppression of HBV can prevent cirrhosis progression and thus reduce the risk of HCC. Once cirrhosis has been established, there has been no robust evidence of the preventive potential of antiviral drugs in chronic hepatitis B. It has only recently been shown that long-term lamivudine and entecavir treatment can reduce the incidence of HCC in HBV-infected patients[55].

2.1.2 Hepatitis C virus infection

Patients with hepatitis C have a high risk of developing HCC, similar to hepatitis B. Approximately 30% of HCC cases worldwide are HCV-related. In most patients, HCV is chronic. It goes hand in hand with a variable degree of hepatic

inflammation and results in 10-40% of patients having cirrhosis. The risk of HCC in HCV-infected individuals is 17 times higher than in non-infected individuals and the risk of HCC development is around 5 percent per year[51]. Tumors occur primarily in the cirrhot liver as opposed to HBV. HCC was previously found to be the leading cause of death (44 %) and the first complication to develop (27 %) followed by ascites, jaundice and upper gastrointestinal bleeding in cirrhotic HCV patients[56]. Recent data suggest that HCC occurs decades after infection and that the risk in patients over 65 years of age is significantly higher than in younger patients[57]. It increases when additional risk factors such as genotype 1b, alcohol or cigarette consumption, HBV or HIV co-infection, or diabetes mellitus are present[58-60].

2.1.3 Alcohol and tobacco

Excessive intake of alcohol is one of the most common causes of cirrhosis of the liver and is therefore an important risk factor for HCC. Recent case-control studies of epidemiology suggest that in addition to alcohol (in 10% of all HCC), tobacco use (in nearly 50% of all HCC) is also a relevant co-factor for tumor development[61]. Particularly in patients with HCV and to a lesser extent with HBV infection, with already moderate alcohol and tobacco consumption, the risk of developing HCC increases significantly[62, 63]. Oxidative stress due to ethanol metabolism and inflammation are important mechanisms involved in alcohol-related hepatocarcinogenesis[64]. Recent data suggest that chronic alcohol consumption leads to cytochrome P450 2E1 (CYP2E1) induction in the liver, leading to ROS generation with direct and indirect carcinogenic effects. CYP2E1 metabolizes various carcinogens that are also present in tobacco smoke with their carcinogenic metabolites, among which nitrosamines appear to be the most important[65].

2.1.4 Aflatoxins

Another important risk factor for HCC is exposure to aflatoxins, depending on the geographic region. In parts of Africa and Asia, the toxins of the fungus *Aspergillus flavus* and *Aspergillus parasiticus* are distributed all the time. They enter the food chain by contaminating maize, nuts and legumes and affect the wide

population[66, 67]. Aflatoxin alone is biologically inactive and has full effect only after ingestion of aflatoxin B 1-8,9-epoxide by activation. The electrophilic epoxy covalently binds to DNA bases and thus becomes mutagenic[66]. In these patients, epidemiological research revealed frequent mutations in the tumor suppressor p53[68]. Simultaneous exposition of aflatoxins and HBV infection results in a more than additive risk for HCC[69].

2.1.5 Non-alcoholic fatty liver disease (NAFLD)

NAFLD encompasses a wide spectrum of liver diseases ranging from simple steatosis to non-alcoholic steatohepatitis (NASH), which may eventually lead to cirrhosis and HCC[70]. Steatohepatitis is present in 20 percent of individuals with NAFLD, while steatosis is present in the majority. Isolated liver steatosis is unlikely to affect liver mortality[71]. With the dramatic increase in obesity prevalence worldwide, NAFLD has become a major issue and is now receiving more attention worldwide. More than 30 percent of the U.S. population was obese at the beginning of this century and there are at least 400 million obese adults worldwide. NAFLD occurs in 90% of obese patients and is the most common liver disease among adults in the United States and other Western countries[70]. In a large prospective study of 900,000 adults it was shown that obesity increases the risk of multiple cancers, the risk of developing liver cancer was significantly increased and 4.5 times higher for men with an index of body mass (BMI) > 35 compared to men with normal BMI (Figure 15)[72]. Similarly, a meta-analysis revealed a relative risk of liver cancer of 1.17 for overweight and 1.89 for obese persons [73]. In addition, a prospective assessment of 315 patients with HCV and 195 patients with NASH revealed that patients with NASH cirrhosis had only a slightly lower risk of liver cancer compared to patients with HCV. Moderate alcohol consumption seemed to be the most significant co-factor in both diseases associated with the risk of HCC development[62]. However, in patients with newly diagnosed HCC, NALFD/NASH is now more frequently identified as the underlying risk factor than in patients with HCV infection[74]. The most frequently reported pathomechanisms of HCC in the setting of NASH are oxidative stress, insulin resistance, adipocytokine functional disorder and cell hyperplasia[75].
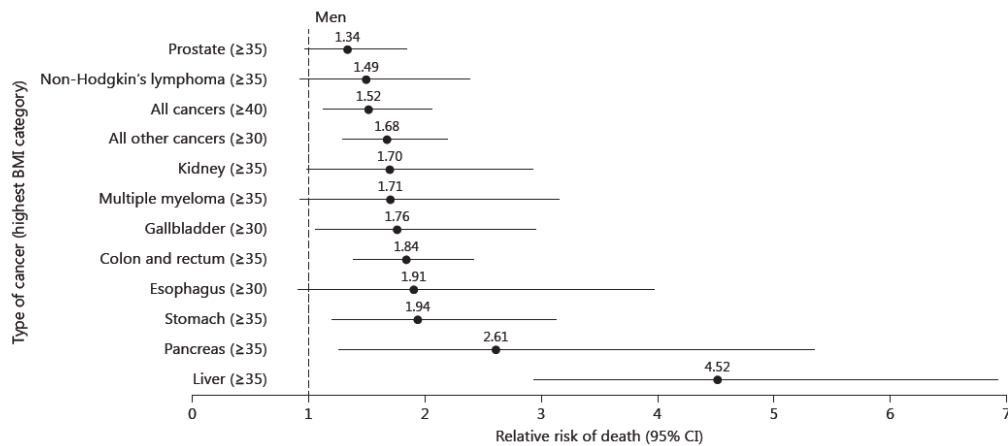
Figure 15 Summary of mortality from cancer

according to BMI for US men in the cancer prevention study II.

Source: Calle EE, Rodriguez C, Walker-Thurmond K, Thun MJ. (2003) Overweight, obesity, and mortality from cancer in a prospectively studied cohort of U.S. adults.

In addition, an increased production of the tumor-promoting cytokines IL-6 and TNF has been identified, resulting in hepatic inflammation and activation of the oncogenic transcription factor STAT3. The development of HCC in NASH was also associated with hepatic iron overload. In NASH, where necroinflammation is prevalent, abnormal iron deposition in the liver is more frequent than in steatosis alone. Iron and hyperinsulinemia coexistence are risk factors for NASH development and can contribute to insulin resistance, disease progression and HCC development[76]. Since HCC is rarely found in pure steatosis without NASH's necroinflammatory component, it remains unclear whether NAFLD is a causative factor for HCC, although it is undeniably a risk factor for HCC[77].

2.2 Staging of HCC

A crucial step in managing these patients is determining the prognosis of HCC patients. Survival after 5 years is associated with early diagnosis and effective treatment[78]. Several classifications have been proposed in order to stratify patients according to their expected outcomes[79]. Obviously, although guidelines and recommendations have been established, therapy decisions should be individualized taking into account the scientific evidence available and the personal profile of the patient. For the time being, most cases of HCC develop in cirrhosis patients, determining the prognosis and therapy of the patient should also consider the baseline level of liver damage due to HCC. Several strategies have been proposed for prognostic staging and decision-making in patients with HCC: Child-Pugh[80], MELD (Model for End-Stage Liver Disease)[81], TNM (Tumor Node Metastasis) classification[82] and tumor volume estimation[83], all characterized and limited by their one-dimensional assessment. The most used classification is developed by the Barcelona Clinic Liver Cancer (BCLC) group[84], a multidimensional strategy. This strategy has been validated in different scenarios and has established recommendations for each stage of the disease[85, 86].

Till now, the BCLC system is the recommended staging system by international guidelines (Figure 16)[78], since it stages the disease and proposes treatment according to the stage:
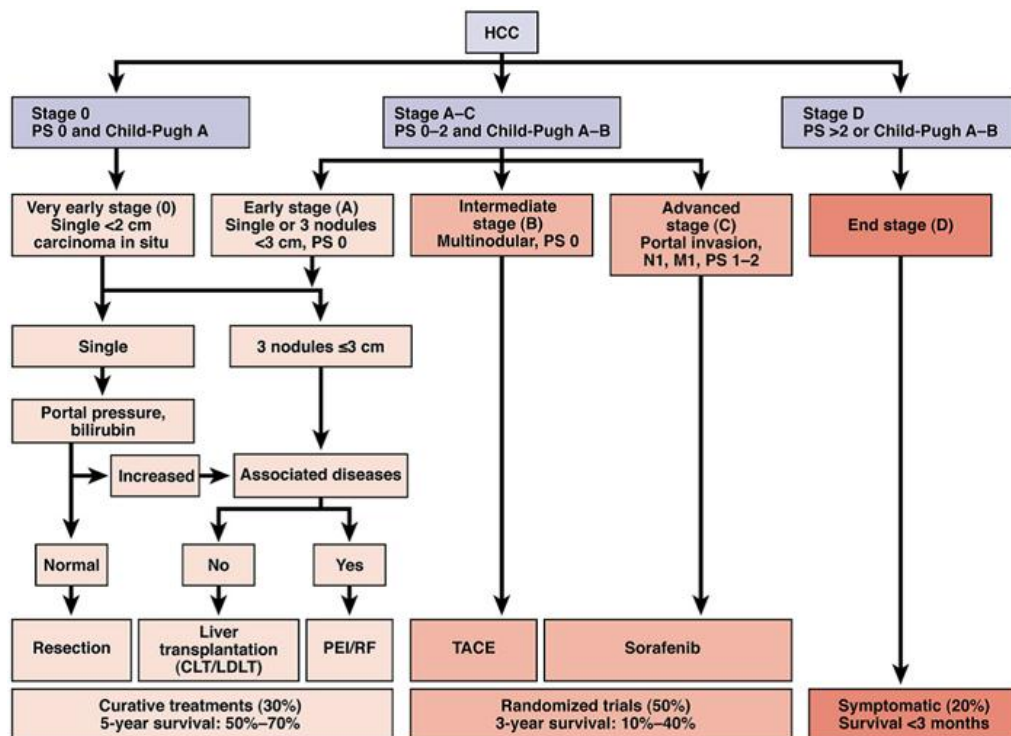
Figure 16 The BCLC classification is based on tumor extent.

Child-Pugh score, vascular invasion and ECOG (Eastern Cooperative Oncology Group) performance status. This algorithm can be used to decide treatment allocation based on tumor stage. BCLC, Barcelona Clinic Liver Cancer; PS, Performance status; HCC, hepatocellular carcinoma; TACE, Transarterial chemoembolization; PEI, Percutaneous ethanol injection; RF, Radiofrequency ablation.

2.2.1 Very early stage (BCLC 0)

Patients with cirrhosis and compensated liver function (Child-Pugh A) are very early patients with no signs of portal hypertension and with a single lesion of about 2 cm ("in situ" carcinoma). ECOG's performance status must be 0. If treated by resection, the 5-year survival of these patients is > 90%[87] and the tumor rarely recurs.

2.2.2 Early stage (BCLC A)

Patients with a single HCC lesion > 2cm or three nodular lesions, each with a diameter of about 3 cm, are early stage. According to the Child-Pugh classification, liver function should be evaluated and limited to groups A and B. The absence of significant portal hypertension and normal serum bilirubin levels are predictors of survival in patients with a single lesion resected[88]. The determined tumor size is a criterion for liver transplantation as set out in the Milan criteria[89]. If these criteria are not fulfilled other therapies are less effective[90]. The risk of invasion by the vascular is directly proportional to the tumor size. Five years of survival in these patients after curative transplantation exceed 50 percent[91].

2.2.3 Intermediate stage (BCLC B)

Intermediate stage includes patients with one, large HCC lesion as well as multifocal disease asymptomatic patients without vascular or extrahepatic lesions. Their reported survival was about 16 mo. It is necessary to preserve liver function (Child-Pugh A and B). These patients may experience transcatheter arterial chemoembolization (TACE) associated with increased survival[92]. A recent meta-analysis of randomized clinical trials suggests that ascites (a contraindication to TACE) in this subgroup of patients is the most important adverse prognostic factor[93].

2.2.4 Advanced stage (BCLC C)

This stage includes patients who do not meet the criteria for BCLC B. They are symptomatic (pain, general malaise or ECOG 1-2), vascular invasion or involvement with extrahepatic HCC. Sorafenib, a tyrosine kinase inhibitor, has recently increased their survival (10.7 mo)[85].

2.2.5 Terminal stage (BCLC D)

This stage includes patients with severe hepatic dysfunction (Child-Pugh C) who are not candidates for liver transplantation and patients with a score of more than 2 ECOG. They have a dire prognosis and survival of less than 6 mo. while taking advantage of conservative therapy (no intervention)[78].

2.3 Treatment

HCC can be cured by surgical resection or liver transplant if diagnosed early; however, only 15% of cases are selected for treatment with these methods [94].

2.3.1 Liver resection

Deciding to carry out a liver resection depends on three conditions: tumor size, location of the tumor and function of the liver. Resection is considered the treatment of choice in patients with liver-limited solitary tumors with no radiological evidence of vascular invasion and normal liver function (normal total bilirubin, 10 mmHg hepatic venous pressure gradient, > 100000 platelets and no endoscopic oesophageal varicose veins)[95]. The 5-year survival rate following tumor resection ranges from 41% to 77%. Resection is also an option in multifocal HCC that meets or does not meet Milan's criteria or is not a candidate for liver transplantation[96]. Loco-regional therapy should be preferably considered in this group of patients, avoiding subsequent liver decompensation. The perioperative mortality after HCC resection in cirrhotic patients is approximately 2-3%, greater than in patients with no cirrhosis. As a general rule, patients with some manifestation of decompensation (bleeding, ascites or portal hypertension), hepatic reserves are insufficient to consider surgical resection. Ideally, resection should only be considered in patients with tumors ≤ 5 cm in diameter[97], although there is consistently more evidence that size may not be a strict criterion in candidate selection; however, it should not be overlooked that the higher the tumor mass, the higher the risk of vascular invasion or spread and the rate of recurrence increases by up to 70% at 5 years[98]. *De novo* tumor development may occur after primary resection, although as a result of primary tumor dissemination, most recurrences appear after 1 or 2 years. The post-resection approach has not yet been well studied, but it is known that repeating the resection is of no value. A viable alternative can be

rescuing liver transplants or loco-regional therapies with or without multikinase inhibitors [99].

2.3.2 Liver transplant

In patients with unresectable tumors, orthotopic liver transplant (OLT) in combination with adjuvant therapies such as transarterial chemoembolization (TACE) or percutaneous ablation is the most feasible surgical option[99]. However, OLT is not an optimal choice for all patients and patients should be well selected when dealing with a scarce resource such as organ donation, despite a necessary and prudent evaluation[95]. In 1996, Mazzaferro et al[100] reported a prospective cohort study including 48 patients transplanted because of HCC and in accordance with the Milan criteria (a single lesion ≤ 5 cm or 3 lesions ≤ 3 cm each). As a result, their 4-year survival rate was 75%. Hence, in these patients, deceased donor liver transplant is a real option. Over time, experience with this method of treatment has increased and current 5-year survival is above 70% with a recurrence rate of 15%, similar to OLT without HCC[101].

Several studies investigate the expansion of the Milan criteria in order not to limit the size of the tumor. The San Francisco criteria were proposed by the University of California, which included patients with a single nodule of 6.5 cm or 3 nodules of 4.5 cm and a total volume not exceeding 8 cm. Other retrospective and prospective studies with very similar results to the Milan criteria are also available[102]. Despite these results, international guidelines insist that they adhere to the Milan criteria while at the same time awaiting stronger data[78, 103]. In downstage interest has recently increased the targeting of patients with HCC that exceed the OLT criteria and are treated with locoregional therapy (TACE and/or RF) to decrease the size of the tumor and then meet the OLT criteria[104]. Current data led to conflicts with some experts recommending OLT only in patients who are effectively down-stage while others favor liver transplantation as a rescue therapy despite the lack of the desired response[105]. Yao et al.[104] studied a downstage protocol using TACE and/or radiofrequency ablation and reported a 1-year survival of 96.2% and 92.1% at 4 years in OLT patients; they were also recurrent-free after an average 25-month follow-up. The downstage approach is

controversial: some experts believe that large or multifocal tumors are at the same risk of recurrence despite successful downstage[105]. After transplantation, one of the main poor response and recurrence biomarkers is AFP. It may indicate microvascular invasion with a cut-off limit above 1000 ng/mL, although further studies are required for confirmation[106]. This group of patients usually have stable liver disease when diagnosed with HCC, a disadvantage when waiting for an OLT. In this context, the United Network for Organ Sharing has determined that patients fulfilling the Milan criteria should have a MELD score of 22 when added to the transplant waiting list and that the score should be increased every 3 months (equivalent to a 10% increase in mortality); this is determined after computed tomography or magnetic resonance confirmation of Milan fulfillment of the criteria[107]. This turns up, depending on the region of the study and the number of patients on the waiting list, as some stay with stable liver disease and up to two years on the list. The Living Donor Living Transplant program is therefore a viable alternative; the risk of death and complications from donors is 0.3% and 2% respectively. This option is limited to excellence centers. It remains to be determined with certainty whether this group of patients has the same long-term survival as recipients of deceased donor livers.

2.3.3 Loco-regional treatments

Loco-regional treatments are selected based on their oncological stage, performance status and underlying liver disease(s) in patients with HCC.

Early Stage (BCLC A): Percutaneous ethanol injection (PEI) and radiofrequency ablation (RFA) are currently the most commonly used methods of ablation. PEI is ethanol directly injected into the HCC. This was the first method of treatment used before RFA was developed[108]. PEI cure capacity in tumors > 2 cm is limited and requires multiple injections in multiple sessions[109]. In 70% of nodules < 3 cm and in about 100% of nodules < 2 cm, PEI can lead to complete tumor necrosis. RFA is currently considered the safest method of ablation and results better in patients with BCLC A[108]. In patients with tumors < 3 cm, 50% in those with tumors between 3 and 5 cm and 25% in tumors >

5 cm, complete response rates can reach 80%. RFA is 76 percent associated with a 5-year survival[109]. To conclude that RFA significantly improves survival and decreases local recurrence compared to PEI, the available data are sufficient. PEI use should be restricted to circumstances where RFA is unavailable or technically unavailable[110].

Intermediate stage (BCLC B): the main method of treatment in unresectable HCC is intra-arterial chemoembolization. This procedure requires a catheter endovascular placement until it reaches the hepatic artery and the segmental and subsegmental branches are guided by a microcatheter. The most commonly used chemotherapeutic agents are cis-platinum and doxorubicin mixed with lipiodol as an emulsion, an oily radio-opaque contrast agent concentrated in the tumor, which promotes the exposure of neoplastic cells to drugs. This emulsion is distributed in the affected segments or lobes and infused in the tumor selectively[110]. Survival rates are 82%, 47%, and 26%, respectively, at 1, 3, and 5 years. Therapy leads to tumor necrosis in 30%-50% of patients, but rarely results in a complete response, especially after a single session[109]. After the emulsion of chemotherapy, embolizing agents are administered after the same procedure. The most frequently used are: Gelfoam®, microparticles of polyvinyl alcohol and microspheres of trisacryl gelatin. Thus, vascular obstruction decreases the washout of chemotherapy agents[109]. The technique of soft embolization is very similar to TACE, but without lipiodol administration of the emulsion of chemotherapy. Embolizing particles are injected directly into the afferent artery of the tumor after diagnostic angiography to produce tumor ischemia and necrosis. This technique is useful in patients with significant tumor load and in patients with no viable treatment options due to future progression. It was also associated with fewer adverse effects[111]. Most of the benefits of soft embolization are shared with TACE and the debate on which technique offers the greatest advantages continues. Among the few controlled trials that compared TACE / soft embolization vs. conservative treatment, survival was the greatest with chemoembolization at 1 and 2 years, 82% and 63% vs. 75% and 50% with soft embolization and 63% and 27% with conservative management. The standard

technique most commonly used at the moment is TACE. Recent evidence shows that TACE can decrease the risk of death in patients with intermediate and advanced HCC by 35% in combination with Sorafenib[112].

Terminal stage (BCLC D): This stage includes patients with Child-Pugh C and some with high score B liver disease associated to other comorbidities and terminal stage oncological symptoms. They must be very carefully evaluated and in most cases, locoregional therapies are not an option since they can lead to the development of severe and even fatal adverse effects[110].

2.3.4 Combined treatment

In lesions between 3 and 5 cm, the combination of chemoembolization and radiofrequency ablation has been shown to control tumor growth better. The benefits of combined therapy include the fact that embolization hypoxic aggression and the effects of chemotherapy agents are synergistic in reducing blood flow and impedance of the tumor. In addition, intra-tumor septa disruption after chemoembolization may promote heat distribution within the tumor and decrease the cooling of the tissue mediated by perfusion, resulting in a larger ablated area. The proposed protocol is to conduct selective chemoembolization first, followed by radiofrequency ablation within 14 days[113]. Combined treatment vs RFA showed an increase in survival rates 92 percent, 66 percent and 61 percent vs 85 percent, 59 percent and 45 percent at within of 1, 3 and 4 years, respectively. Recurrence-free survival rates were reported as 79%, 60% and 54% vs 66%, 44% and 38% over the same follow-up periods[114].

2.4 Molecular pathways in HCC

Several molecular alterations have been observed in HCC. Accumulation of these genetic alterations and aberrant activation of several signaling pathways have been thought to play a role in the development of HCC[115]; specifically, those involving vascular endothelial growth factor (VEGF)-mediated angiogenesis, Wnt, phosphatidylinositol 3-kinase (PI3K)/Akt/mammalian target of rapamycin (mTOR), AMP-activated protein kinase (AMPK), and c-MET.

Angiogenesis and the production of angiogenic factors are fundamental for tumor growth, invasion and metastasis[116]. New vessels promote growth by transmitting oxygen and nutrients and removing catabolites, while endothelial cells secrete tumor cell growth factors and a variety of matrix-degrading proteinases that facilitate invasion of tumors[117]. In normal tissues, the dominant influence of endogenous angiogenesis inhibitors on angiogenic stimuli maintains vascular quiescence. On the other hand, tumor angiogenesis is induced by increased angiogenic factor secretion and/or down-regulation of angiogenesis inhibitor. There are two types of microvascular structures in the liver: large vessels, such as portal and central venules and hepatic arterioles, lined with continuous endothelial cells and fenestrated sinusoids lined with discontinuous sinusoidal endothelial cells (SEC)[118]. The adult liver is highly vascularized. Its cells are flanked by SEC-lined sinusoids and separated from them by the space of Disse[119]. Capillaries are formed in liver tumors and sinusoidal fenestration is lost. Stellate cells are considered pericytes resident in the liver. Through mechanisms other than those attributed to pericytes they can contribute to angiogenesis and become activated. Extracellular fibrillar matrix accumulates and microvilli is lost by hepatocytes. The result is a distorted sinusoidal structure that is characterized by capillarization and neovessel formation. Paramount evidence revealed several angiogenic endogenous stimulators responsible for the onset of angiogenesis in HCC, including vascular endothelial growth factor (VEGF), fibroblast growth factor-2 (FGF-2), angiogenin, and angiopoietins (Ang). Secretion of angiogenic factors such as VEGF, FGF-2, angiogenin, and Ang induced by HCC cells, infiltrating inflammatory cells, and hepatic stellate cells promote sprouting of new vessels from pre-existing ones. In fact, angiogenesis of the tumor does not depend on a single molecule, as many angiogenic inducers and inhibitors are expressed simultaneously. Hypoxia in the center of growing tumors results in intracellular stabilization of the hypoxia-inducible factor (HIF)-1α, the key transcription factor in hypoxic tissues, and induces the expression of several hypoxia-response genes such as VEGF (Figure 17)[120, 121].
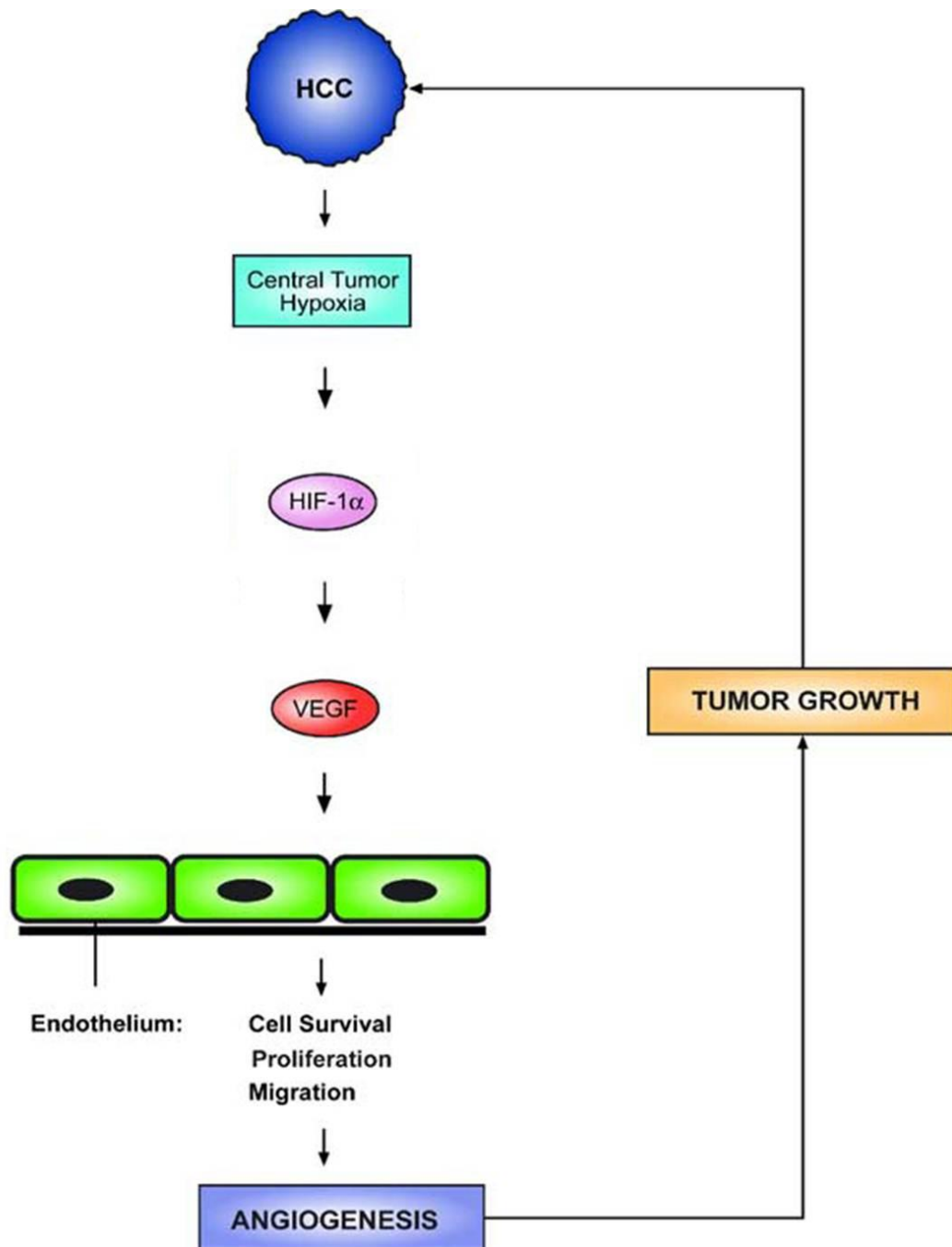
Figure 17 Role of hypoxia as main trigger for tumor angiogenesis.

Source: Semela D and Dufour JF. (2004) Angiogenesis and hepatocellular carcinoma.

2.4.1 VEGF-mediated angiogenesis pathway

VEGF is one of the strongest angiogenic stimulating factors in most human tumors and is up-regulated. The main VEGF mediating angiogenesis of the tumor is VEGF-A. VEGF signals on the cell surface via the VEGF receptor (tyrosine kinase receptor). VEGF ligand binding induces VEGF receptors to be dimerized and autophosphorylated. Residues of phosphorylated tyrosine in the receptor serve as a docking site for different signal transduction proteins that can eventually activate angiogenesis-involved cellular processes. For example, phosphorylation by VEGFR-2 activates PLC-which in turn results in activation of protein kinase C (PKC). PKC can activate MAP kinase signals and promote cell proliferation and increase vascular permeability by activating endothelial synthesis of nitric oxide[122]. VEGF also induces Rho GTPase activation, which plays an important role in angiogenesis processes such as vascular permeability, extracellular matrix degradation, cell migration and invasion[123]. For HCC pathogenesis, the VEGF pathway is clearly important. Most HCC patients found expression of VEGF mRNA in liver tumors. And with the progression of the hepatocarcinogenic process from a normal liver to a dysplastic nodule to HCC, VEGF expression is steadily increasing[124]. In tumors with tumor emboli and poorly encapsulated tumors, the levels of VEGF mRNA expression were higher than those without tumor emboli and in well encapsulated tumors. The main route of HCC dissemination and metastasis is through the portal vein in the liver. VEGF mRNA level well correlated with the formation of HCC portal vein tumor thrombus (PVTT), suggesting that VEGF can play a significant role in HCC invasion and metastasis[125]. In well differentiated HCC as well as in area surrounding the HCC tissues where inflammatory cell filtration was apparent, immunohistochemical staining also detected very high VEGF expression. High serum VEGF levels among HCC patients have been shown to correlate with poor chemotherapy response and poor survival. Increased preoperative serum VEGF can also predict tumor recurrence after surgical resection[126]. Furthermore, increased VEGF expression has also been detected in cirrhotic and dysplastic livers, which often lead to liver cancer[127].
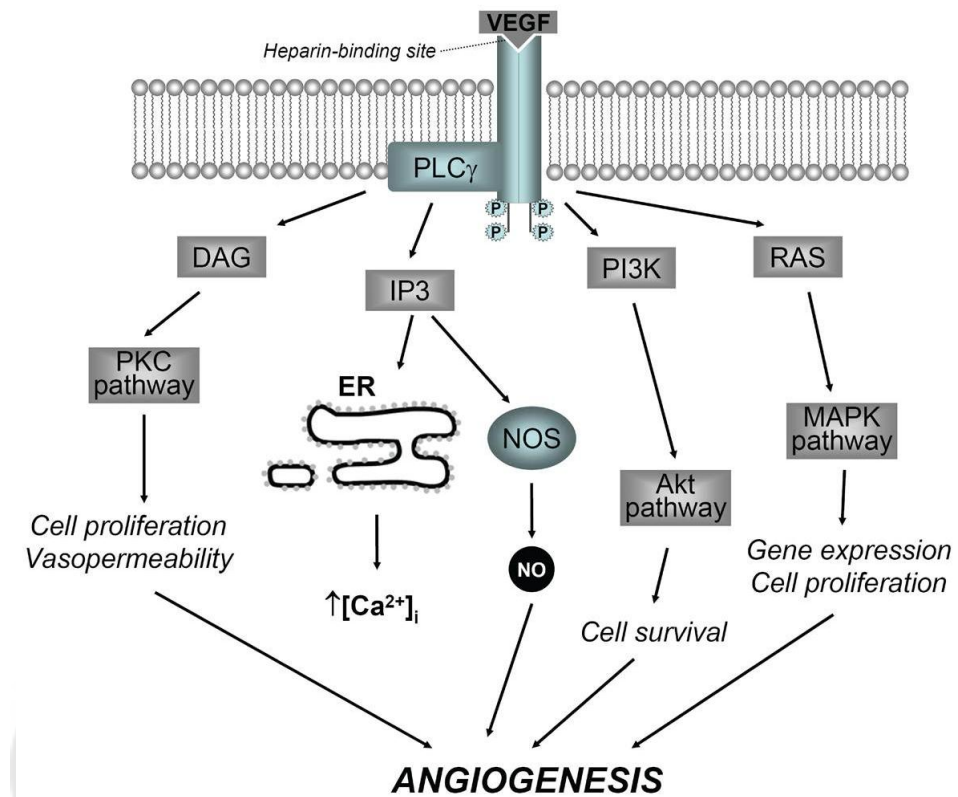
Figure 18 VEGF signaling pathway

Source: Trujillo CA, Nery AA, Alves JM, Martins AH, Ulrich H. (2007) Development of the anti-VEGF aptamer to a therapeutic agent for clinical ophthalmology.

2.4.2 Wnt pathway

Wnt signaling pathway involves three main components which include the cell surface, the cytoplasm, and the nucleus[128]. At the cell membrane, Wnt ligands form complexes with Frizzled receptors and LRP5 or LRP6 co-receptors[129]. β-catenin is associated with a multiprotein complex in the cytoplasm that includes APC, axin, and Ser / Thr kinase glycogen synthase kinase-3 beta (GSK3β) tumor suppressor proteins.

Axin and adenomatous polyposis coli (APC) form a structural scaffold enabling β-catenin to be phosphorylated by GSK3β. Ubiquitination and protein degradation targets β-catenin phosphorylation[130]. Thus, in the absence of Wnt ligands, β-catenin is continuously degraded in the cytosol under basal conditions. On Wnt binding, LPR5 recruits axin to the membrane and then inactivates the β-catenin destruction complex. This allows the accumulation and translocation of unphosphorylated β-catenin into the nucleus[130]. Then nuclear β-catenin forms a complex with DNA binding transcription factors in the TCF / LEF family to activate target genes for T-cell factor / lymphoid enhancer-binding factor (TCF/LEF). Many of the target genes, such as cyclin D1, are involved in cell proliferation[131]. In addition to regulating the transcription of genes, β-catenin is also involved in cell-cell adhesion. It regulates cadherin-mediated adhesion. Multiple lines of evidence link HCC signaling with aberrant Wnt. Activation of the Wnt signaling pathway in liver carcinoma is frequently reported. Subcellular localization of β-catenin and β-catenin-associated cell adhesion molecules in HCC has been shown to have significant changes[132]. Studies have shown that 50-70% of liver tumors have increased levels of β-catenin in the cytoplasm and in the nucleus[133]. Such accumulation by promoting proliferation and inhibiting differentiation can potentially provide a growth advantage for tumor cells. Accumulation and stabilization of β-catenin may result directly from point mutations or deletions of the β-catenin gene found in 12-26% of HCC[128]. Such dominant gain-of-function mutations typically occur on β-catenin N-terminal phosphorylation sites, including GSK3β-phosphorylated sites that regulate β-catenin degradation[134]. Mutations in these positions interfere with GSK3β recognition leading to a more stable β-catenin protein. In HCC pathogenesis, it is important to recognize that the disease development is highly context-dependent, involves cross-talking with other pathways, and is often not the result of mutation induced only by one pathway. Therefore, Wnt pathway components may represent potential therapeutic points for the treatment of HCC.
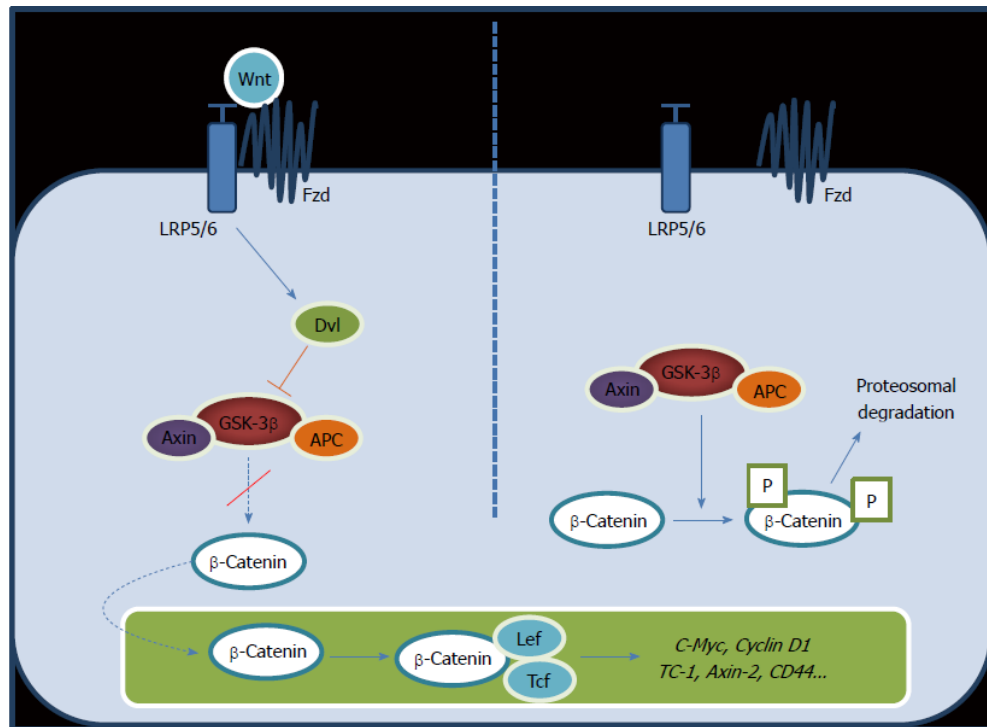
Figure 19 The signaling pathway for Wnt/β-catenin.

Source: Vilchez V, Turcios L, Marti F, Gedaly R. (2016) Targeting Wnt/beta-catenin pathway in hepatocellular carcinoma treatment

Wnt protein binding initiates a cascade resulting in β-catenin activation, cytoplasm accumulation and translocation into the nucleus to enhance target gene transcription (Left); when Fz / LRP receptors are not engaged and GSK3β sequentially phosphorylate β-catenin binding. As a result, β-catenin is ubiquitinated and targeted by the proteasome (right) for rapid destruction[8].

2.4.3 PI3K/AKT/mTOR pathway

The PI3K/AKT/mTOR pathway plays an important role in cell regulation. This pathway is involved in many cellular processes, such as cell division, cell growth, and programmed cell death[135], and can be activated by many different stimuli, such as activated tyrosine kinase growth factor receptors, G-protein-coupled receptors, and

oncogenes such as RAS[136]. The mTOR complex is also an important therapeutic target, as it is a key intracellular node for a number of cellular signaling pathways. Inhibiting mTOR can prevent abnormal cell proliferation, tumor angiogenesis, and abnormal cell metabolism, rationalizing mTOR inhibitors as potential targeting agents[137]. Several studies have shown that selective mTOR inhibition can result in AKT activation, mediated by the receptor pathway of insulin-like growth factor 1[138]. AKT activation can limit mTOR inhibitors' anti-tumor activity leading to resistance. This pathway is activated in a subset of HCC patients and it has been shown that the use of rapalogs inhibits growth in HCC cell lines and experimental models[115].

2.4.4 AMPK pathway

AMPK is a preserved heterotrimeric serine / threonine kinase that plays a key role in linking the development of metabolism and cancer. AMPK is activated when a stressful condition such as low glucose, hypoxia, ischemia, or heat shock increases AMP / ATP activity. Once activated, by regulating the cell cycle, apoptosis, autophagy, and protein synthesis inhibition, AMPK suppresses cell proliferation in tumor and non-tumor cells. There is growing evidence that AMPK levels in different cancers, specifically HCC, are altered[139]. Zheng et al. showed that in most HCC patients AMPK was down-regulated, which correlated with a worse prognosis[139]. Another study by Lee et al. showed that AMPK is a HCC tumor suppressor and its inactivation by destabilizing p53 can lead to hepatocarcinogenesis. These studies show that AMPK plays a role in HCC and that its loss can contribute to HCC's progress[140].

2.4.1 c-MET pathway

The hepatocyte growth factor (HGF)/mesenchymal-epithelial transition factor (MET), a tyrosine kinase receptor, is frequently dysregulated in many malignancies and plays a key role in HCC[141]. It encourages tumor cell growth, survival, migration, invasion, angiogenesis, and metastasis when c-MET is activated[142]. Activating this path can therefore lead to a more aggressive form of HCC and a poor outcome[141]. Aberrant c-MET signaling is seen in HCC and Sorafenib patients, and MET overexpression is associated with poor prognosis[142]. The proto-oncogene c-MET

encodes the ligand Hepatocyte growth factor (HGF) receptor. Binding a ligand to the HGF receptor leads to homodimerization, subsequent downstream residue autophosphorylation, and downstream MAPK and PI3K pathways activation. In the absence of HGF, c-MET phosphorylation may occur through interaction with the epidermal growth factor receptor (EGFR), cell attachment, or alternate ligand des-gamma carboxyprothrombin binding. Regardless of how HGF is activated, this results in c-MET dimerisation, autophosphorylation and kinase activity needed for malignant transformation[143].

3 Hepatocellular carcinoma induction

3.1 Stages of carcinogenesis

Studies carried out using *in vivo*, *in vitro* studies and epidemiological assays enabled researchers to conclude that neoplastic pathogenesis is a complex process that can be divided from an operational point of view into three distinct stages. These are: initiation, promotion and progression[144, 145].
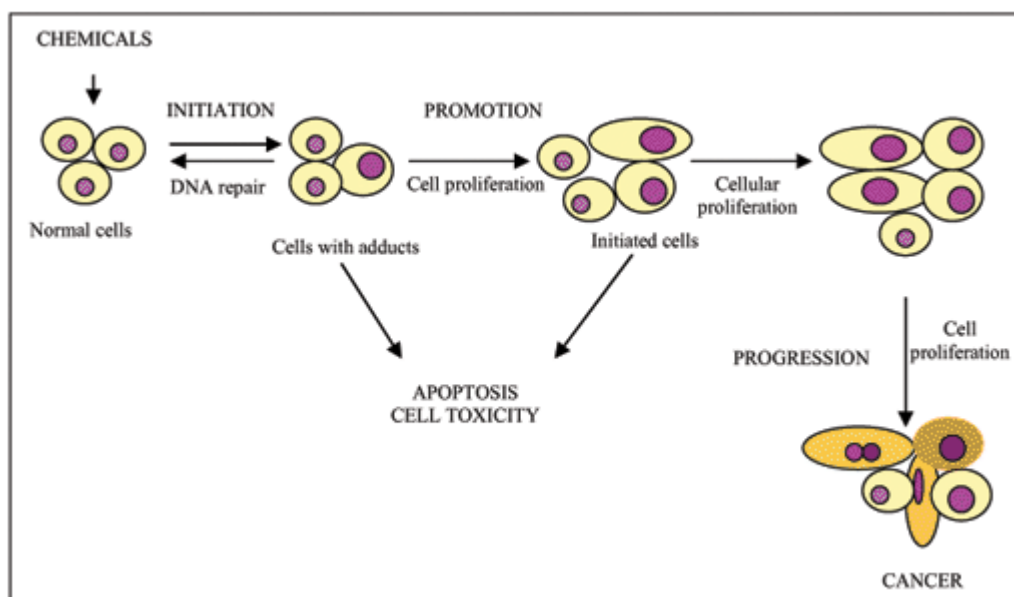
Figure 20 Chemical carcinogenesis stages and the occurrences involved in each one.

Source: Oliveira PA, Colaco A, Chaves R, Guedes-Pinto H, De-La-Cruz PL, Lopes C. (2007) Chemical carcinogenesis

3.1.1 Initiation

Since 1947, initiation has been labeled as the first stage of carcinogenesis. The findings from several experiments made it possible to draw the conclusion that initiation is caused by irreversible genetic changes that predispose susceptible normal cells to malignant evolution and immortality. The initiated cell is not a neoplastic cell but, after successive genotypic and phenotypic changes, has taken its first step towards this state. The initiated cell is similar to the remaining cells from a phenotypic perspective. It is mutated and causes proliferation but not differentiation[146].

The initiated cells may stay latent for weeks, months, or years at this stage, or they may grow autonomously and clonally. This initiation process ensures that by creating two new initiated cells, cell division remains symmetrical. The clonal expansion of initiated cells results from autogenic processes caused by an increase in

the number of new cells and an inhibition of apoptosis that prevents the death of initiated cells[146].

Increasing DNA damage is particularly important for stem cells as they survive for a long time and are found in several tissues. Stem cells are, by definition, immortal cells until they differentiate or induce death. Potter explained in 1978 that neoplastic cells could display a phenotype between the embryonic aspect and terminal differentiation, and that all neoplastic cells had monoclonal origin from a stem cell. They become initiated and accumulate in tissues as clones of abnormal cells if we delay their differentiation. Although stem cells in most tissues are not identifiable, it is believed that each tissue has a stem cell population[147].

Initiation is a phenomenon that is fast and irreversible and is transmitted to daughter cells. For this stage, cell proliferation is essential if cell division takes place before DNA repair systems can act, then the injury becomes permanent and irreversible. Initiation is an additive process, the development of neoplasms depends on the carcinogenic dose, increasing the dose increases the incidence and multiplicity of resulting neoplasms and reduces the latent period of its manifestation. Not all cells of a living organism that are exposed to an initiator agent are initiated even if mutations have occurred, and the genes that regulate terminal differentiation must also be mutated[148].

In all living organisms there are spontaneously initiated cells. Initiation can start with spontaneous mutations, supported by normal events such as depuration and deamination of DNA. Initiation is also associated with errors in DNA replication. Although spontaneous initiation is less common than initiation, the occurrence of spontaneous neoplasia in laboratory animals has confirmed its existence[149].

3.1.2 Promotion

The promotion concept was introduced when chemical substances with low carcinogenic activity were found that could still induce cancer development under experimental conditions[150].

Promoter compounds do not interact directly with biological effects of DNA and unchain without being activated metabolically. These agents increase the

proliferation of cells in susceptible tissues, help fix mutations, enhance changes in genetic expression and cause changes in the control of cell growth. On the other hand, through oxidation, these promoters may indirectly damage DNA. These events were initially linked to epigenetic mechanisms, but it is widely accepted nowadays that promotion also involves genetic changes[151].

Promoters delay the quiescent cells (G0)'s natural inhibition through gap junctions. The most important activity of the promoters is mitogenesis, there is no need for genotoxic and mutational actions at this stage. In order to be effective, the promoter must be present for weeks, months and years, and its effectiveness depends on its target tissue concentration. Promotion is a reversible stage, a regression in cell proliferation may occur after the disappearance of a promoter, possibly through apoptosis. It is a stage that can be shaped by physiological factors, thus limiting the extent of experimental carcinogenesis. Some promoter agents are specific to a specific tissue, but others affect several tissues simultaneously[152].

Even without the previous application of initiator agents, exposure to phenobarbital, benzene, asbestos, and arsenic leads to neoplastic development. Not all cells exposed to promoters are involved in the promotion stage, only cells stimulated to divide, undifferentiated and survived apoptosis can contribute to instability between growth and cell death and lead to malignant neoplasia[146].

3.1.3 Progression

The lesion sequence identified between initiation and promotion through histopathology is referred to as preneoplastic lesions and/or benign neoplasia. Their transformation into malignant lesions is the final stage of carcinogenesis and the most widespread-it is progression labeled. In progression, genetic and epigenetic mechanisms acquire a neoplastic phenotype. Cell proliferation is independent of stimulation during progression[153].

Previous study, HCC was induced by injection of diethylnitrosamine (DEN) i.p. 200 mg/kg as a single dose, and after 2 weeks, the mice were given i.p. injection of thioacetamide (TAA) 100 mg/kg twice per week for 4 weeks[154].

3.2 Diethylnitrosamine or N-nitrosodiethylamine (DEN)

N-nitrosodiethylamine (DEN) is often used as a carcinogenic reagent. The target organ in which DEN induces malignant tumors is species specific. Mice mainly develop not only liver tumors, but also gastrointestinal[155], skin, respiratory[156] and haematopoietic tumors[157]. The carcinogenic capacity of DEN is situated in its capability of alkylating DNA structures. In the first step, DEN is hydroxylated to α-hydroxylnitrosamine [158]. This step of bioactivation is oxygen-and NADPH-dependent and is mediated by cytochrome P450, an enzyme with its highest activity in the hepatocytes of the central lobe. An electrophilic ethyldiazonium ion is formed after acetaldehyde cleavage. By reacting with nucleophiles such as DNA-bases, this ethyldiazonium ion causes DNA damage. DEN operates on a dose-dependent basis[159]; a single low initiation dose does not lead to the formation of neoplasms, administration of a high dose induces HCC after a period of latency. Several DNA-repair mechanisms, such as nonhomologous end joining, recombinational repair, basic excision repair and much more, prevent DNA-adduct mutagency when DEN is given in a single low dose[160].

Furthermore, oxidative stress caused by DEN can contribute to hepatocarcinogenesis[161]. By forming hydrogen peroxide and superoxide anions, reactive oxygen species (ROS) generated by the P450-dependent enzymatic system may induce oxidative stress. ROS production is known to cause damage to DNA, proteins and lipids; therefore, oxidative stress can play a significant role in cancer[162].

Mouse tumors induced by DEN is due to activating mutations in the H-ras proto-oncogene[163]. These mutations are rarely seen in humans and are correlated with metastasis and poor prognosis[164]. However, as a relatively frequent event in hepatocarcinogenesis, Ras-activation that does not involve ras-oncogene mutations also occured[165]. Genetically, the DEN-model proves to be a good representation of HCC associated with poor prognosis[166].

The time required to develop HCC after a single DEN-injection depends not only on the dose given, but also on mice's sex, age and strain[167]. The younger the mice,

the faster the HCC due to the high rates of proliferation of juvenile animals[168]. HCC develops in 100 percent of male mice and 30 percent of females after a long-term repetitive administration of DEN. The gender difference in HCC incidence is due to the estrogen inhibitory effect and the stimulating effect of androgens on hepatocarcinogenesis[169]. One of the genetic factors that differs between tumor-sensitive and tumor-resistant strains may be the methylation status of certain genes that contribute to the susceptibility to hepatocarcinogens[170]. Tumor-sensitive mice, such as C3H / HE-strain, are characterized by hypermethylation in promoter regions of tumor suppressor gene after hepatocarcinogen exposure[171].

A dose-dependent formation of carcinoma after a single injection (5-90 mg/kg) of DEN in 15-day-old mice is observed after 45-104 weeks[172]. When B6C3F1 mice are exposed to a single dose of 5.0 mg/kg DEN, it takes approximately 64 weeks to develop HCC[173]. HCC occurs either within existing adenomas visible after 24 weeks, or within the hepatocellular parenchyma. Metastasis to the lungs happens quite fast after HCC develops[174]. The time and percentage of tumor development differ between strains, for example sv129[160, 172] (20 mg/kg DEN, 80-100% HCC after 30-55 weeks), C3H/HE[175] (90 mg/kg DEN, 100% HCC after 45-75 weeks), C57BL6/J[176] (5 mg/kg DEN, 84% HCC after 40-70 weeks). When adult mice undergo short weekly DEN administration, it results in a higher incidence of tumor in a shorter span of time. Six weeks of intraperitoneal injections (3 weeks of 75 mg/kg followed by 3 weeks of 100 mg/kg) result in 100% tumor incidence after 52 weeks and the first tumors begin to occur in male mice after 30 weeks[177]. Long-term, weekly administration of 35 mg/kg DEN to mice leads to HCC after 20-35 weeks[178].

A two-stage model where a promotional phase follows the initiation by a genotoxic compound is often used to induce HCC. DEN can be used as an initiator and phenobarbital (PB) as a promoter. The tumor-promoting effect of PB may be responsible for several mechanisms. First, PB can increase cytochrome P450 a 100-fold expression, leading to increased DEN effect[179]. Second, the increased cytochrome P450 activity induces oxidative stress[180]. Third, PB can cause hypermethylation in promoter regions

of tumor suppressor genes, therefore, enhancing hepatocarcinogenesis[181]. Fourth, PB also interferes with the intracellular communication and might influence cell proliferation. Promotion with PB leads to tumors with mutations in the β-catenin proto-oncogene[182].

Also, the effects of PB promotion on DEN-initiated mice vary greatly depending on the mice's strain, sex and age. While PB tumor activity is generally accepted, a tumor-inhibiting effect is seen when juvenile (15-day-old) B6C3F1 mice are treated with DEN followed by long-term (36-week) PB exposure[183]. The inhibitory effect is not seen in juvenile female B6C3F1 mice[185]. Or other mice strains, such as Balb/c[184] and C3H[185], initiated with DEN promoted with PB.

3.3 Thioacetamide (TAA)

3.3.1 TAA mechanism

In general, metabolism of TAA occurs by following pathway in Figure 21. TAA has been used extensively in the development of suitable animal models of acute and chronic liver injury. It is a model hepatotoxicant due to its effects on protein synthesis, RNA, DNA and gamma-glutamyl transpeptidase activity. Prolonged this compound directs to macro liver nodules, liver cell adenomas, cholangiomas and hepatocarcinomas, histologically similar to that caused due to viral hepatitis infection (Figure 21)[186].
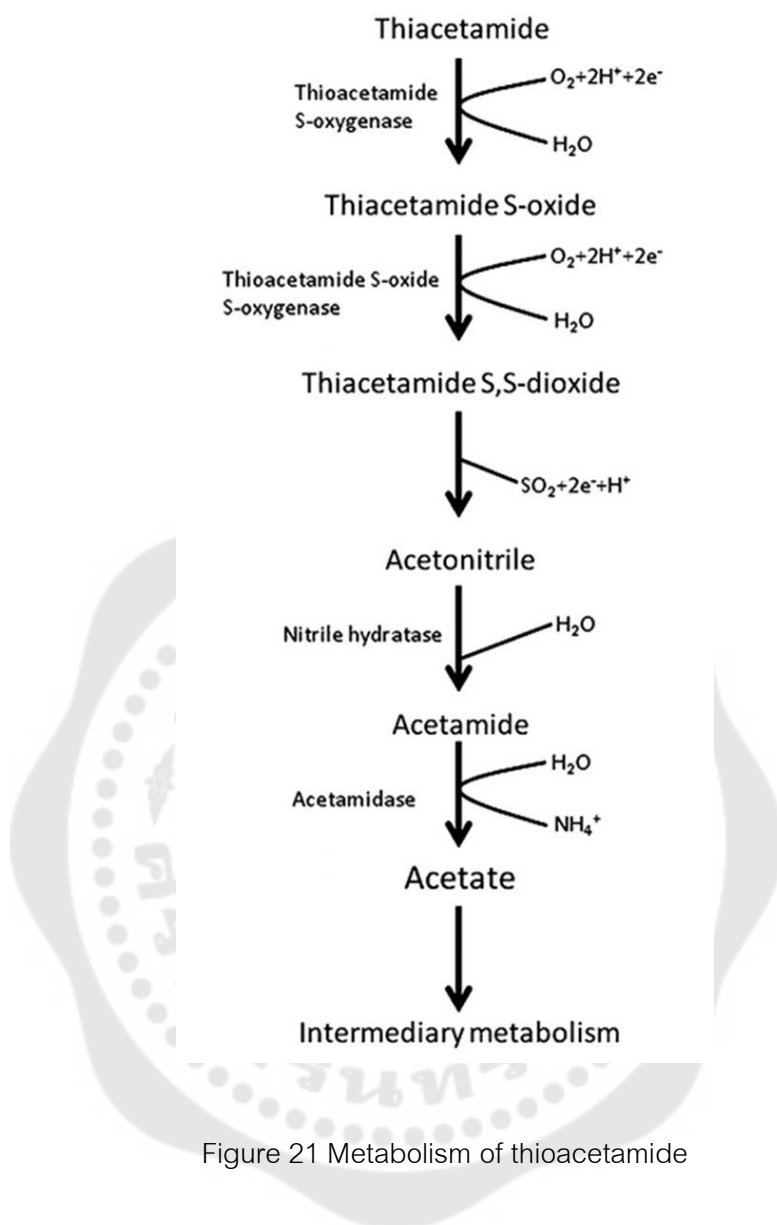
Figure 21 Metabolism of thioacetamide

Source: Akhtar T and Sheikh N. (2013) An overview of thioacetamide-induced hepatotoxicity

3.3.2 Bioactivation of TAA

Cellular enzymes, including the cytochrome P450 (CYP) system, mediate the biotransformation of chemical toxicants and carcinogens. CYP is an enzyme containing heme that catalyzes the oxidation of a wide variety of endogenous and exogenous compounds, including drugs, carcinogenic substances and other

xenobiotics. Sulfine (sulfoxide) and sulfene (sulfone) metabolites are generally considered to be bioactivated by CYP systems[187, 188]. TAA undergoes a two-step bioactivation interceded with sulfine by microsomal CYP2E1 and subsequently active metabolite to sulfene. The CYP450 system in rat liver is believed to be responsible for the TAA metabolism. TAA is biotransformed or metabolized by monooxygenase (FMO) and CYP450 flavin-containing systems. CYP450 enzymes are present in the liver microsomes that convert TAA to thioacetamide S-oxide (TAASO), a toxic reactive intermediate; and due to the oxidation process, it induces oxidative stress in the hepatic cells that ultimately leads to central-lobular necrosis and hepatic injury (Figure 22)[186].
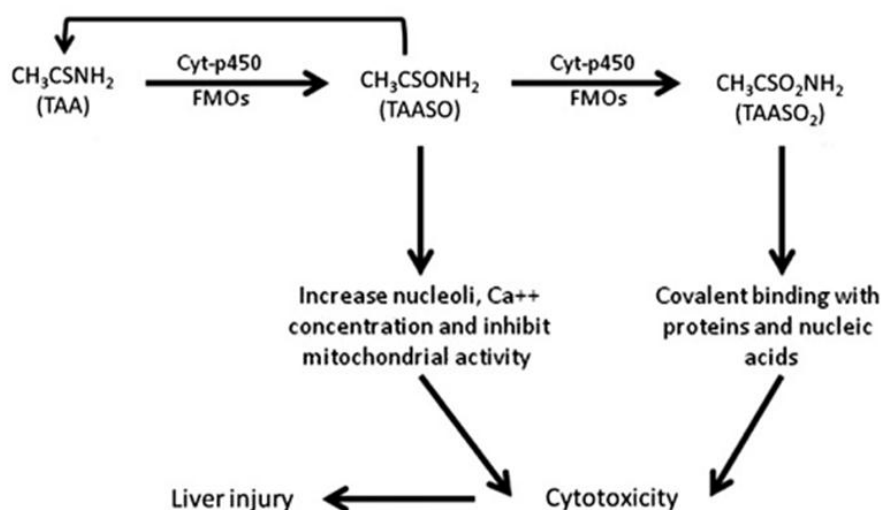
Figure 22 The mode of action of TAA during liver injury.

Source: Akhtar T and Sheikh N. (2013) An overview of thioacetamide-induced hepatotoxicity

The kinetics of a two-step bioactivation where both steps are catalyzed by the similar combination of enzymes involve that as the concentration of the initial substrate increases, it will compete with the intermediate metabolite (TAASO) for the second oxidation and thereby inhibit the formation of the ultimate reactive metabolite TAASO$_2$[186].

TAA's hepatotoxic effects are expressed only after metabolic conversion to thioacetamide S-oxide, which undergoes further metabolic conversion to an unidentified metabolite, possibly the unstable reactive thioacetamide sulfone. Since much of the TAA bioactivation mechanism and toxicity work was carried out largely before the discovery of CYP450 isozymes was discovered, information on specific isozymes involved in TAA bioactivation remained completely blurred and uninvestigated, previous studies showed that TAA bioactivation is primarily mediated by hepatic CYP2E1[187]. TAA and its initial metabolite thioacetamide S-oxide (TASO) give rats a range of hepatotoxic responses depending on the dose and duration of administration. TAA is a powerful inhibitor of TASO's oxidation to its reactive TASO metabolite S,S-dioxide. TAA and TASO in vivo metabolism leads to the formation of acetamide derivatives on the side chains of protein lysine. TASO metabolism results in extensive modification of both the protein lysine side chains and the amine groups of phosphatidylethanolamine lipids in isolated hepatocytes[189].

3.3.3 Cellular dysfunction caused by TAA

TAASO is responsible for nuclei enlargement, increased nuclear volume, increased intracellular Ca2+, concentration, cell permeability change, and inhibition of mitochondrial activity. TAASO2 is available in two tautomeric forms and reacts by changing lycin side chains with proteins. TAASO2 is responsible for releasing synthase of nitric oxide (iNOS), which leads to necrosis of the central lobbies. TAASO2 denatures proteins by modifying their load. It forms derivatives of acetylimidolysine after protein reaction. Several protein systems, including those involved in mitochondrial respiration, those in the endoplasmic reticulum, and stress response proteins such as heat shock proteins, gave an idea of being harmed. Due to lipid peroxidation, TAA-generated free radicals can injure various cells. It alters lipoprotein metabolism through the synthesis of long-chain polyunsaturated fatty acids and the lipid properties of hepatocyte lysosomes and leads to sphingomyelin accumulation in the endoplasmic reticulum. It also impairs the urea cycle and ornithine activity, leading to severe changes in the amino acid profile of the serum[190].

3.3.4 Experimental hepatotoxicity of TAA

The experimental hepatotoxicity of TAA in rodents was first studied in 1948. More recently, the in *vivo* use of TAA in rodents as a model hepatotoxin produced highly selective liver damage including fibrosis, cirrhosis and hepatic necrosis or apoptosis[191]. TAA requires metabolic activation to elicit its toxicity. Activation of TAA occurs via two oxidations, leading first to its S-oxide (TASO) and then to its chemically reactive S,S-dioxide (TASO$_2$). The latter, which can potentially exist in two tautomeric forms, then reacts with proteins by modifying lysine side chains. This presumably leads to impairment of function and cytotoxicity. The oxidation of TAA and TASO can be carried out by hepatic cytochrome P450 enzymes[191]. On the other hand, metabolic activation of TAA leads to the formation of reactive metabolites represented by thioacetamide-S-oxide-derived radicals and intermediate-generated reactive oxygen species (ROS). Administering TAA to rodents simultaneously resulted in cell death through apoptosis and necrosis. Lipid peroxidation followed the production of ROS resulting from TAA administration[192].

3.3.5 Histopathological variations caused by TAA

The liver sections of Wistar rats received chronic TAA treatment showed hepatic cells with toxicity typified by vascular fibrosis, giant hepatocytes, degenerated hepatic lobular architecture, increased hematopoiesis, low-degree cirrhosis, high infiltration of necrotic cells, occurrence of plasma cells in sinusoidal spaces, especially in the vicinity of necrotic areas, increased sinusoidal infiltration. Inflammation is a feature of liver toxicity that is characteristic and usually prominent. Kupffer cells are loaded with pigment by hepatocellular debris phagocytosis through hyperplasia and hypertrophy. Portal tracts usually infiltrate a mixture of inflammatory cells, causing apoptosis of periportal hepatocytes. Chronic liver injury histological characteristics range from extremely modest to rigorous. In the modest forms of TAA liver injury, inflammation consists of macrophages, lymphocytes, sometimes plasma cells, and rare eosinophils or neutrophils, and is limited to portal tracts. Liver architecture is generally well

preserved, but in all forms of liver injury, smoldering hepatocyte apoptosis can occur throughout the lobule[186].

    In chronic liver injury, necrosis is also a very prominent feature. Swelling occurs as a result of water, fat and protein accumulation. Almost always, chronic liver injury is accompanied by prominent activation of sinusoidal stellate cells and portal tract fibroblasts, resulting in fibrosis. Fibrosis is most commonly sinusoidal and perivenular, separating parenchymal cells; periportal fibrosis may occasionally predominate. Persistent loss of hepatocytes and fibrosis resulted in cirrhosis under prolonged chronic conditions. Usually, the ultimate and permanent type of liver disorder develops slowly and insidiously. Delicate fibrous septa develops and expands from central regions to portals. The activity of parenchymal hepatocytes generates uniform micronodules. With the passage of time, the liver surface shows an appearance of " hobnail " created by large scattered nodules. As fibrous septa divides the nodules and encircles them, the liver becomes extra fibrotic, loses fat, and gradually minimizes its size. Fibrous tissue with wider bands encompassing parenchymal islands; in addition, the liver is transformed into a mixed micronodular and macronodular pattern. Finally, fibrous nodular obliteration and ischemic necrosis make a wide stretch of hard, pale scar tissue. Bile stasis often develops; at this stage, mallory bodies are rarely apparent[190].

4 Sorafenib

    Sorafenib is currently the only approved treatment for unresectable HCC by the Food and Drug Administration (FDA). Sorafenib is an oral multityrosine kinase and angiogenesis inhibitor with activity against VEGF, PDGFR, c-KIT receptor, BRAF and p38 signaling pathways[142]. For patients with advanced HCC taking Sorafenib, the median time for disease progression is 5.5 months and the median overall survival (OS) time is 10.7 months[85]. In a Phase II study, twice daily Sorafenib was received by 137 patients with inoperable HCC in Belgium, France, Italy, Israel, and the United States. Disease control in 42 percent of patients was reported. The median progression time (TTP) was 5.5 months and the median operating system was 9.2 months[193]. In two large

phase III randomized trials done by Llovet et al. (2008) and Cheng et al. (2012), Sorafenib significantly improved overall survival compared to placebo[85, 194]. In the Asian population, a study conducted by Cheng et al. (2012) showed improvement in median OS (5.9 vs. 4.1 months) and median TTP (2.7 vs. 1.4 months)[194]. In the SHARP study by Llovet et al. (2008), majority of the patients had hepatitis C and alcohol compared to few patients with hepatitis B[85]. In contrast, in the study done by Cheng et al. (2012), 71% and 78% of the patients in the Sorafenib and placebo group were positive for hepatitis B[194]. Though both trials had similar design, the higher rate of hepatitis C in the SHARP compared to hepatitis B in Asian population indicates that these two populations are distinct from each other[85, 194]. Furthermore, Sorafenib has a category 1 recommendation for patients with a Child-Pugh class A and category 2A for those with Child- Pugh class B with a special caution in the latter group specifically the bilirubin level. Presently there is no additional therapy for individuals whose disease progresses on Sorafenib or who have poor tolerance for this drug. Some common side effects seen with the use of Sorafenib are skin rash, hand-foot syndrome, diarrhea, and hypertension[195]

5 Benja-ummarit

Benja-ummarit is Thai traditional medicine dispensatory from Thai scripture called Tadbunjob. It consists of 8 herbs as follow: aloe (*Aloe barbadensis*; Yadum) 2.48%, red physic nut (*Baliospermum montanum*; Thongtak) 9.92%, kaffir lime (*Citrus hystrix*; Makrut) 33.06%, asafoetida (*Ferula assafoetida*; Mahahing) 2.48%, gamboge resin (*Garcinia hanburyi*; Rongthong) 4.96%, Javanese long pepper (*Piper chaba*; Deeplee) 2.48%, black pepper (*Piper nigrum*; Prikthaidum) 2.48%, ginger (*Zingiber officinale*; Khing) 2.48%, and 1 chemical is epsom salt or magnesium sulfate (Deegleuafarang) 39.67%

5.1 *Aloe barbadensis* Miller

A. Vera is one of about 420 Aloe genus species. It is also referred to as the Liliaceae family's *Aloe barbadensis* Miller. *A. Vera* is believed to have originated in Sudan and was subsequently introduced worldwide. It is used in several countries such

as India, China, South Africa, and Japan as a folk medicine. However, due to its ability to increase collagen synthesis, it was first clinically used for the treatment of skin burns and wound healing in 1930. It is used as a laxative due to reduced intestinal water absorption and improved intestinal movement[196]. It is also used as a functional food, particularly in food industry health drinks and beverages, and as an active ingredient in pharmaceutical industry gels, ointments, tablets and capsules. A number of phytochemicals are present in *A. Vera*, including anthraquinones (barbaloin), phytosterols, carbohydrates, chromiums, enzymes, vitamins, amino acids, and proteins[197].

      A. vera is being used for anti-obesity, antidiabetic, anti-inflammatory, immune modulator, antioxidant, and anticancer effects since ancient periods. The possible mechanism of action of *A. vera* on different organs has been depicted in Figure 23. A hypoglycemic (lowering of blood glucose levels) property of *A. vera* is associated with pancreatic insulin synthesis and its secretion[198]. However, phytosterols that are present in the *A.vera* are not extensively absorbed from the intestine, but they can bind to the cholesterol and prevent its absorption to show a hypolipidemic effect (lowering of blood lipid levels)[199]. Ishii et al. (1990) reported that anthraquinones (barbaloin and isobarbaloin) are poorly absorbed in the small intestine and are broken down into active metabolites aloe-emodin-9-anthrone and aloe-emodin in the large intestine[200]. These active metabolites have laxative properties inhibiting Na+/K+ATPase activity to prevent water absorption. Furthermore, aloe-emodin is a powerful urokinase inhibitor (convert plasminogen to active plasmine), whose secretion involves angiogenesis[201]. The polysaccharide (acemannan) of *A. vera* is responsible for the activation of macrophages to secrete cytokines, viz. tumor necrosis factor-alpha (TNF-α), interleukin 1 & 6 (IL-1 & 6) and interferon-γ. The active components present in the *A.vera* showed an anti-inflammatory activity by inhibiting the cyclooxygenase in arachidonic acid pathway[202]. The pancreatic β islets destruction is associated with its DNA damage by free radicals, which further leads to damage of other organs. The low antioxidant effect is associated with the lower levels of glutathione peroxidase and

superoxide dismutase in pancreatic cells[203]. The presence of phenolic and flavanoid compounds in the *A. vera* is responsible for the scavenging of both superoxide and peroxyl radicals, respectively[204]. Phytosterols (lophenol, 24-methyl-lophenol, 24-ethyl-lophenol, cycloartanol, and 24-methylene-cycloartanol) isolated from *A. vera* gel extract (AVGE) showed a significant decrease in the fasting blood glucose and glycated hemoglobin (HbA1C) levels in diabetic mice[205, 206].
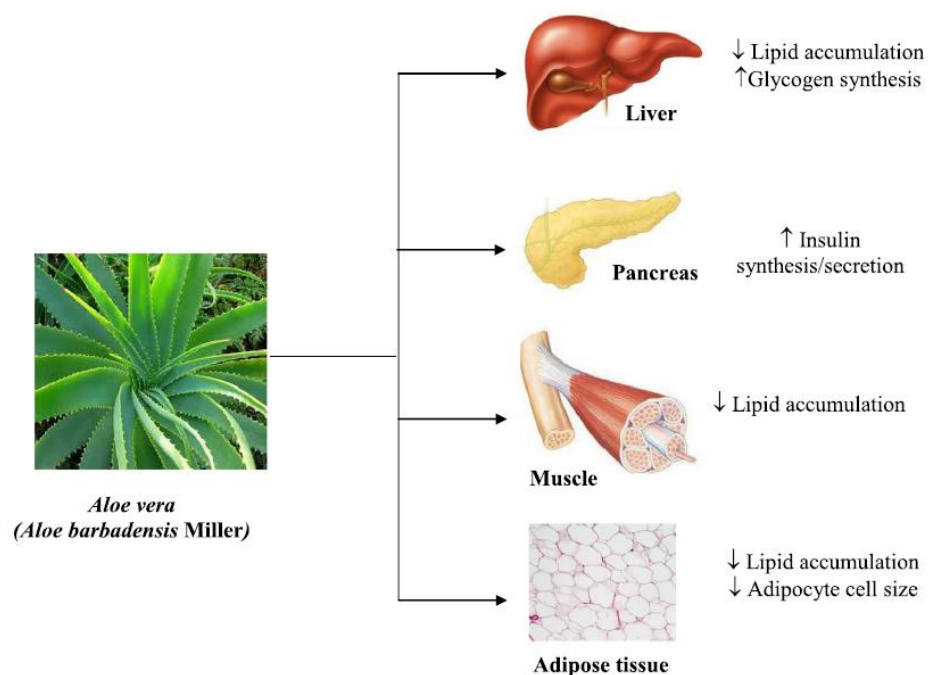
Figure 23 Effect of Aloe vera on different organs in obesity and diabetes management.

Source: Pothuraju R, Sharma RK, Onteru SK, Singh S, Hussain SA. (2016) Hypoglycemic and Hypolipidemic Effects of Aloe vera Extract Preparations

Figure 24 Dry latex from *Aloe barbadensis* Miller

5.2 *Baliospermum montanum*

Baliospermum montanum (Willd.) Muell Arg is a predominant woody medicinal plant categorized in the family Euphorbiaceae and is noted to possess extensively diverse medicinal properties[207]. The various parts of the plant such as the roots, leaves, and seeds are used traditionally for the treatment of different ailments. The roots of *B. montanum* are ascribed to possess anticancer[208], antimicrobial[209], immunomodulatory[210] and antihelmintic[211] properties. Its root is proclaimed to contain axillarenic acid, baliospermin, and montanin which is responsible for all the wide range of activities[212]. Five phorbol esters (montanin, baliospermin, 12-deoxyphorbol-13-palmitate, 12-deoxy-5b-hydroxyphorbol-13-myristate, and 12-deoxy-16-hydroxy phorbol-13-palmitate) were isolated from *B. montanum* roots and was reported for their antitumor activity[208]. Phytochemical analysis of *B. montanum* found compounds such as glycosides, flavonoids, tannins and triterpenoids in aqueous and alcohol extracts of the plant[209]. *B. montanum* was a rich source of flavonoids which also accounted for this plant's antioxidant and anticancer properties[213]. *B. montanum* has been used to treat abdominal tumors since ancient times. The plant's aqueous and alcoholic extracts present an interesting cytotoxic activity on lines of cancer cells in the human colon HT-29. *In vitro* cytotoxic activity against HT-29 cell line was evaluated at different concentrations and the calculated IC50 value was below 50 g/mL, indicating the potential of extracts *Baliospermum montanum* Muell Arg[214]. An aqueous extract of

alcohol from the root of *B. Montanum* had activity with P-388 *in vivo* lymphocytic leukemia[208].

Figure 25 *Baliospermum montanum*

5.3 *Citrus hystrix*

Citrus hystrix (*C. hystrix*), kaffir lime, contains abundant naringenin and hesperidin, considered to be flavonoid compounds[215]. A study reported that the highest extraction yield was obtained from peels among parts of the plant[216]. Numerous researchers have examined antioxidant activity and free radicals scavenging properties of naringenin and hesperidin using different assay systems[217]. Naringenin may increase the ratio of CD4+/CD8+ to T cells responsible for the immune system[218], whereas hesperidin may improve the innate and adaptive immune system[219], and cardioprotective effect on doxorubicin-induced rats[18].

Figure 26 *Citrus hystrix*

5.4 *Ferula assafoetida*

Asafoetida (*Ferula assafoetida*) is a member of the family Apiaceae and was used in traditional medicine [220]. This medicinal plant is made up of three major fractions, including resin (40-64 %), gum (25 %) and essential oil (10-17%)[221]. The fraction of resin contains ferulic acid and its esters, coumarins, coumarins of sesquiterpene and other terpenoids. The gum contains glucose, galactose, L-arabinose, rhamnose, glucuronic acid, polysaccharides and glycoproteins, and the volatile fraction contains compounds containing sulfur, monoterpenes and other volatile terpenoids[222]. Recent Ferula pharmacological and biological studies have shown several activities including: antioxidant, antifungal, antiviral, antidiabetic, antispasmodic, cancer chemopreventive and hypotensive [223-226]. Sprague Dawley rat studies revealed that Ferula significantly increased the activity and detoxification of antioxidant enzymes in the liver and protects rats from toxins[227].
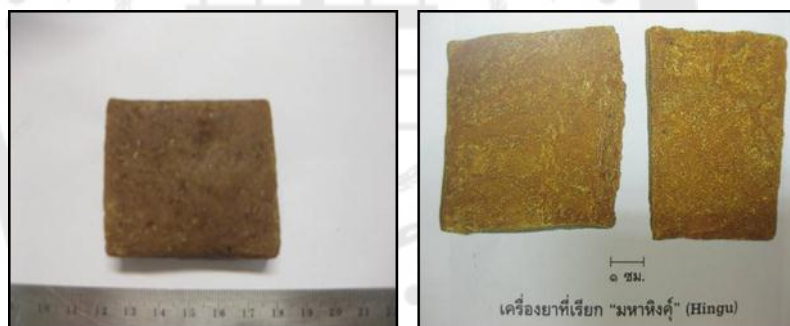
Figure 27 *Ferula assafoetida*

5.5 *Garcinia Hanburyi*

Garcinia hanburyi Hook. f., a plant belonging to the Guttiferae family, is a small tree distributed throughout Thailand, Cambodia, India, and the southern part of China. It was developed for clinical testing in the 1970s as an anti-tumor drug through intravenous injection in China[228]. It had been developed in the 1970s as an anti-tumor drug via intravenous injection in China for clinical testing[229]. Gambogic acid (GA), a

caged polyprenylated xanthone, is a natural product isolated from Garcinia hanburyi trees resin in south-east Asia[230]. Recent studies from several labs have shown that this natural product has a powerful *in vitro* and *in vivo* anti-cancer activity[15, 231]. The potent anticancer activity of GA is mainly attributed to its activation of the impaired apoptosis pathways in cancerous cells via down-regulation of telomerase[232]. In addition, GA is a potent angiogenesis inhibitor that inhibits angiogenesis by suppressing the endothelial vascular growth factor (VEGF)-induced tyrosine phosphorylation of KDR/Flk-1 and GA showed *in vitro* and *in vivo* anti -angiogenesis activity[15, 17]. GA inhibited the proliferation of cells not only by suppressing hTERT transcription activity but also by post-translational modification of hTERT[233].). GA had potent cytotoxicity to various cancers of humans such as hepatoma[232], gastric carcinoma[234] and lung cancer[231].

Figure 28 Gamboge resin from *Garcinia Hanburyi*

5.6 *Piper chaba*

Piper chaba HUNTER (syn. *P. retrofractum* VAHL., Piperaceae) is distributed widely in Southeast Asia. In Thailand, the fruit of this plant is called "Dee Plee" and has a wide range of applications in traditional medicine, for example, as an anti-flatulent, expectorant, antitussive, antifungal, uterus-contracting agent, sedative-hypnotic, appetizer, and counterirritant [235]. The aqueous acetone extract and isolates were found to have a range of protective effects: they decreased the rate of ethanol-or indomethacin-induced gastric lesions in rats; they inhibited increased levels of serum aspartate aminotransaminase (AST) and serum alanine aminotransaminase (ALT)

induced by D-galactosamine (D-GalN)/lipopolysaccharide (LPS) induced liver injury in mice; and they decreased levels of D-galactosamine (D-GalN)/lipopolysaccharide (LPS) induced liver injury in mice and they reduced the rate of cell death in primary cultured mouse hepatocytes induced by D-GalN/tumor necrosis factor-**α** (TNF-**α**)[236-238].

Figure 29 *Piper chaba*

5.7 *Piper nigrum*

In folk medicine, *P. nigrum* is widely used. *P. nigrum* may not only be used to relieve symptoms of the digestive system, such as diarrhea and indigestion, but also to treat problems with the respiratory system, such as colds, fevers and asthma[239]. Black pepper, long pepper and ginger in traditional Indian medicine are "Trikatu" ingredients used to control respiratory and digestive system diseases[240] as well as tumors[241].

Black pepper's anti-cancer bioactivities were due to wide bioactivity spectrum. The anti-cancer bioactivities of pure *P. nigrum* compounds, especially piperine, have been investigated by many modern research. In lung cancer, piperine had an anti-cancer property[242]. Pipernonaline inhibits the growth of PC3 cells in prostate cancer lines and induces cell apoptosis associated with ROS[243]. Purpurogallin suppresses angiogenesis and metastasis of tumor cells[244]. Research focusing on crude extracts of *P. nigrum*, however, has been limited, exhibiting multiple bioactivities including anti-inflammatory, anti-tumor, and selective tumor cell killing[245]. *P. nigrum* (PFPE) crude extract exhibited a strong effect on the cell line of breast cancer (MCF-7).

IC_{50} PFPE was 7.45 mg / ml for MCF-7 cells with higher cytotoxic activity than piperine and pellitorine[246].

Figure 30 *Piper nigrum*

Source: www.Thaicrudedrug.com

5.8 *Zingiber officinale*

Zingiber officinale Roscoe (Zingiberaceae), commonly referred to as ginger, is native to tropical Asia, primarily southern China and India. The plant's rhizome has a wide variety of prophylactic and therapeutic properties[247]. Recently, 6-shogaol has been reported to have pharmacological effects including the properties of anti-cancer, anti-inflammatory and antioxidant[248]. Previous studies reported apoptosis induced by 6-shogaol in hepatocellular carcinoma[249], colorectal carcinoma[250], leukemia[251], and non-small cell lung cancer cells[252]. Molecular mechanisms underlying the anti-cancer effects of 6-shogaol can be associated with activation of caspase[250, 251, 253] and the inhibition of Akt signaling pathway[252]. In addition, previous studies have reported that gingerol has increased the apoptosis induced by tumor necrosis factor-related apoptosis-inducing ligand (TRAIL) in gastric cancer cells[254], and that 6-shogaol has been found to be more potent anti-inflammatory and anti-tumor agent compared to 6-gingerol[250].

Figure 31 *Zingiber officinale*

5.9 Magnesium sulphate

Magnesium sulfate ($MgSO_4$) is the main course of treatment for patients with severe symptoms with preeclampsia and is often used to prevent the disease from preeclampsia to eclampsia from progressing. Preeclampsia complicates about 5-8% of pregnancies in the United States[255] and nearly 20% of pregnancies in African American[256]. Preeclampsia is characterized by new-onset proteinuric hypertension, low platelet count, renal insufficiency, impaired liver function, pulmonary edema, or cerebral or visual symptoms after 20 weeks of gestation[257]. Preeclampsia affects several organs including the kidney, liver, and brain. It should be noted that cerebrovascular events are the cause of all deaths associated with preeclampsia/eclampsia in 40% of cases[258].

Although in recent years the analgesic effect of magnesium sulfate (MS) has been extensively studied, it remains to elucidate its prognostic effect. Studies have shown that systemic MS in both somatic and visceral inflammatory pain exerted antihyperalgesia/ antinociception[259, 260].

The magnesium ion is involved in various cellular processes, including metabolic pathway regulation, signal transduction, cell proliferation, differentiation, apoptosis, and angiogenesis[261-263].

Figure 32 Magnesium sulphate

CHAPTER 3

MATERIALS AND METHODS

1 Chemicals, antibodies and Benja-ummarit preparation

1.1 Chemicals

Diethylnitrosamine (DEN), thioacetamide (TAA), hematoxylin-eosin stain, and the lipid peroxidation (MDA) assay kit were purchased from Sigma-Aldrich (St. Louis, Mo). The Benja-ummarit extract was obtained from Assoc.Prof. Arunporn Itharat, Department of Applied Thai Traditional Medicine, Faculty of Medicine, Thammasat University, Thailand. Protein Assay Dye Reagent Concentrate, Clarity™ western ECL Subsrate, the high capacity cDNA reverse transcriptase Kit, and the SsoAdvanced™ SYBR® Green gene assay were purchased from Bio-Rad (Hercules, CA). TRIzol reagent was purchased from Invitrogen (Carlsbad, CA, USA). Diethylpyrocarbonate (DEPC)-treated water was purchased from Applied Biosystems (Foster City, CA, USA). All other chemicals used in this study were analytical grade and obtained from Sigma-Aldrich (St. Louis, MO, USA) or Lab-Scan Analytical Science (Dublin, Ireland).

1.2 Antibodies

Mouse monoclonal antibodies against VEGF, β-catenin, and cyclin D1 were purchased from Santa Cruz Biotech (Santa Cruz, CA, USA). Mouse monoclonal antibody against actin was purchased from Millipore (Billerica, MA, USA). Horseradish peroxidase (HRP)-conjugated horse anti-mouse IgG antibody was purchased from Cell Signaling Technology (Danvers, MA, USA). The alkaline phosphatase-conjugated goat anti-mouse IgG antibody and normal goat serum were purchased from Sigma-Aldrich.

1.3 Benja-ummarit preparation

Each components of Benja-ummarit as show in Table 2 were cleaned, sliced slab, dried in a hot air oven at 50°C and made to be powder. These powders were weighted and mixed according to Benja-ummarit dispensatory formula. Dried component materials 300 g were macerated by 95% ethanol for 3 days, filtered through a Whatman No.1 filter paper and concentrated using an evaporator.

Table 2 The components of Benja-ummamrit dispensatory

Scientific name	Thai name	Part	Percentage
Aloe barbadensis	Ya-dum	latex	2.48
Baliospermum montanum	Thong-tak	root	9.92
Citrus hystrix	Ma-krut	peel	33.06
Ferula assafoetida	Ma-ha-hing	resin	2.48
Garcinia hanburyi	Rong-thong	latex	4.96
Piper chaba	Dee-plee	fruit	2.48
Piper nigrum	Prik-thai-dum	fruit	2.48
Zingiber officinale	Khing	rhizome	2.48
Magnesium sulfate	Dee-gleua-fa-rang	-	39.67

2 Experimental animals

Male Wistar rats weighing 200-250 g were obtained from the National Laboratory Animal Center, Mahidol University. They were housed individually in stainless-steel wire cages in a temperature and humidity controlled room with a 12h:12h light-dark cycle. The animals were supplied water and food *ad libitum*. They were acclimatized for 1 week before the experiment started. All procedures involving animals were followed and approved by the Animal Ethics Committee of the Faculty of Medicine, Srinakharinwirot University (Number 3/2558).

3 Experimental designs

After acclimatization, the rats were randomly divided into eight groups of seven animals each (Figure 33).
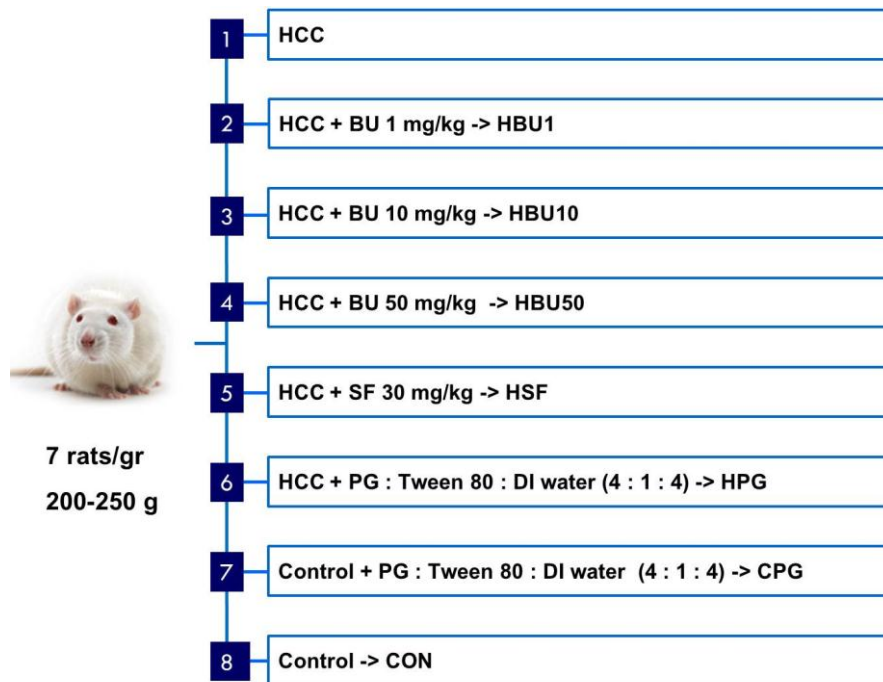
Figure 33 Diagram illustrating the experimental group:

HCC, TAA-induced hepatocellular carcinoma; BU, Benja-ummarit; SF, Sorafenib; PG, propylene glycol. In order to induce HCC in rat models, single dose of 200 mg/kg of diethylnitrosamine (DEN) was administered intraperitoneally. Two weeks later the rat was subjected to intraperitoneal injection of 300 mg/kg of thioacetamide (TAA) thrice weekly for 4 consecutive weeks (Figure 34).
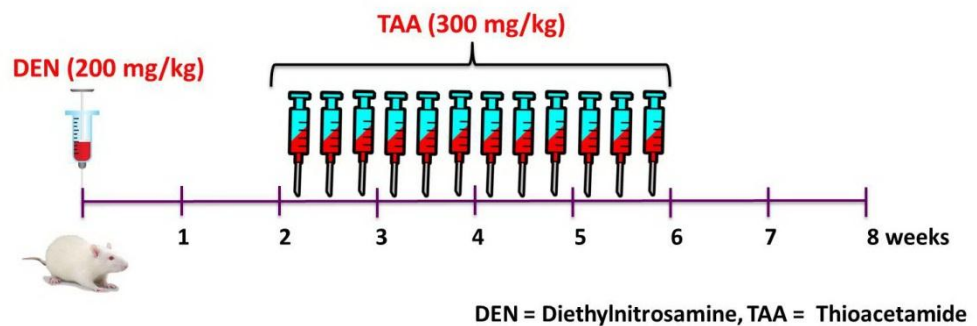
Figure 34 Diagram illustrating the HCC induction

After the completion of the TAA treatment regimen, the HCC rats were divided into 6 groups; 1 received no further treatment; group 2 was treated with 1 mg/kg Benja-ummarit extract; group 3 was treated with 10 mg/kg Benja-ummarit extract; group 4 was treated with 50 mg/kg Benja-ummarit extract; group 5 was treated with 30 mg/kg Sorafenib, a multikinase inhibitor used to treat human HCC; group 6, finally, was treated with a solvent mixture of propylene glycol : Tween80 : distilled water (4:1:4 (v/v)). In addition, two groups of control rats were treated with the solvent mixture or not treated at all. Treatments in all groups were administered orally on a daily basis for consecutive 8 weeks.

After sacrifice under nembutal anesthesia, blood samples were collected via cardiac punture. Liver tissue samples were collected for histological analysis or stored a -80°C for Western blot analysis, lipid peroxidation (MDA), and mRNA quantification with real-time quantitative PCR.

4 Methods

4.1 Gross examination of the liver

The liver of rats was isolated, dissected, and then rinsed in phosphate buffered saline (PBS). Gross examination checked for visible abnormalities of the organs and photographs were taken. Furthermore, body and liver weight were determined. The liver indices were calculated as the percentage of the body weight.

4.2 Liver function tests

Aspartate aminotransferase (AST), alanine aminotransferase (ALT), alkaline phosphatase (ALP), and albumin levels were measured in serum samples.

4.3 Histopathological analysis.

4.3.1 Tissue preparation

The liver specimens were immediately removed and rinsed in PBS. Five pieces were excised: 3 pieces from the left lateral lobe, 1 piece from the left medial lobe and 1 piece from right medial lobe. All samples fixed in 4% paraformaldehyde at 4°C

and then dehydrated in a graded series of alcohol. The specimens were then embedded in paraffin blocks.

4.3.2 Histopathological analysis

The paraffin blocks were sectioned at 5-7 micron thickness. The sections were deparaffinized in xylene and hydrated in a graded series of alcohol. The sections were stained with hematoxylin and eosin covered with Permount® and observed under a light microscope (Olympus, Tokyo, Japan). The slides were scanned with a panoramic digital slide scanner. We randomly selected an area of 4000 x 2500 μm^2 to locate the cancer area with the case viewer program. We calculated the size of the cancer area and the relative size of its surface (as a fraction of the total area analyzed). To eliminate bias, a blind evaluation was performed by three specialists in liver histopathology using the following criteria to determine the the boundaries of the carcinomatous area (Figure 35)
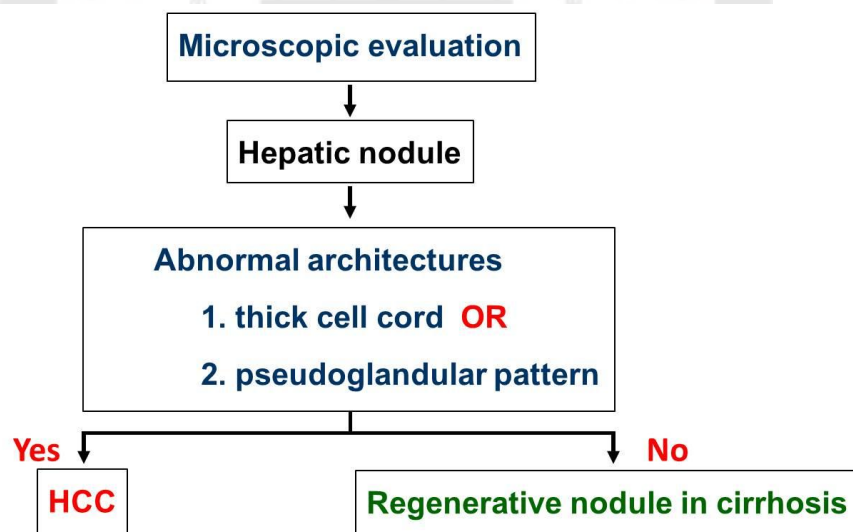
Figure 35 Diagram illustrating the assessment criteria for the boundaries of the cancer area

4.3.3 Immunohistochemical staining

Paraffin sections were mounted on poly-L-lysine coated glass slides. Specimens were deparaffinized and rehydrated in a graded series of ethanol. After washing, specimens were processed for antigen retrieval by boiling in 10 mmol/L sodium citrate buffer (pH 6.0) for 10 minutes at 120°C. After cooling down at room temperature and washing in PBS, the specimens were incubated in TENG-T with 10% normal goat serum for 30 minutes in a humidified box. The samples were then incubated with mouse anti-VEGF monoclonal antibody (diluted 1:50) overnight at room temperature in the humidified box. Subsequently washed in PBS, and further incubated in alkaline phosphatase-conjugated goat anti-mouse IgG (diluted 1:100) for 2 hours at room temperature. Then the samples were washed again in PBS and incubated in substrate (NTM+NBT/BCIP) for 30 minutes to 2 hours to visualize the immunopositive regions in the tissue. After stopping the development of stain with double distilled water, the sections were dehydrated quickly in a graded series of ethanol, cleared in xylene and covered with Permount® before being examined and photographed under a light microscope (Olympus, Tokyo, Japan).

4.4 Malondialdehyde (MDA) assay

After sacrifice, the liver was immediately removed and stored at -80°C until use. Liver samples of ∼10 mg were homogenized with MDA lysis buffer and centrifuged at 3500 rpm for 10 minutes at 4°C. The supernatant was collected for estimation of lipid peroxidation products and MDA content with a thiobarbituric acid (TBA). The absorbance of the supernatant was measured at 532 nm.

4.5 Western blot analysis

After sacrifice, the liver was immediately removed and stored at -80°C. Liver samples of ∼50 mg were homogenized in RIPA lysis buffer (50 mM Tris-HCl pH 7.4, 150 mM NaCl, 1 mM EDTA, 1% Triton X-100, 1% sodium deoxycholate, 0.1% sodium dodecylsulfate and 1% protease inhibitor) and then centrifuged at 12,000 rpm for 15 minutes at 4°C. The supernatants were used for Western blot analysis. The concentration of protein was determined with the Bradford method, using bovine serum

albumin as protein standard. The samples were denatured in sample buffer (62.5 mM Tris-HCl pH 6.8, 2% SDS, 10% glycerol, 2% mercaptoethanol and 0.01% bromophenol blue) at 95°C for 5 minutes. Protein samples were size-separated in 12% SDS-PAGE gels and the resolved proteins were transferred electrophoretically onto a polyvinylidene difluoride (PVDF) membrane. The transfer efficiency was checked by Ponceau-S red staining of the membranes. The membranes were washed with Phosphate-buffered saline (PBS) for 5 minutes, incubated in blocking buffer (5% BSA in PBS containing 0.1% Tween-20 (PBST) for 1 hour at room temperature before mouse anti-VEGF (diluted 1:1,000 in PBST), rabbit anti-β-catenin (diluted 1:1,000 in PBST), rabbit anti-cyclin D1 (diluted 1:1,000 in PBST), or mouse anti-actin (diluted 1:5,000 in PBST). All primary antibodies were incubated at 4°C overnight. After washing with PBST (3X), the membranes were incubated in horse-reddish peroxidase(HRP)-conjugated anti-mouse IgG antibodies (diluted 1:10,000 in PBST) for VEGF and actin, and HRP-conjugated anti-rabbit IgG antibodies (diluted 1:10,000 in PBST) for β-catenin and cyclin D1 at room temperature for 1.5 hours, followed by washing in PBST. Finally, the proteins were visualized by enhanced chemiluminescence using ECL Plus™ Western blotting detection reagents and were exposed on Hyperfilm ECL. The immunoblot bands were quantified by measuring the density of each band using the densitometry program of Scion image (National Institutes of Health, Bethesda, MD).

4.6 Real-time quantitative PCR

The real-time qPCR was performed in the CFX96 Real-time PCR Detection System (Bio-Rad, Hercules, CA, USA) by SsoAdvanced™ SYBR® Green Gene Expression Assays and PrimePCR™ SYBR® Green gene assay which is a primer set design for the detection and quantitation of rat VEGF (*Vegfa*), β-catenin (*Ctnnb1*) and cyclin D1 (*Ccnd1*) genes in RNA samples converted to cDNA. Assay of rat β-actin (*Actb*) gene was performed as an endogenous control for relative quantification study.

4.6.1 RNA extraction

Total RNA was extracted from frozen rat liver (20 mg) using the TRIzol reagent. Briefly, the tissue samples were homogenized with a sonicator (130 Watt, 20

kHz, and 35% Amp) for 10 seconds in 1 ml of TRIzol reagent and then incubated at room temperature for 5 minutes before adding 0.2 ml of chloroform ($CHCl_3$). The suspension was then mixed vigorously by hand for 15 seconds, incubated at room temperature for another 3 minutes and centrifuged at 12,000 g for 15 minutes at room temperature. After centrifugation, the RNA in the upper aqueous phase was collected, transferred to a fresh tube, precipitated with 0.5 ml of isopropanol, mixed gently by vortex and incubated at room temperature for 10 minutes. The pellet of total RNA was collected by centrifugation at 12,000 g for 10 minutes. The supernatant was discarded. The RNA pellet was washed with 0.1 ml cold 75% ethanol, mixed, and centrifuged at 7,500 g for 5 minutes. The ethanol was discarded. The RNA pellet was air-dried for 15 minutes. Finally, the RNA was dissolved in a small volume of DEPC-treated water (30-40 µl) and stored at $-80°C$.

4.6.2 RNA qualification

The amount of total RNA was determined using a NanoDrop® spectrophotometer (Thermo Scientific, Waltham, MA, USA). RNA quality was assessed by the 260/280 nm absorbance ratio (minimally 1.8) and gel electrophoresis.

4.6.3 Reverse transcription

Total RNA was reverse-transcribed using high capacity cDNA reverse transcriptase Kit (Applied Biosystems™). First strand cDNA was synthesized according to the manufacturer's protocol.

4.6.4 Real time quantitative PCR

The real-time PCR reactions were set up using the SsoAdvancedTM SYBR® Green Supermix (Bio-Rad, California, USA) along with 1 μl of cDNA and gene-specific primers (Bio-Rad, Hercules, CA, USA). The primers used were: rat *Vegfa* (Unique Assay ID: qRnoCED0002159), rat *Ctnnb1* (Unique Assay ID: qRnoCID0053256), and rat *Ccnd1* (Unique Assay ID: qRnoCED0004966). The differences in sample RNA content were normalized rat *Actb* expression (Unique Assay ID: qRnoCID0056984). The real-time PCR reactions were carried out in a CFX96 Real-Time PCR Detection System (Bio-Rad, Hercules, CA, USA). The thermal cycler protocol

consisted of 2 minutes activation at 95°C followed by 40 cycles of denaturation at 95°C for 5 seconds, and then annealing/extension at 60°C for 30 seconds was employed. At the end of each run, a melting curve analysis was performed from 65-95°C with a heating rate of 0.1°C per second. Target genes and *Actb* reactions were performed in separate tubes and all samples were run in triplicate to ensure the accuracy of data. Analysis of the mRNA expression levels was performed by Bio-Rad CFX manager[TM] software version1.3.1 (Hercules, CA) and quantification of relative mRNA expression was calculated using the $\Delta\Delta$Ct method of relative quantification. The change of target mRNA expression is calculated as the fold change relative to the amount of ΔCt calibrator, using the equation $2^{-\Delta\Delta Ct}$, where $\Delta\Delta$Ct = ΔCt (calibrator) - ΔCt (target).

5 Statistical analysis

All values were represented as mean ± SEM. The data was analyzed using one-way analysis of variance (ANOVA) with Tukey's post hoc test to compare between groups. The significance level was set at $p < 0.05$.

CHAPTER 4
RESULTS

1 Gross examination of the livers

1.1 External morphology

The gross appearance of the rat livers in the normal control (CON) and control with propylene glycol- (CPG-)treated groups was smooth, soft, reddish-brown, and glossy, and had sharp edges. The livers in the HCC and HCC with propylene glycol- (HPG-) treated groups were firm with numerous cancer nodules. However, rats with HCC that we treated with 30 mg/kg Sorafenib (HSF), 1 mg/kg (HBU1), 10 mg/kg (HBU10), or 50 mg/kg Benja-ummarit (HBU50) had far fewer nodules (Figure 37).

1.2 The liver-to-body weight ratio

The liver weight in the HSF group was lower than that of all other groups (Table 3). Moreover, the liver-to-body weight ratio in this group was significantly decreased when compared with the HCC, HPG, HBU1, HBU10 and HBU50 groups ($p<0.05$) (Figure 38).

Diaphragmatic surface   Visceral surface

CON
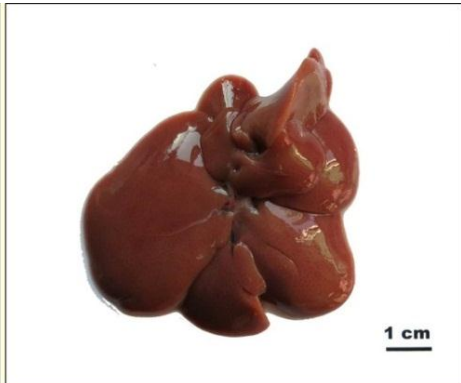
CPG
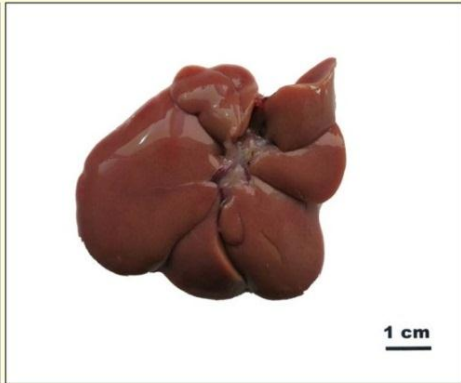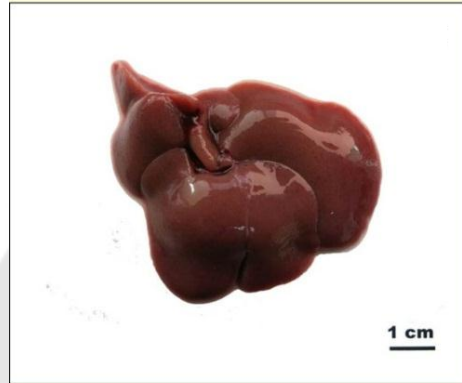
HCC
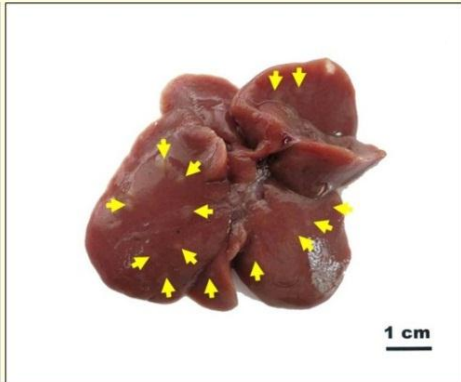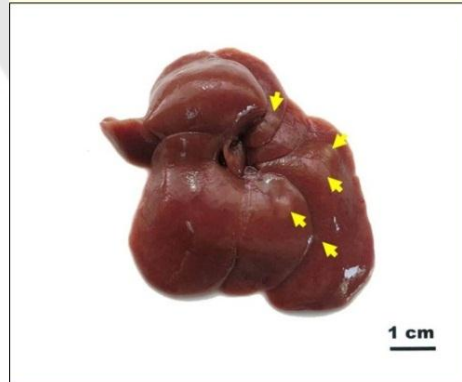
HPG
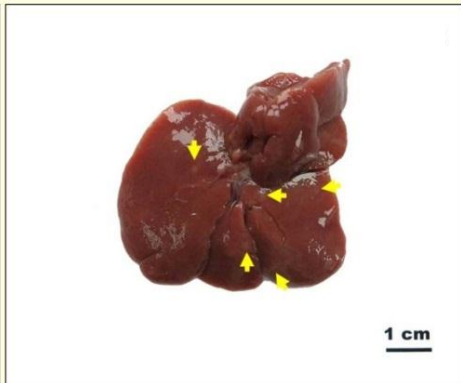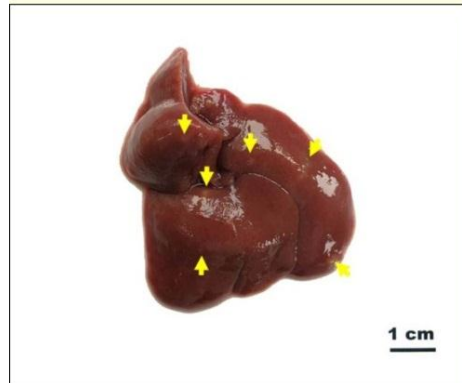
Figure 36 Gross morphology of the diaphragmatic and visceral surfaces of rat livers demonstrates the hepatic cancer nodules (yellow arrows) in normal control (CON), control with propylene glycol (CPG), HCC, and HCC with propylene glycol (HPG) groups.

Diaphragmatic surface   Visceral surface

HSF
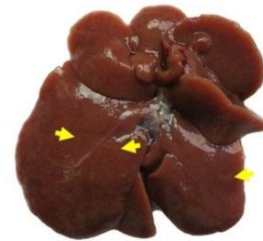
HBU1
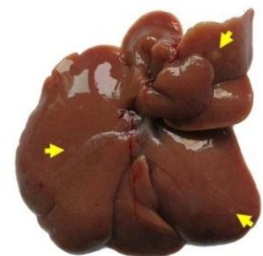
HBU10
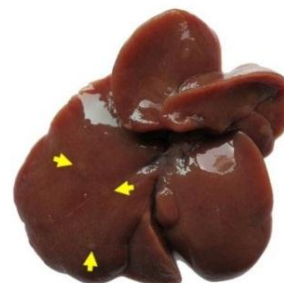
HBU50
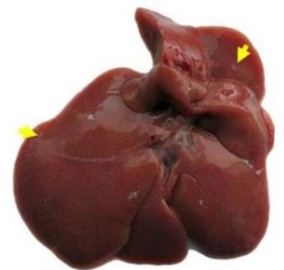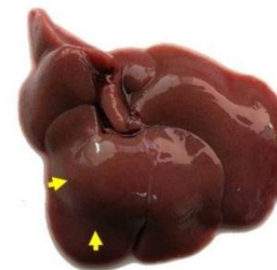
Figure 37 Gross morphology of the diaphragmatic and visceral surfaces of rat livers shows hepatic cancer nodules (yellow arrows) in the groups   HCC treated with Sorafenib at 30 mg/kg (HSF), Benja-ummarit at 1 mg/kg (HBU1), 10 mg/kg (HBU10) and 50 mg/kg (HBU50).

Table 3 The liver-to-body weight ratio among the respective control and experimental groups.

Values were presented as the mean ± SEM (n = 7).

Groups	Parameters		
	Liver weight (g)	Body weight (g)	Liver weight to Body weight ratio (%)
CON	14.5±0.6	466.0±17.1	3.1±0.2
CPG	14.4±0.7	496.9±12.4	2.9±0.2
HCC	15.1±0.6	455.6±10.8	3.3±0.1
HPG	14.1±0.6	423.3±10.1	3.3±0.1
HSF	10.6±0.4	392.8±5.4	2.7±0.1*
HBU1	13.5±0.4	405.6±5.9	3.3±0.1
HBU10	14.2±0.4	430.4±9.4	3.3±0.1
HBU50	13.8±0.9	408.6±14.3	3.4±0.1

*$p<0.05$ compared to HCC, HPG, HBU1, HBU10 and HBU50 groups.

I-- Control --I I------------------ Cancer --------------------I
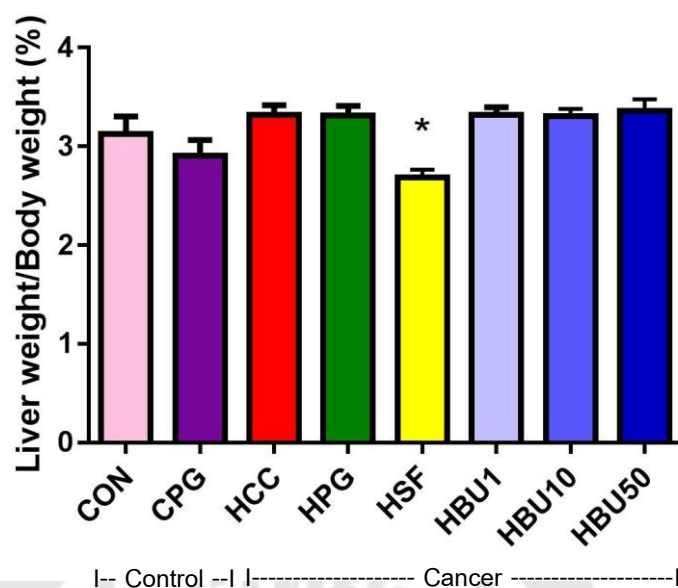
Figure 38 Graphs showing the liver-to-body weight ratio

of the normal control (CON), and, control treated with propylene glycol (CPG) groups, the nontreated HCC and, HCC groups treated with propylene glycol (HPG), 30 mg/kg of Sorafenib (HSF), 1 mg/kg of Benja-ummarit (HBU1), 10 mg/kg of Benja-ummarit (HBU10), or 50 mg/kg of Benja-ummarit (HBU50) . Values were presented as the mean ± SEM (n = 7). *p<0.05 compared to HCC, HPG, HBU1, HBU10 and HBU50 groups.

2 Liver function tests

2.1 Aspartate aminotransferase (AST)

The serum concentration of AST in the HBU1, HBU10 and HBU50 groups was not significantly different from the CON, CPG and HCC groups. It was noteworthy, however, that the serum level in the HSF group increased ∼ 1.5 fold relative to the CON, CPG and HCC groups ($p<0.05$) (Figure 39).
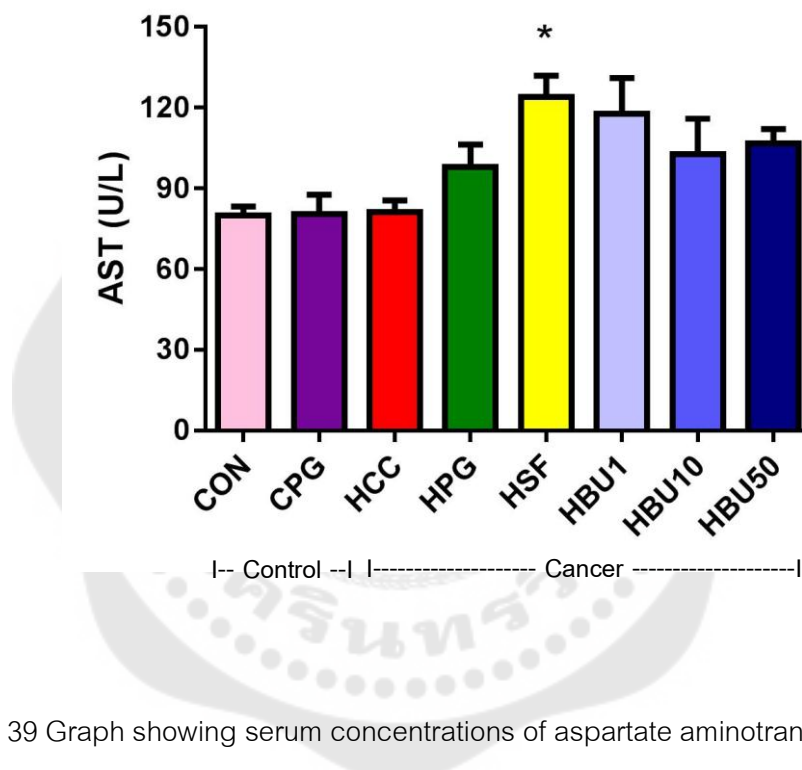
Figure 39 Graph showing serum concentrations of aspartate aminotransferase (AST) in the normal control (CON) and control treated with propylene glycol (CPG) groups, the nontreated HCC and HCC groups treated with propylene glycol (HPG), 30 mg/kg of Sorafenib (HSF), 1 mg/kg of Benja-ummarit (HBU1), 10 mg/kg of Benja-ummarit (HBU10), or 50 mg/kg of Benja-ummarit (HBU50). Values were presented as the mean ± SEM (n = 7). *$p< 0.05$ compared with CON, CPG and HCC groups.

2.2 Alanine aminotransferase (ALT)

The concentration of serum ALT in the HSF group was 2-3 fold increased relative to all other groups ($p<0.05$). However, its concentration in the HBU1, HBU10 and HBU50 groups was not significantly different from the CON, CPG, HCC and HPG groups (Figure 40).
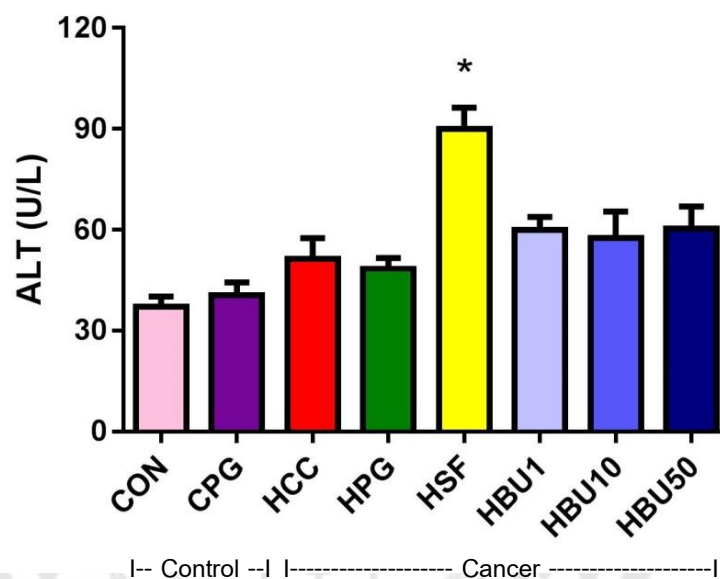
Figure 40 Graph demonstrating the serum levels of alanine aminotransferase (ALT) of the normal control (CON) and control treated with propylene glycol (CPG) groups, the nontreated HCC and HCC groups treated with propylene glycol (HPG), 30 mg/kg of Sorafenib (HSF), 1 mg/kg of Benja-ummarit (HBU1), 10 mg/kg of Benja-ummarit (HBU10), or 50 mg/kg of Benja-ummarit (HBU50). Values were presented as the mean ± SEM (n = 7). *$p<0.05$ compared with the CON, CPG, HCC, HPG, HBU1, HBU10 and HBU50 groups.

2.3 Alkaline phosphatase (ALP)

The serum concentration of ALP in the HSF, HBU1, HBU10 and HBU50 groups was not significant different from that in the CON, CPG, HCC and HPG groups (Figure 41).

I-- Control --I I------------------- Cancer -------------------I
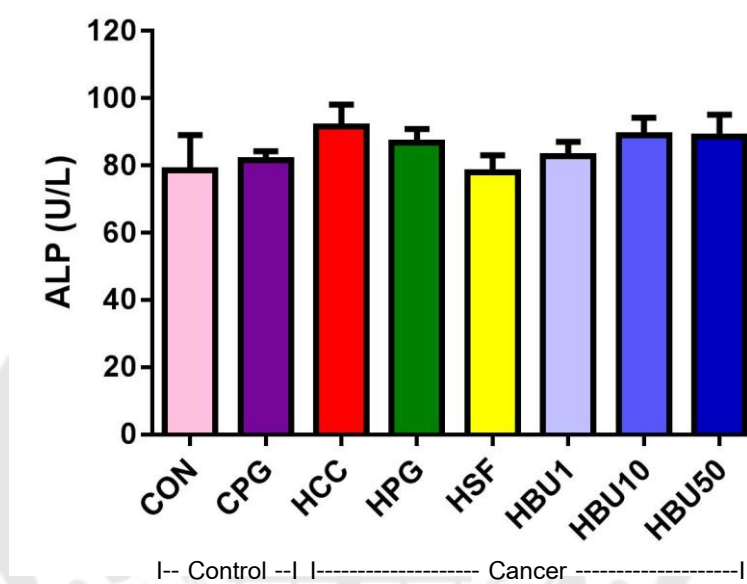
Figure 41 Graph depicting the serum levels of alkaline phosphatase (ALP) of the normal control (CON) and control treated with propylene glycol (CPG) groups, the nontreated HCC and HCC groups treated with propylene glycol (HPG), 30 mg/kg of Sorafenib (HSF), 1 mg/kg of Benja-ummarit (HBU1), 10 mg/kg of Benja-ummarit (HBU10), or 50 mg/kg of Benja-ummarit (HBU50). Values were presented as the mean ± SEM (n = 7).

2.4 Albumin

The serum albumin concentration decreased significantly in the HSF group compared with the CPG, HBU1, HBU10 and HBU50 groups ($p<0.05$). Albumin concentration in the HBU1, HBU10 and HBU50 groups was, however, similar to that in the CON, CPG, HCC and HPG groups (Figure 42).

I-- Control --I I------------------ Cancer -------------------I
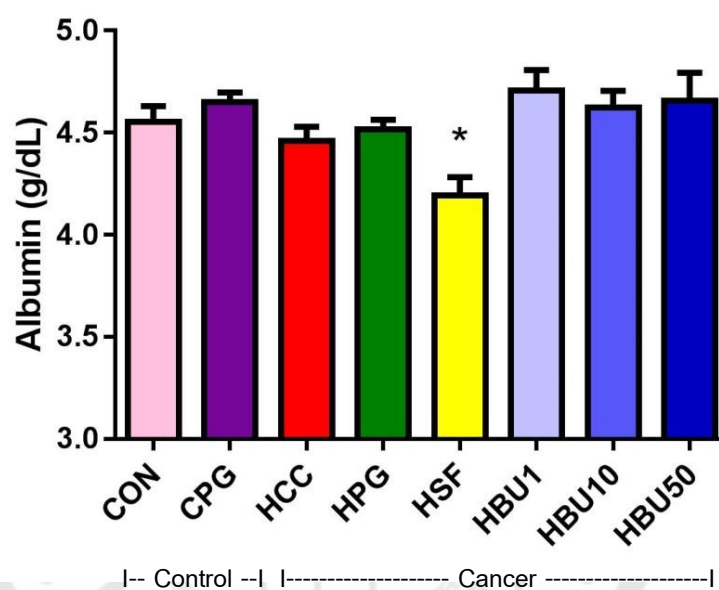
Figure 42 Graph showing the serum levels of albumin

of the normal control (CON) and control treated with propylene glycol (CPG) groups, the nontreated HCC and HCC groups treated with propylene glycol (HPG), 30 mg/kg of Sorafenib (HSF), 1 mg/kg of Benja-ummarit (HBU1), 10 mg/kg of Benja-ummarit (HBU10), or 50 mg/kg of Benja-ummarit (HBU50). Values were presented as the mean ± SEM (n = 7). *$p<0.05$ compared with the CPG, HBU1, HBU10 and HBU50 groups.

Table 4 Comparison of liver function tests in the respective control and experimental groups .

Values were presented as the mean ± SEM (n = 7).

Groups	Liver function test			
	AST (U/L)	ALT (U/L)	ALP (U/L)	Albumin (g/dL)
CON	80.1±3.2	37.1±3.1	78.7±10.3	4.6±0.1
CPG	80.6±7.2	40.4±3.9	81.5±2.8	4.7±0.1
HCC	81.2±4.4	51.3±6.3	91.5±6.7	4.46±0.1
HPG	98.1±8.3	48.4±3.2	86.9±4.0	4.5±0.1
HSF	124.0±7.9*	90.1±6.2*	78.0±5.0	4.2±0.1*
HBU1	117.8±13.3	60.0±3.9	82.8±4.3	4.7±0.1
HBU10	102.8±13.1	57.6±7.9	89.0±5.2	4.6±0.1
HBU50	106.8±5.3	60.5±6.5	88.7±6.5	4.7±0.1

AST; *$p < 0.05$ compared with CON, CPG and HCC groups

ALT; *$p < 0.05$ compared with the CON, CPG, HCC, HPG, HBU1, HBU10 and HBU50 groups

Albumin; *$p < 0.05$ compared with the CPG, HBU1, HBU10 and HBU50 groups

3. Histopathological studies

3.1 Hematoxylin and eosin staining (H&E)

The cancer areas could be demonstrated in paraffin-embedded rat liver sections stained with H&E. Classical histomorphological features of hepatocellular carcinoma were the presence of hepatic nodules with, thick cell cords arranged in a pseudoglandular pattern[264]. The livers of the HCC, HPG, HSF, HBU1, HBU10 and HBU50 groups showed various sizes of cancer areas.
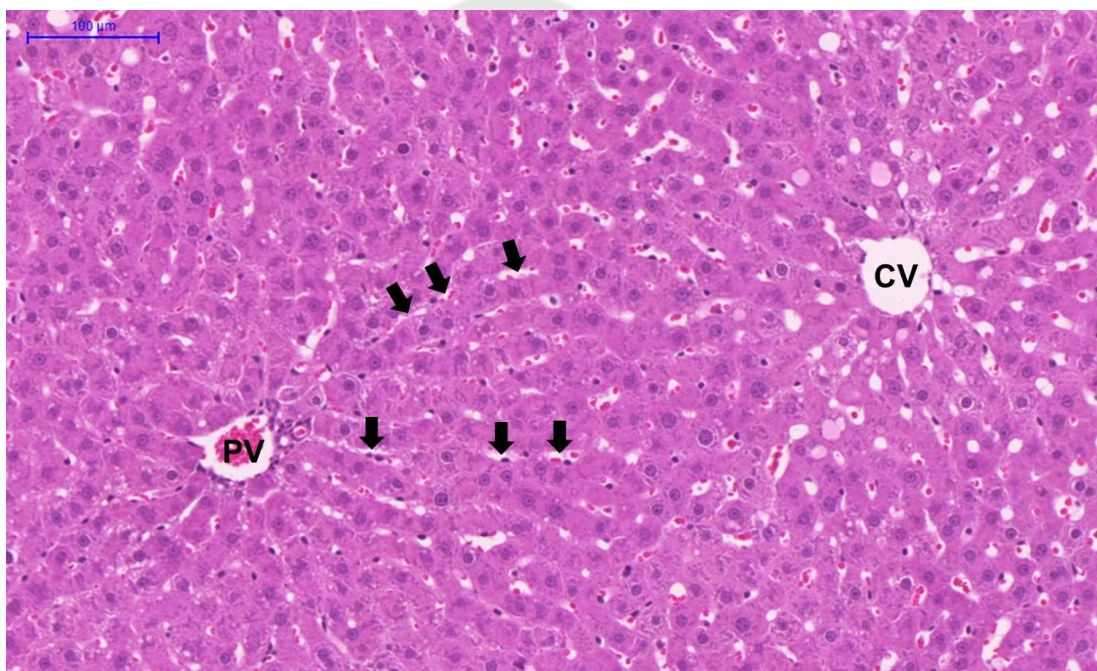
Figure 43 Light micrograph illustrating the histology of normal liver with radial arrays of hepatocytes converging towards the central (CV) or portal veins (PV). Note the liver cords appear to be discontinuous at the periphery of the central and portal fields. Further note the sinusoidal space (arrows) between adjacent cords. Bar: 100 μm.
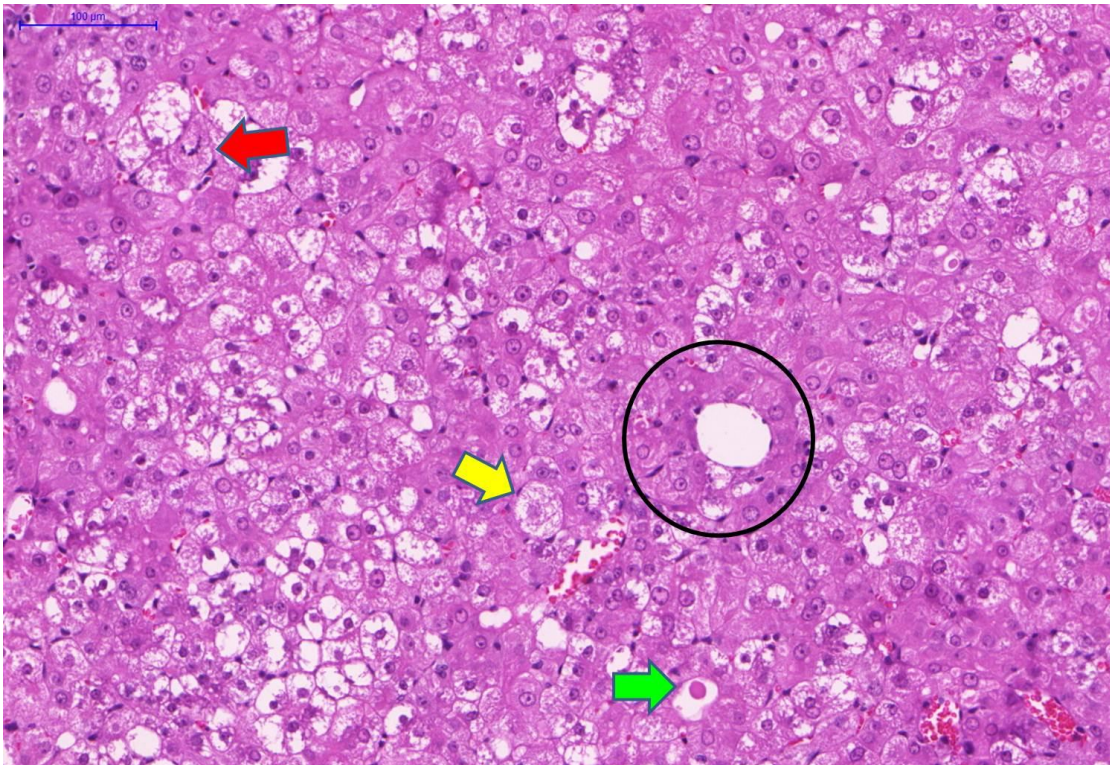
Figure 44 Light micrograph demonstrating the histopathology of the liver cancer containing thick cell cords and no sinusoidal spaces between the cords. Note the cells with mitotic figure (red arrow) hydropic degeneration (yellow arrow), hyaline globule (green arrow), pseudoglandular transformation (inside black circle), or large diameter with hyperchromatic nuclei. Bar: 100 μm.
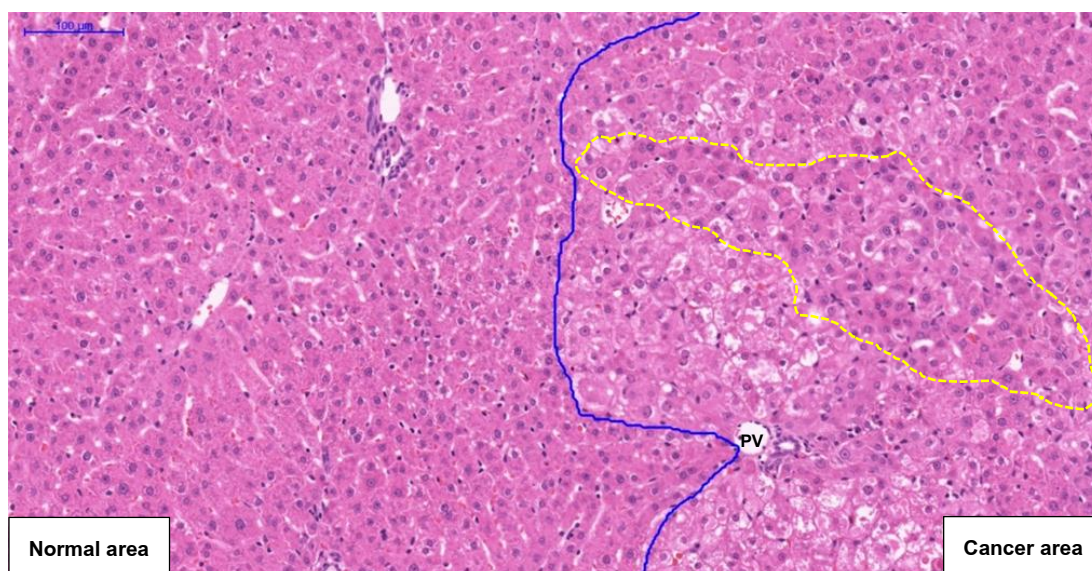
Figure 45 Light micrograph depicting the histology of normal and cancerous areas. Note the cancerous area is characterized by hyperchromatic cells (in the dashed line area) and thick cell cords. PV; portal vein. Bar: 100 μm.

Histological examination of the liver sections of the CON and CPG groups showed normal architecture of the hepatic cell cords separated by hepatic sinusoids radiating from a central or portal vein (Figure 43, 46).

Liver sections of rats in the HCC and HPG groups showed the severe histopathological characteristics of cancer (nodules with thick cell cord and hyperchromatic cells) when compared with the CON and CPG groups. (Figure 44- 46). In the HSF group, the occurrence of thick cell cords was markedly reduced. In addition, the cancer area was greatly diminished as compared with the HCC and HPG groups (Figure 46).

The liver sections of the HCC groups treated with Benja-ummarit groups (HBU1, HBU10 and HBU50) showed that thick cell cords decreased in a dose-dependent manner. The number of cancer area was also markedly decreased as compared with HCC and HPG groups (Table 5, Figure 46).

Additionally, intrahepatic bile duct dilatation and hyperchromatic nuclei were observed in the HCC and HPG groups, but not in the other groups (Figure 47). The brownish granule -containing cells in the periportal area were often seen in sections of HCC and HPG groups (Figure 48).
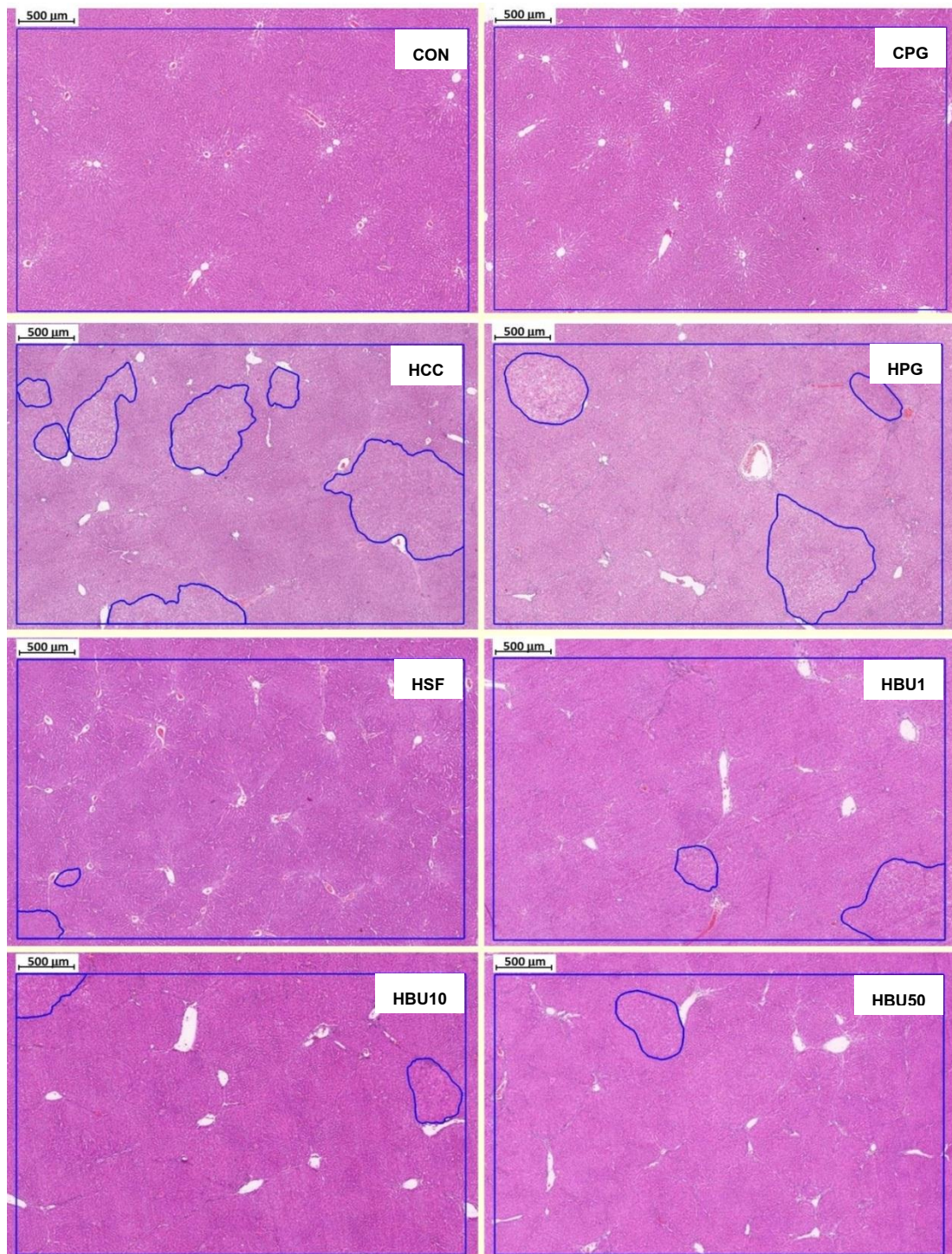
Figure 46 Photomicrographs of H&E-stained sections cancer areas (bounded by blue lines) in the normal control (CON) and control treated with propylene glycol (CPG) groups, the nontreated HCC and HCC groups treated with propylene glycol (HPG), 30 mg/kg of Sorafenib (HSF), 1 mg/kg of Benja-ummarit (HBU1), 10 mg/kg of Benja-ummarit (HBU10), or 50 mg/kg of Benja-ummarit (HBU50). Bar: 500 μm
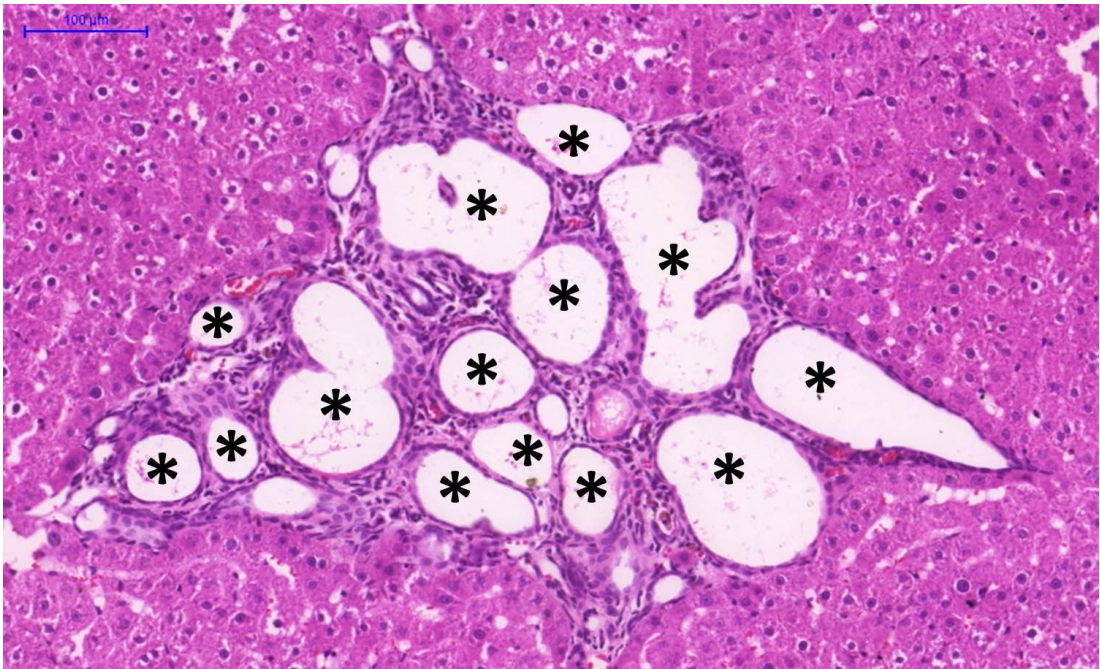
Figure 47 Light micrograph of section in HCC group
shows intrahepatic bile duct dilatation (asterisks) surrounded by elongated hyperchromatic cells. Bar: 100 μm
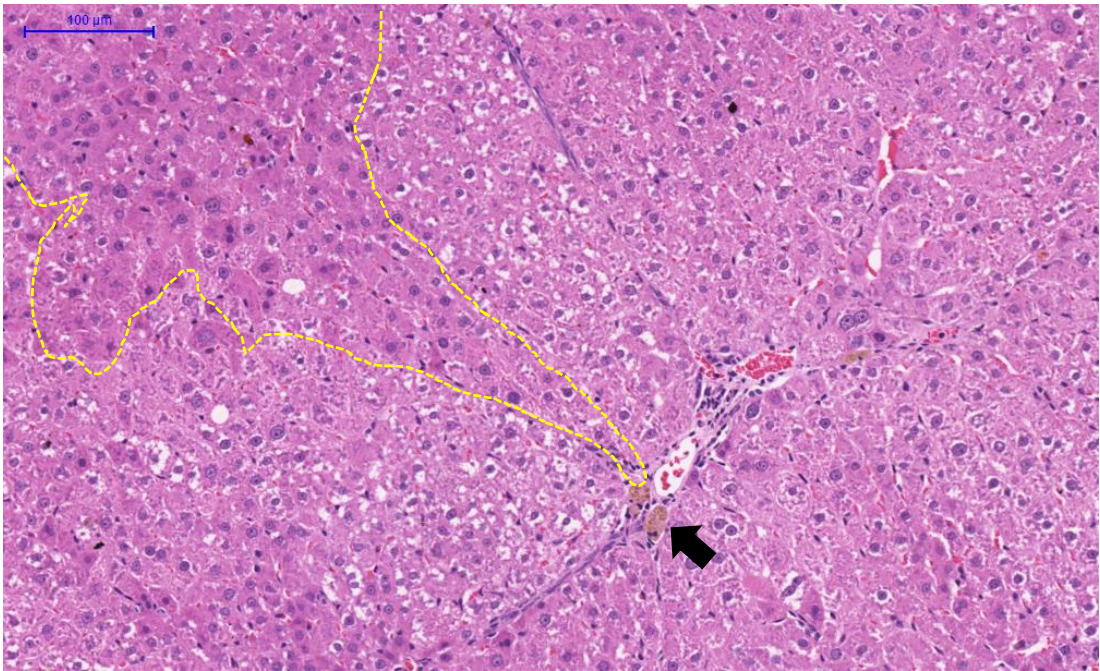
Figure 48 Light micrograph demonstrating hepatocytes with hyperchromatic staining (area surrounded by dashed line) in the HCC and HPG groups. Note the brownish cells (arrow) in the periportal area. Bar: 100 μm

Table 5 Comparison of the percentage of cancer area in liver sections among respective experimental groups.

Values were presented as the mean ± SEM (n = 7).

Groups	Cancer area (%)
HCC	21.5±3.2
HPG	18.1±1.6
HSF	1.5±0.6*
HBU1	2.7±0.5*
HBU10	2.6±0.3*
HBU50	2.1±0.3*

*p<0.05 compared to HCC and HPG groups.
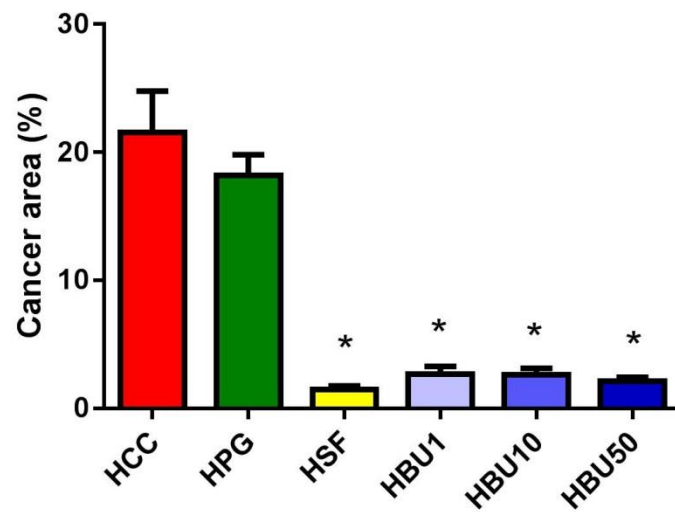
Figure 49 Graph showing the percentage cancer areas

as determined by the case viewer program in the livers the normal control (CON) and control treated with propylene glycol (CPG) groups, the nontreated HCC and HCC groups treated with propylene glycol (HPG), 30 mg/kg of Sorafenib (HSF), 1 mg/kg of Benja-ummarit (HBU1), 10 mg/kg of Benja-ummarit (HBU10), or 50 mg/kg of Benja-ummarit (HBU50). Values were presented as the mean ± SEM (n = 7) *p<0.05 compared to HCC and HPG groups.

3.2 Immunohistochemical staining

VEGF, a biomarker for angiogenesis, was immunolocalized in all livers. Only low concentrations of VEGF were present in the CON and CPG groups, although more densely stained area of VEGF was found in the cytoplasm of some hepatocytes. In contrast, larger area of more densely staining hepatocytes was found in the HCC and HPG groups. However,VEGF-immunopositive areas were seldom seen in liver of the HSF, HBU1, HBU10 and HBU50 groups (Figure 50).
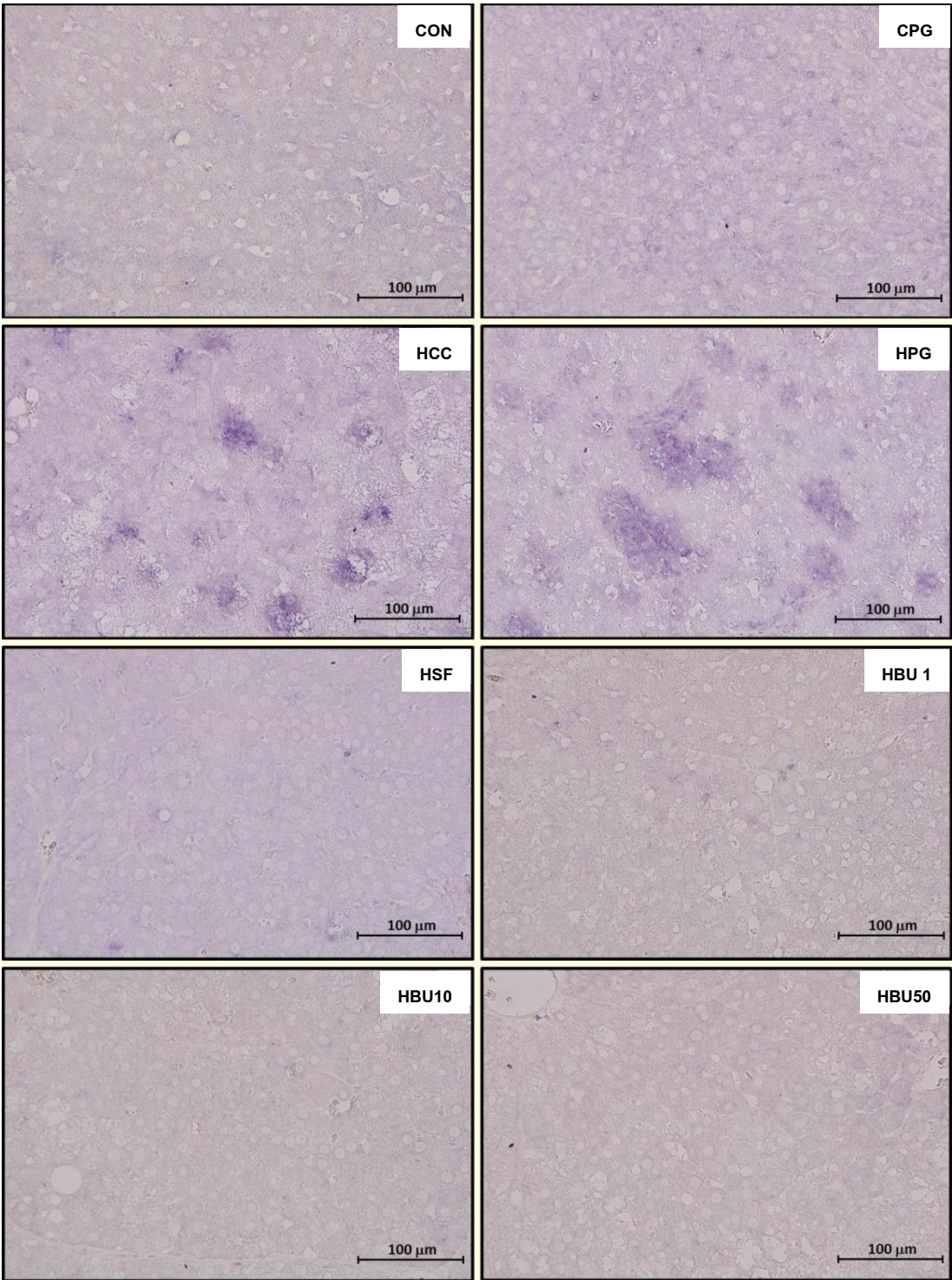
Figure 50 Light micrographs showing the distribution of VEGF in liver sections of the normal control (CON) and control treated with propylene glycol (CPG) groups, the nontreated HCC and HCC groups treated with propylene glycol (HPG), 30 mg/kg of Sorafenib (HSF), 1 mg/kg of Benja-ummarit (HBU1), 10 mg/kg of Benja-ummarit (HBU10), or 50 mg/kg of Benja-ummarit (HBU50). Note more immunopositive area of VEGF in HCC and HPG groups. Bar: 100 μm

4. Malondialdehyde (MDA) assay

Malondialdehyde (MDA), a widely accepted biomarker of lipid peroxidation, was employed to evaluate the level of oxidative stress. The concentration of MDA reflects the degree of lipid peroxidation in liver sample. MDA concentrations in liver samples from all treated groups (HSF, HBU1, HBU10, HBU50) were not significantly different from the control group. MDA concentrations (mmol/L) in the rat liver are shown in Table 6 and Figure 51.

Table 6 MDA concentrations (mmol/L) in liver tissues among groups.

Values were presented as the mean ± SEM (n = 7).

Groups	MDA (mmol/L)
CON	0.13±0.005
CPG	0.12±0.005
HCC	0.14±0.009
HPG	0.14±0.008
HSF	0.13±0.009
HBU1	0.14±0.009
HBU10	0.14±0.011
HBU50	0.13±0.006

I-- Control --I I------------------ Cancer --------------------I
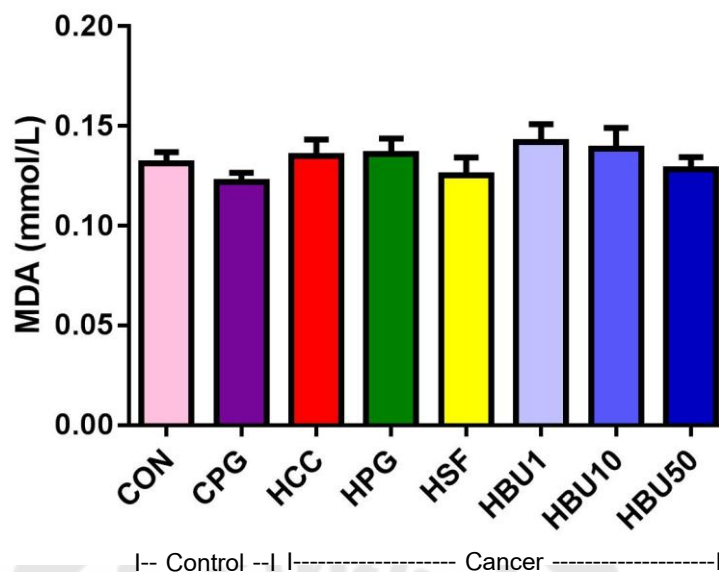
Figure 51 Graphs showing the MDA concentration (mmol/L)
determined by spectrophotometry in the liver tissues of the normal control (CON) and
control treated with propylene glycol (CPG) groups, the nontreated HCC and HCC
groups treated with propylene glycol (HPG), 30 mg/kg of Sorafenib (HSF), 1 mg/kg of
Benja-ummarit (HBU1), 10 mg/kg of Benja-ummarit (HBU10), or 50 mg/kg of Benja-
ummarit (HBU50). Values were presented as the mean ± SEM (n = 7).

5 Western blot analysis

Quantification of VEGF, β-catenin and cyclinD1 protein expression was done by Western blot analysis. Liver VEGF, β-catenin and cyclinD1 protein contents in HCC group were ∼ 3, 1.2 and 1.4 folds increased respectively compared to the CON group. In contrast, VEGF expression in the HSF, HBU1, HBU10 and HBU50 groups was decreased significantly comparing with the HCC group. The β-catenin and cyclinD1 expressions in the HBU10 and HBU50 groups tended to decrease compared to the HCC group, but the change was not statistically significant. Among three Benja-ummarit-treated groups (HBU1, HBU10, HB50), the liver content of VEGF, β-catenin and cyclinD1 protein was reduced in a dose-dependent manner (50>10>1 mg/kg of BU; Table 7 and Figure 52-54).

Table 7 The expression of VEGF, β-catenin and cyclin D1 proteins in liver tissues performed by Western blot analysis. Values were presented as the mean ± SEM (n = 7).

Groups	Parameters		
	VEGF/Actin	β-catenin/Actin	Cyclin D1/Actin
CON	1.0±0.0[*,#]	1.0±0.0	1.0±0.0
CPG	1.3±0.2[*,#]	1.0±0.3	0.9±0.2
HCC	3.0±0.2	1.2±0.2	1.4±0.2
HPG	3.4±0.4	1.4±0.3	1.7±0.2
HSF	1.6±0.1[*,#]	1.4±0.3	2.1±0.3
HBU1	2.4±0.2[#]	1.3±0.4	1.2±0.2
HBU10	1.7±0.3[*,#]	1.3±0.4	1.0±0.2
HBU50	1.1±0.3[*,#]	0.8±0.2	0.9±0.4

[*]$p<0.05$ compared to HCC group; [#]$p<0.05$ compared to HPG group.
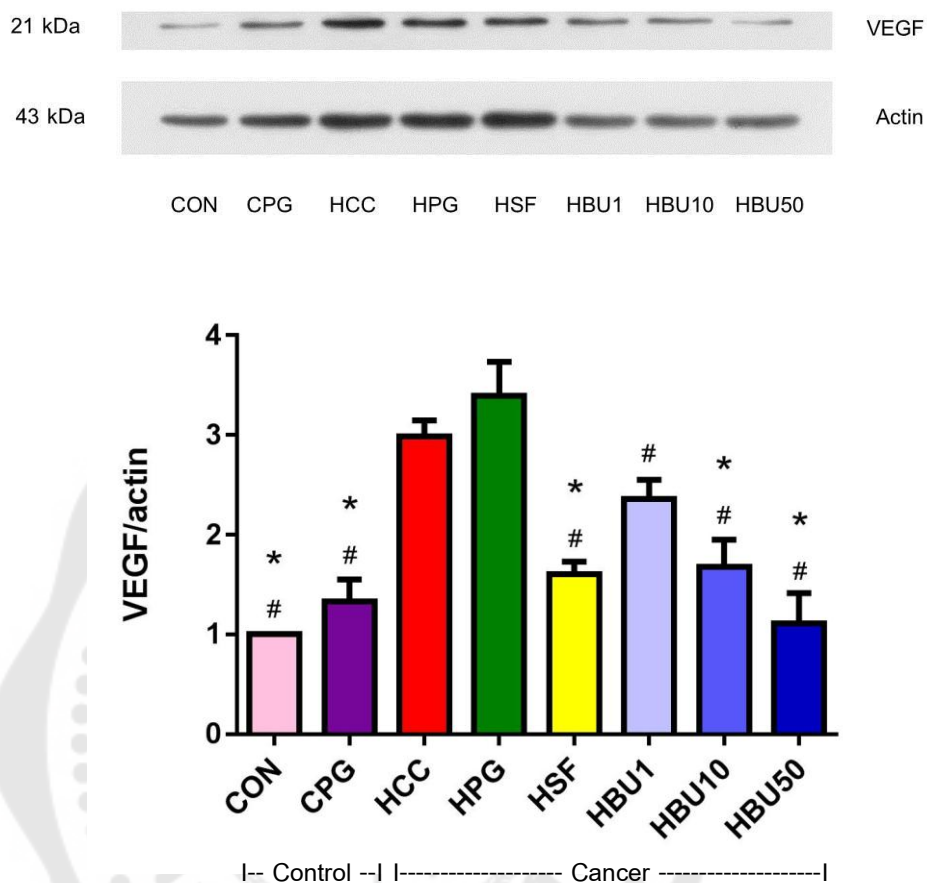
Figure 52 Graphs showing the level of VEGF expression in the liver tissues determined by Western blot analysis the normal control (CON) and control treated with propylene glycol (CPG) groups, the nontreated HCC and HCC groups treated with propylene glycol (HPG), 30 mg/kg of Sorafenib (HSF), 1 mg/kg of Benja-ummarit (HBU1), 10 mg/kg of Benja-ummarit (HBU10), or 50 mg/kg of Benja-ummarit (HBU50). Protein bands were quantified by using densitometry. Values were presented as the mean ± SEM (n = 7). *p<0.05 compared to HCC group; #p<0.05 compared to HPG group.
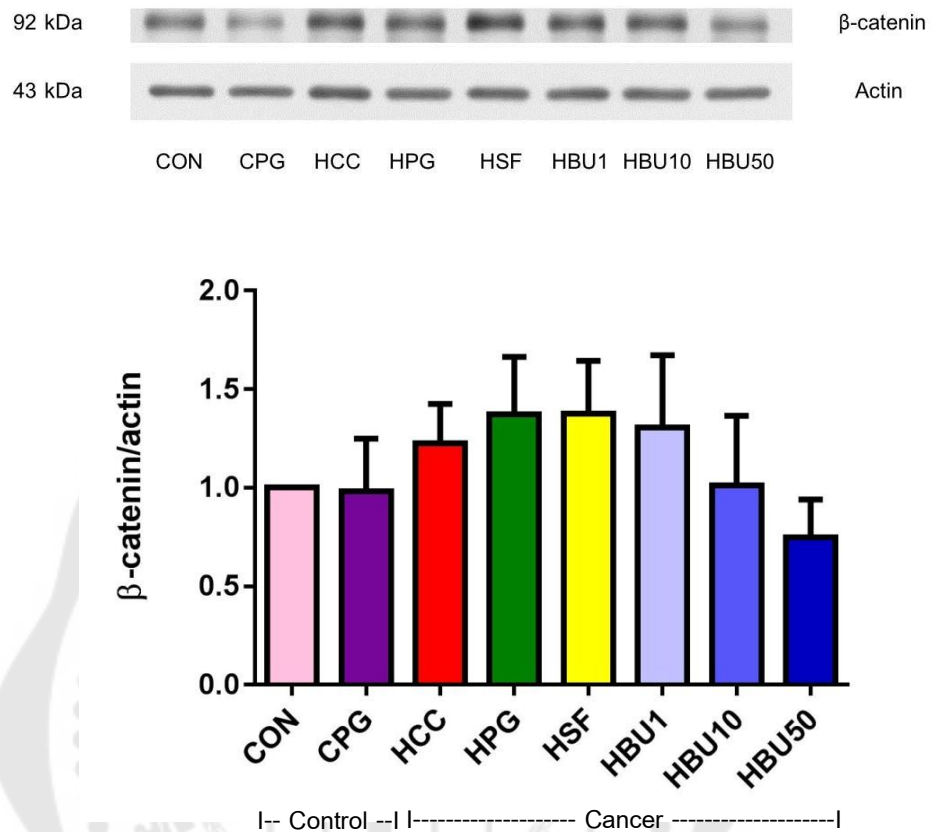
Figure 53 Graphs showing the level of β-catenin expression in the liver tissues determined by Western blot analysis the normal control (CON) and control treated with propylene glycol (CPG) groups, the nontreated HCC and HCC groups treated with propylene glycol (HPG), 30 mg/kg of Sorafenib (HSF), 1 mg/kg of Benja-ummarit (HBU1), 10 mg/kg of Benja-ummarit (HBU10), or 50 mg/kg of Benja-ummarit (HBU50). Protein bands were quantified using densitometry. Values were presented as the mean ± SEM (n = 7) Note no statistically difference was determined among groups.
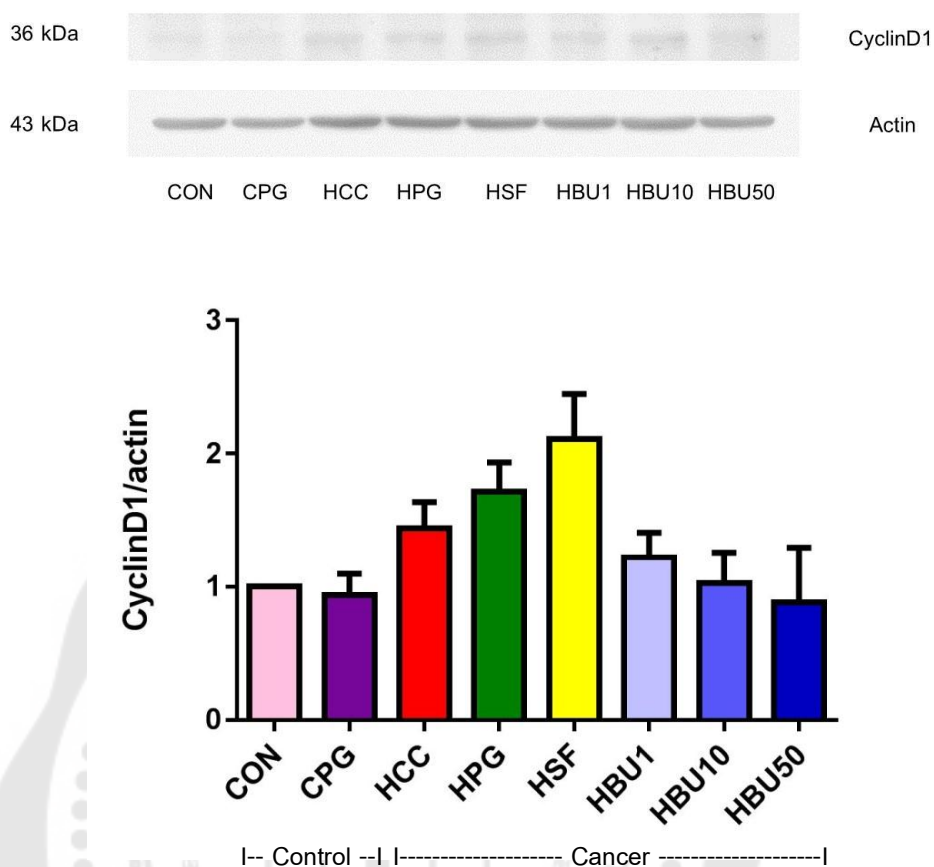
Figure 54 Graphs showing the level of cyclinD1 expression in the liver tissues determined by Western blot analysis of the normal control (CON) and control treated with propylene glycol (CPG) groups, the nontreated HCC and HCC groups treated with propylene glycol (HPG), 30 mg/kg of Sorafenib (HSF), 1 mg/kg of Benja-ummarit (HBU1), 10 mg/kg of Benja-ummarit (HBU10), or 50 mg/kg of Benja-ummarit (HBU50). Protein bands were quantified using densitometry. Values were presented as the mean ± SEM (n = 7). Note no statistically difference was determined among groups.

6 Real-time quantitative PCR

The expression of *Vegfa*, *Ctnnb1* and *Ccnd1* mRNAs were determined by real-time PCR in rat liver samples. The expression of the three genes in the HCC and HPG groups was ～ 2-fold increased compared to CON and CPG groups. When treated with Sorafenib (HSF) or with Benja-ummarit (HBU1, HBU10 and HBU50), *Vegfa, Ctnnb1* and *Ccnd1* expression was significantly reduced when compared to the HCC and HPG groups. In addition, the reduction in the BU-treated groups was dose-dependent (50>10>1mg/kg; Table 8 and Figure 55-57).

Table 8 Expression of *Vegfa*, *Ctnnb1* and *Ccnd1* mRNA

in liver samples of the respective control and experimental groups. Values were presented as the mean ± SEM (n = 7).

Groups	Parameters		
	Vegfa/Actb	*Ctnnb1/Actb*	*Ccnd1/Actb*
CON	$1.0\pm0.0^{*,\#}$	$1.0\pm0.0^{*,\#}$	$1.0\pm0.0^{*,\#}$
CPG	$1.2\pm0.1^{*,\#}$	$1.1\pm0.1^{*,\#}$	$1.1\pm0.1^{*,\#}$
HCC	2.1 ± 0.4	1.8 ± 0.1	2.0 ± 0.3
HPG	1.8 ± 0.3	1.7 ± 0.1	1.9 ± 0.3
HSF	$1.3\pm0.2^{*}$	$1.5\pm0.1^{*}$	$1.4\pm0.2^{*}$
HBU1	$1.1\pm0.1^{*,\#}$	$1.4\pm0.1^{*}$	$1.3\pm0.2^{*,\#}$
HBU10	$0.9\pm0.2^{*,\#}$	$1.3\pm0.1^{*,\#}$	$0.9\pm0.2^{*,\#}$
HBU50	$0.6\pm0.1^{*,\#}$	$1.3\pm0.1^{*,\#}$	$0.8\pm0.1^{*,\#}$

*p<0.05 compared to the HCC group; #p<0.05 compared to the HPG group.
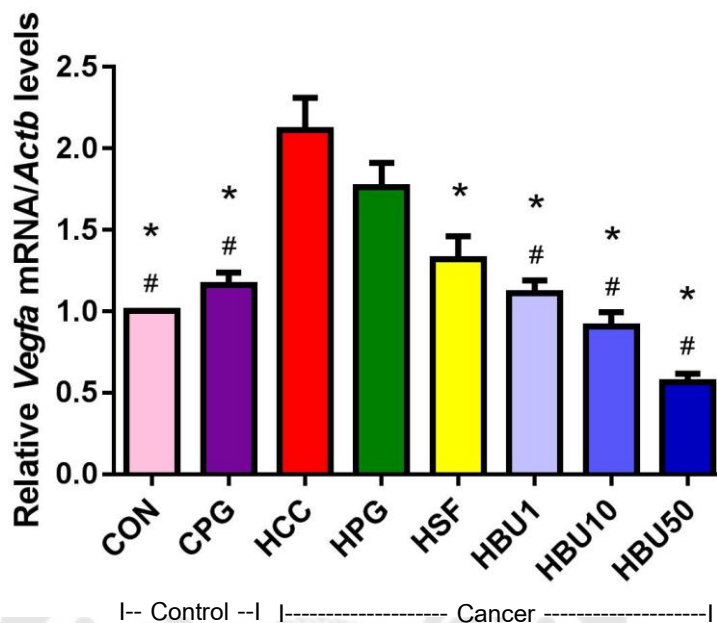
Figure 55 Graphs showing the level of *Vegfa* gene expressions
analyzed by real-time PCR in the rat liver samples of the normal control (CON) and
control treated with propylene glycol (CPG) groups, the nontreated HCC and HCC
groups treated with propylene glycol (HPG), 30 mg/kg of Sorafenib (HSF), 1 mg/kg of
Benja-ummarit (HBU1), 10 mg/kg of Benja-ummarit (HBU10), or 50 mg/kg of Benja-
ummarit (HBU50). Values were presented as the mean ± SEM (n = 7). *$p<0.05$
compared to the HCC group; #$p<0.05$ compared to the HPG group.
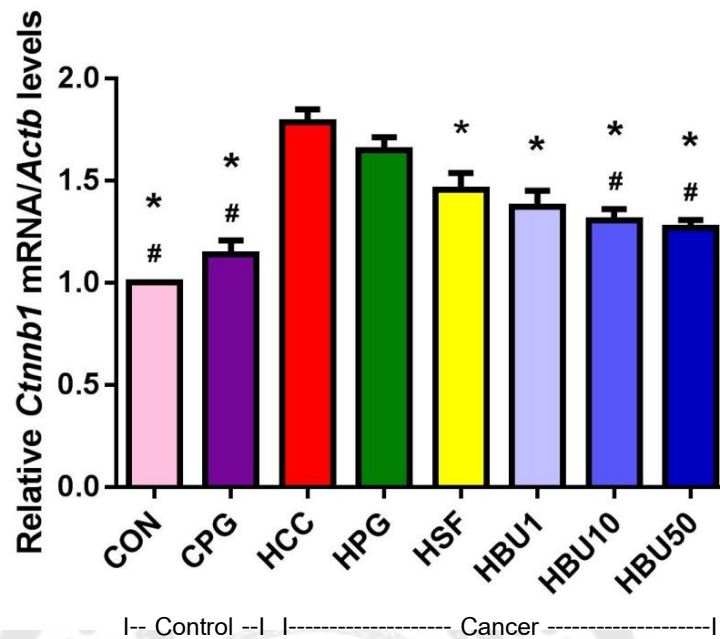
Figure 56 Graphs showing the level of *ctnnb1* gene expressions
analyzed by real-time PCR in the rat liver samples of the normal control (CON) and
control treated with propylene glycol (CPG) groups, the nontreated HCC and HCC
groups treated with propylene glycol (HPG), 30 mg/kg of Sorafenib (HSF), 1 mg/kg of
Benja-ummarit (HBU1), 10 mg/kg of Benja-ummarit (HBU10), or 50 mg/kg of Benja-
ummarit (HBU50). Values were presented as the mean ± SEM (n = 7). *p<0.05
compared to the HCC group; #p<0.05 compared to the HPG group.
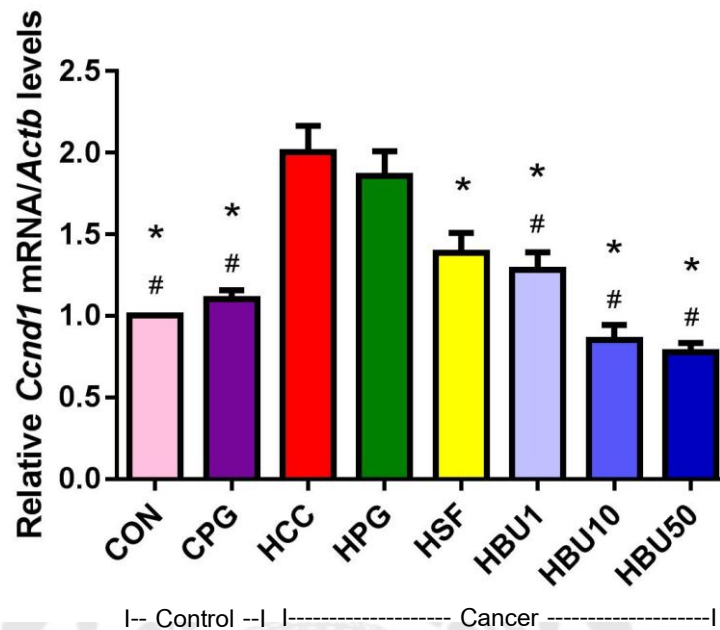
Figure 57 Graphs showing the level of *Ccnd1* mRNA expressions

in rat liver samples of the normal control (CON) and control treated with propylene glycol (CPG) groups, the nontreated HCC and HCC groups treated with propylene glycol (HPG), 30 mg/kg of Sorafenib (HSF), 1 mg/kg of Benja-ummarit (HBU1), 10 mg/kg of Benja-ummarit (HBU10), or 50 mg/kg of Benja-ummarit (HBU50). Values were presented as the mean ± SEM (n = 7). *p<0.05 compared to HCC group; #p<0.05 compared to HPG group.

CHAPTER 5

DISCUSSION AND CONCLUSION

Benja-ummarit (BU) is a traditional Thai herbal medicine consisting of many ingredients. The word "Benja-ummarit" is a combination of two Thai words: "Benja" means five and "Ummarit" means holy compound or nectar. Even though Benja-ummarit typically comprises 9 compounds, its main active ingredients are only 5 compounds: gamboge resin (*Garcinia hanburyi)*, *aloe vera* (*Aloe barbadensis)*, asafoetida (*Ferula assafoetida)*, red physic nut (*Baliospermum montanum)*, and epsom salt (magnesium sulfate). The other four ingredients are kaffir lime (*Citrus hystrix)*, ginger (*Zingiber officinale)*, Javanese long pepper (*Piper chaba)*, and black pepper (*Piper nigrum).* These compounds are added during preparation of Benja-ummarit to reduce its toxicity, to eliminate the gas accumulating in the alimentary canal, and to increase appetite[265, 266]

We have carried out our experiments with a crude extract of BU instead of admixing highly purified components of BU. In 2012, Intharit and coworkers[9] compared the cytotoxicity of crude extracts of BU with single ingredient of BU in the HepG2 cell line (Table 9) and found that the IC_{50} value was lower for the BU crude extract, which implies that a higher activity for inhibiting cancer cell growth could be realized than with single compounds of BU.

Table 9 Comparison of the cytotoxic effect the Benja-ummarit crude extract and its individual ingredient in HepG2 cancer cell lines

Name	$IC_{50}\pm SEM$ (μg/ml)
Benja-ummarit dispensatory	0.22±0.01
Gamboge resin	0.62±0.01
Red physic nut	3.03±0.91
Ginger	11.46±0.21

Table 9 (Continued)

Kaffir lime	26.43±2.76
Black pepper	37.96±1.22
Javanese long pepper	39.97±2.63
Aloe	>50
Asafoetida	>50
Epsom salt	>50

These results are in agreement with the outcome of our preliminary study in thioacetamide induced rat liver carcinoma. Following treatment with 1 mg/kg of BU crude extract and 1 mg/kg of gamboge resin, the cancer areas in rat liver specimens were reduced to 16% and 11% of their size in non-treated livers, respectively (unpublished data). Treatment with crude extract of BU, therefore, appears superior both *in vitro* and *in vivo* to treatment with a single active ingredient of BU (at least from gamboge resin). For these reasons, we decided to study the medicinal effects of crude extracts of BU instead of those of individual compounds of BU[9]

The gross and histopathological findings show that treatment with a crude extract of Benja-ummarit reduces the size of the cancer nodules and the cancer area in a dose-dependent manner (50 mg/kg > 10 mg/kg > 1 mg/kg). BU treatment probably improves the cancer parameters via its anti-angiogenic and /or anti-proliferative properties. This hypothesis is supported by our immunohistochemical, real-time PCR, and Western blot analyses of vascular endothelial growth factor (VEGF), β-catenin and cyclin D1. Its anti-angiogenic property is supported by the lower expression of VEGF mRNA and protein following BU treatment. In the same vein, expression of β-catenin and cyclin D1 mRNA and protein were decreased following BU treatment, which points to the anti-proliferation effect of the compound.

The anti-angiogenic effect of BU is probably due to the effects of gambogic acid in the gamboge resin[9, 15, 16, 19], aloe-emodin and aloin in *aloe vera*[267, 268], galbanic

acid in asafetida[268], 6-gingerol in ginger[269-271], piplartine in javanese long pepper[272], as well as piperine in black pepper[273]. Among the mentioned substances the gambogic acid appears to have the strongest anti-angiogenic activity[15-17, 19]. Gambogic acid is claimed to act via inhibition of the vascular endothelial growth factor receptor 2 (VEGFR2)[19] and its downstream protein kinases, c-Src, FAK, ERK, p38 and AKT[15, 17] or by inhibiting the PHD2-VHL-HIF-1α pathway[16].

The anti-proliferative property of a crude extract of BU may be an effect of gambogic acid in gamboge resin[17, 274], aloe-emodin in aloe vera[275, 276], galbanic acid in asafetida[277], 6-gingerol or zingerone in ginger[270, 271, 278, 279], piplartine in black pepper[280] as well as piperine in black pepper[281-285]. 6-Gingerol or zingerone in ginger inhibits cell proliferation by stoping the cell cycle at G1 phase[270] via down-regulation of cyclin D1[278, 279] or via inhibition of NF-κB activation[271]. Similarly, piperine in black pepper may induce cell cycle arrest at G0/G1 phase[281] or at G1 phase[285] via down-regulation of cyclin D1[281, 282]. Piperine in black pepper stops cell proliferation in breast cancer stem cells by inhibiting Wnt/β-catenin signaling[282]. In contrast, aloe-emodin in *aloe vera* appears to inhibit cell proliferation via phosphorylation of AKT and ERK[275]. Piplartine in long pepper inhibits cell-cycle progression in various tumor cells by inactivating CDK2 and destabilizing cyclin D1[280].

In addition to the anti-angiogenic and anti-proliferative properties of BU, each ingredient could have further effects. Aloe-emodin in *aloe vera*, 6-gingerol in ginger, and piperine in black pepper were all reported to inhibit tumor invasion and metastasis through suppression expression of MMP-2/9[267, 269]. All ingredients of BU except epsom salt have been shown to exert apoptotic activity in various cancer cell lines including SMMC-7721[286], human glioblastoma cell line (U87MG)[287], prostate cancer[288], H460 non-small cell lung carcinoma (NSCLC)[289], adriamycin-resistant human leukemia (K562/ADR)[290], MCF-7[291], IOMM-Lee and CH157MN[292] via overexpression of BAX[271, 288], caspase 3[271, 287], caspase 8[287], caspase 9[288] induced ROS accumulation[286, 291] or via the Akt/MAPK pathway[290]

A potentially important histopathological observation in the HCC- and HPG-induced groups is the appearance of intrahepatic bile duct dilatation and cholestasis. This bileduct dilatation or cholestasis totally disappeared following treatment with 1-50 mg/kg BU. We hypothesize that bile-duct dilatation disappears due to regression in the size of the cancer masses. In agreement, no developed in a HCC patient treated with Benja-ummarit[293, 294]

Sorafenib is, an oral multikinase inhibitor that is used worldwide for treatment of the advanced or metastatic hepatocellular carcinoma[295]. Irrespective of this status, the present study shows that the Sorafenib-treated group had the lowest liver-to-body weight ratio and albumin level, and the highest ALT level compared to the CON, CPG, HCC, HPG, and all BU-treated groups. This finding suggests that the the Sorafenib can harm hepatocytes. Accordingly, Kuroda et al. reported in 2016 that hepatocellular carcinoma patients treated with 400 mg Sorafenib twice daily for 2 months had higher levels of serum proteins in liver function tests (ALT 1098 IU/L; AST 1611 IU/L; total bilirubin 28.6 mg/dL). In addition, histopathology of these livers showed hepatocyte degeneration and necrosis in addition to lymphocyte infiltration and cholestasis[296]

In conclusion an extract of Benja-ummarit in 95% ethanol has a potent anti-carcinogenic effect via its anti-angiogenic and anti-proliferative effects. Therefore, Benja-ummarit is a good alternative herbal agent for treatment of hepatocellular carcinoma, since it seems to be less toxic than the standard drug Sorafenib.

REFERENCES

1.	Forner A, Reig M, Bruix J. Hepatocellular carcinoma. Lancet. 2018;391(10127): 1301-14.

2.	El-Serag HB. Epidemiology of viral hepatitis and hepatocellular carcinoma. Gastroenterology. 2012;142(6):1264-73.

3.	Tajiri H, Tanaka H, Brooks S, Takano T. Reduction of hepatocellular carcinoma in childhood after introduction of selective vaccination against hepatitis B virus for infants born to HBV carrier mothers. Cancer Causes Control. 2011;22(3):523-7.

4.	Tanaka Y, Hanada K, Mizokami M, Yeo AE, Shih JW, Gojobori T, et al. A comparison of the molecular clock of hepatitis C virus in the United States and Japan predicts that hepatocellular carcinoma incidence in the United States will increase over the next two decades. Proc Natl Acad Sci U S A. 2002;99(24):15584-9.

5.	Altekruse SF, McGlynn KA, Reichman ME. Hepatocellular carcinoma incidence, mortality, and survival trends in the United States from 1975 to 2005. J Clin Oncol. 2009;27(9):1485-91.

6.	El-Serag HB. Hepatocellular carcinoma: recent trends in the United States. Gastroenterology. 2004;127(5 Suppl 1):S27-34.

7.	Li T, Zhu Y, Qin CY, Yang Z, Fang A, Xu S, et al. Expression and prognostic significance of vascular endothelial growth factor receptor 1 in hepatocellular carcinoma 2012.

8.	Vilchez V, Turcios L, Marti F, Gedaly R. Targeting Wnt/beta-catenin pathway in hepatocellular carcinoma treatment. World J Gastroenterol. 2016;22(2):823-32.

9.	Intharit N. Cytotoxic activity of Benjaummarit remedy against cancer cells and its biological activities. Patumthani: Thammasat; 2012.

10.	Yan F, Wang M, Li J, Cheng H, Su J, Wang X, et al. Gambogenic acid induced mitochondrial-dependent apoptosis and referred to phospho-Erk1/2 and phospho-p38 MAPK in human hepatoma HepG2 cells. Environ Toxicol Pharmacol. 2012;33(2):181-90.

11.	Xie H, Qin YX, Zhou YL, Tong LJ, Lin LP, Geng MY, et al. GA3, a new gambogic

acid derivative, exhibits potent antitumor activities in vitro via apoptosis-involved mechanisms. Acta Pharmacol Sin. 2009;30(3):346-54.

12. Zou Z, Xie L, Wei J, Yu L, Qian X, Chen J, et al. Synergistic anti-proliferative effects of gambogic acid with docetaxel in gastrointestinal cancer cell lines. BMC Complement Altern Med. 2012;12:58.

13. Guo XK, Sun HP, Shen S, Sun Y, Xie FL, Tao L, et al. Synthesis and evaluation of gambogic acid derivatives as antitumor agents. Part III. Chem Biodivers. 2013;10(1):73-85.

14. Qiang L, Yang Y, You QD, Ma YJ, Yang L, Nie FF, et al. Inhibition of glioblastoma growth and angiogenesis by gambogic acid: an in vitro and in vivo study. Biochem Pharmacol. 2008;75(5):1083-92.

15. Yi T, Yi Z, Cho SG, Luo J, Pandey MK, Aggarwal BB, et al. Gambogic acid inhibits angiogenesis and prostate tumor growth by suppressing vascular endothelial growth factor receptor 2 signaling. Cancer Res. 2008;68(6):1843-50.

16. Lu N, Hui H, Yang H, Zhao K, Chen Y, You QD, et al. Gambogic acid inhibits angiogenesis through inhibiting PHD2-VHL-HIF-1alpha pathway. Eur J Pharm Sci. 2013;49(2):220-6.

17. Lu N, Yang Y, You QD, Ling Y, Gao Y, Gu HY, et al. Gambogic acid inhibits angiogenesis through suppressing vascular endothelial growth factor-induced tyrosine phosphorylation of KDR/Flk-1. Cancer Lett. 2007;258(1):80-9.

18. Abdel-Raheem IT, Abdel-Ghany AA. Hesperidin alleviates doxorubicin-induced cardiotoxicity in rats. J Egypt Natl Canc Inst. 2009;21(2):175-84.

19. Wen J, Pei H, Wang X, Xie C, Li S, Huang L, et al. Gambogic acid exhibits anti-psoriatic efficacy through inhibition of angiogenesis and inflammation. J Dermatol Sci. 2014;74(3):242-50.

20. Cascao R, Vidal B, Raquel H, Neves-Costa A, Figueiredo N, Gupta V, et al. Potent anti-inflammatory and antiproliferative effects of gambogic acid in a rat model of antigen-induced arthritis. Mediators Inflamm. 2014;2014:195327.

21. Panthong A, Norkaew P, Kanjanapothi D, Taesotikul T, Anantachoke N, Reutrakul V. Anti-inflammatory, analgesic and antipyretic activities of the extract of gamboge from

Garcinia hanburyi Hook f. J Ethnopharmacol. 2007;111(2):335-40.

22.	Qi Q, Lu N, Li C, Zhao J, Liu W, You Q, et al. Involvement of RECK in gambogic acid induced anti-invasive effect in A549 human lung carcinoma cells. Mol Carcinog. 2015;54:13-25.

23.	Xin ZF, Shen CC, Tao LJ, Yan SG, Wu HB. Gambogic acid inhibits invasion of osteosarcoma via upregulation of TIMP-1. Int J Mol Med. 2013;31(1):105-12.

24.	Chen J, Gu HY, Lu N, Yang Y, Liu W, Qi Q, et al. Microtubule depolymerization and phosphorylation of c-Jun N-terminal kinase-1 and p38 were involved in gambogic acid induced cell cycle arrest and apoptosis in human breast carcinoma MCF-7 cells. Life Sci. 2008;83(3-4):103-9.

25.	Li R, Chen Y, Zeng LL, Shu WX, Zhao F, Wen L, et al. Gambogic acid induces G0/G1 arrest and apoptosis involving inhibition of SRC-3 and inactivation of Akt pathway in K562 leukemia cells. Toxicology. 2009;262(2):98-105.

26.	Li C, Lu N, Qi Q, Li F, Ling Y, Chen Y, et al. Gambogic acid inhibits tumor cell adhesion by suppressing integrin beta1 and membrane lipid rafts-associated integrin signaling pathway. Biochem Pharmacol. 2011;82(12):1873-83.

27.	Wu X, Li Y. Signaling Pathways in Liver Cancer. In: Julianov A, editor. Liver Tumors. Shanghai: InTech China; 2012. p. 37-58.

28.	Tso P, McGill J. The Physiology of the Liver. In: Rhoades RA, Tanner GA, editors. Medical Physiology. 2 ed: Lippincott Williams & Wilkins; 2004. p. 514-25.

29.	Sibulesky L. Normal liver anatomy. Clinical Liver Disease. 2013;2(S1).

30.	Martins PN, Neuhaus P. Surgical anatomy of the liver, hepatic vasculature and bile ducts in the rat. Liver Int. 2007;27(3):384-92.

31.	Kogure K, Ishizaki M, Nemoto M, Kuwano H, Makuuchi M. A comparative study of the anatomy of rat and human livers. J Hepatobiliary Pancreat Surg. 1999;6(2):171-5.

32.	Madrahimov N, Dirsch O, Broelsch C, Dahmen U. Marginal hepatectomy in the rat: from anatomy to surgery. Ann Surg. 2006;244(1):89-98.

33.	Fiebig T, Boll H, Figueiredo G, Kerl HU, Nittka S, Groden C, et al. Three-dimensional in vivo imaging of the murine liver: a micro-computed tomography-based

anatomical study. PLoS One. 2012;7(2):e31179.

34.   Krishna M. Microscopic anatomy of the liver. Clinical Liver Disease. 2013;2(S1).

35.   Saxena R, Theise ND, Crawford JM. Microanatomy of the human liver-exploring the hidden interfaces. Hepatology. 1999;30(6):1339-46.

36.   Bhunchet E, Wake K. The portal lobule in rat liver fibrosis: a re-evaluation of the liver unit. Hepatology. 1998;27(2):481-7.

37.   Dancygier H. Gross anatomy. Clinical Hepatology: Springer-Verlag Berlin Heidelberg; 2010.

38.   Krishna M. Microscopic anatomy of the liver. Clinical Liver Disease. 2013;2(S1):S4-S7.

39.   Jungermann K, Kietzmann T. Zonation of parenchymal and nonparenchymal metabolism in liver. Annu Rev Nutr. 1996;16:179-203.

40.   Henderson NC, Iredale JP. Liver fibrosis: cellular mechanisms of progression and resolution. Clin Sci (Lond). 2007;112(5):265-80.

41.   Stankova P, Kucera O, Lotkova H, Rousar T, Endlicher R, Cervinkova Z. The toxic effect of thioacetamide on rat liver in vitro. Toxicol In Vitro.24(8):2097-103.

42.   Kisseleva T, Brenner DA. Hepatic stellate cells and the reversal of fibrosis. J Gastroenterol Hepatol. 2006;21 Suppl 3:S84-7.

43.   Friedman SL. Hepatic stellate cells: protean, multifunctional, and enigmatic cells of the liver. Physiol Rev. 2008;88(1):125-72.

44.   Highleyman L, Franciscus A. An Introduction to the Liver. HCSP. 2012;4.

45.   El-Serag HB. Hepatocellular carcinoma. N Engl J Med. 2011;365(12):1118-27.

46.   Farazi PA, DePinho RA. Hepatocellular carcinoma pathogenesis: from genes to environment. Nat Rev Cancer. 2006;6(9):674-87.

47.   Baffy G, Brunt EM, Caldwell SH. Hepatocellular carcinoma in non-alcoholic fatty liver disease: an emerging menace. J Hepatol. 2012;56(6):1384-91.

48.   Thorgeirsson SS, Grisham JW. Molecular pathogenesis of human hepatocellular carcinoma. Nat Genet. 2002;31(4):339-46.

49.   Han ZG. Functional genomic studies: insights into the pathogenesis of liver cancer.

Annu Rev Genomics Hum Genet. 2012;13:171-205.

50.   Chang MH, Chen CJ, Lai MS, Hsu HM, Wu TC, Kong MS, et al. Universal hepatitis B vaccination in Taiwan and the incidence of hepatocellular carcinoma in children. Taiwan Childhood Hepatoma Study Group. N Engl J Med. 1997;336(26):1855-9.

51.   Ganem D, Prince AM. Hepatitis B virus infection-natural history and clinical consequences. N Engl J Med. 2004;350(11):1118-29.

52.   Chen CJ, Yang HI, Su J, Jen CL, You SL, Lu SN, et al. Risk of hepatocellular carcinoma across a biological gradient of serum hepatitis B virus DNA level. JAMA. 2006;295(1):65-73.

53.   Yu MW, Yeh SH, Chen PJ, Liaw YF, Lin CL, Liu CJ, et al. Hepatitis B virus genotype and DNA level and hepatocellular carcinoma: a prospective study in men. J Natl Cancer Inst. 2005;97(4):265-72.

54.   Szpakowski JL, Tucker LY. Causes of death in patients with hepatitis B: a natural history cohort study in the United States. Hepatology.58(1):21-30.

55.   Hosaka T, Suzuki F, Kobayashi M, Seko Y, Kawamura Y, Sezaki H, et al. Long-term entecavir treatment reduces hepatocellular carcinoma incidence in patients with hepatitis B virus infection. Hepatology. 2013;58(1):98-107.

56.   Sangiovanni A, Prati GM, Fasani P, Ronchi G, Romeo R, Manini M, et al. The natural history of compensated cirrhosis due to hepatitis C virus: A 17-year cohort study of 214 patients. Hepatology. 2006;43(6):1303-10.

57.   Asahina Y, Tsuchiya K, Tamaki N, Hirayama I, Tanaka T, Sato M, et al. Effect of aging on risk for hepatocellular carcinoma in chronic hepatitis C virus infection. Hepatology. 2010;52(2):518-27.

58.   Donato F, Tagger A, Gelatti U, Parrinello G, Boffetta P, Albertini A, et al. Alcohol and hepatocellular carcinoma: the effect of lifetime intake and hepatitis virus infections in men and women. Am J Epidemiol. 2002;155(4):323-31.

59.   Lok AS, Seeff LB, Morgan TR, di Bisceglie AM, Sterling RK, Curto TM, et al. Incidence of hepatocellular carcinoma and associated risk factors in hepatitis C-related advanced liver disease. Gastroenterology. 2009;136(1):138-48.

60.   Veldt BJ, Chen W, Heathcote EJ, Wedemeyer H, Reichen J, Hofmann WP, et al. Increased risk of hepatocellular carcinoma among patients with hepatitis C cirrhosis and diabetes mellitus. Hepatology. 2008;47(6):1856-62.

61.   Trichopoulos D, Bamia C, Lagiou P, Fedirko V, Trepo E, Jenab M, et al. Hepatocellular carcinoma risk factors and disease burden in a European cohort: a nested case-control study. J Natl Cancer Inst. 2011;103(22):1686-95.

62.   Ascha MS, Hanouneh IA, Lopez R, Tamimi TA, Feldstein AF, Zein NN. The incidence and risk factors of hepatocellular carcinoma in patients with nonalcoholic steatohepatitis. Hepatology. 2010;51(6):1972-8.

63.   Chuang SC, Lee YC, Hashibe M, Dai M, Zheng T, Boffetta P. Interaction between cigarette smoking and hepatitis B and C virus infection on the risk of liver cancer: a meta-analysis. Cancer Epidemiol Biomarkers Prev. 2010;19(5):1261-8.

64.   Seitz HK, Stickel F. Risk factors and mechanisms of hepatocarcinogenesis with special emphasis on alcohol and oxidative stress. Biol Chem. 2006;387(4):349-60.

65.   Seitz HK, Wang XD. The role of cytochrome P450 2E1 in ethanol-mediated carcinogenesis. Subcell Biochem. 2013;67:131-43.

66.   McGlynn KA, London WT. Epidemiology and natural history of hepatocellular carcinoma. Best Pract Res Clin Gastroenterol. 2005;19(1):3-23.

67.   Wu HC, Santella R. The role of aflatoxins in hepatocellular carcinoma. Hepat Mon. 2012;12(10 HCC):e7238.

68.   Lunn RM, Zhang YJ, Wang LY, Chen CJ, Lee PH, Lee CS, et al. p53 mutations, chronic hepatitis B virus infection, and aflatoxin exposure in hepatocellular carcinoma in Taiwan. Cancer Res. 1997;57(16):3471-7.

69.   Sun Z, Lu P, Gail MH, Pee D, Zhang Q, Ming L, et al. Increased risk of hepatocellular carcinoma in male hepatitis B surface antigen carriers with chronic hepatitis who have detectable urinary aflatoxin metabolite M1. Hepatology. 1999;30(2):379-83.

70.   Lazo M, Clark JM. The epidemiology of nonalcoholic fatty liver disease: a global perspective. Semin Liver Dis. 2008;28(4):339-50.

71.   Turati F, Edefonti V, Talamini R, Ferraroni M, Malvezzi M, Bravi F, et al. Family

history of liver cancer and hepatocellular carcinoma. Hepatology. 2012;55(5):1416-25.

72. Calle EE, Rodriguez C, Walker-Thurmond K, Thun MJ. Overweight, obesity, and mortality from cancer in a prospectively studied cohort of U.S. adults. N Engl J Med. 2003;348(17):1625-38.

73. Larsson SC, Wolk A. Overweight, obesity and risk of liver cancer: a meta-analysis of cohort studies. Br J Cancer. 2007;97(7):1005-8.

74. Ertle J, Dechene A, Sowa JP, Penndorf V, Herzer K, Kaiser G, et al. Non-alcoholic fatty liver disease progresses to hepatocellular carcinoma in the absence of apparent cirrhosis. Int J Cancer. 2011;128(10):2436-43.

75. Petta S, Craxi A. Hepatocellular carcinoma and non-alcoholic fatty liver disease: from a clinical to a molecular association. Curr Pharm Des. 2010;16(6):741-52.

76. Pietrangelo A. Iron in NASH, chronic liver diseases and HCC: how much iron is too much? J Hepatol. 2009;50(2):249-51.

77. Duan XY, Zhang L, Fan JG, Qiao L. NAFLD leads to liver cancer: do we have sufficient evidence? Cancer Lett. 2013;345(2):230-4.

78. Bruix J, Sherman M. Management of hepatocellular carcinoma: an update. Hepatology. 2011;53:1020-2.

79. Maida M, Orlando E, Camma C, Cabibbo G. Staging systems of hepatocellular carcinoma: a review of literature. World J Gastroenterol. 2014;20(15):4141-50.

80. Reichman TW, Bahramipour P, Barone A, Koneru B, Fisher A, Contractor D, et al. Hepatitis status, child-pugh classification, and serum AFP levels predict survival in patients treated with transarterial embolization for unresectable hepatocellular carcinoma. J Gastrointest Surg. 2005;9(5):638-45.

81. Huo TI, Lin HC, Hsia CY, Wu JC, Lee PC, Chi CW, et al. The model for end-stage liver disease based cancer staging systems are better prognostic models for hepatocellular carcinoma: a prospective sequential survey. Am J Gastroenterol. 2007;102(9):1920-30.

82. Kee KM, Wang JH, Lin CY, Wang CC, Cheng YF, Lu SN. Validation of the 7th edition TNM staging system for hepatocellular carcinoma: an analysis of 8,828 patients in

a single medical center. Dig Dis Sci. 2013;58(9):2721-8.

83.   Pawlik TM, Delman KA, Vauthey JN, Nagorney DM, Ng IO, Ikai I, et al. Tumor size predicts vascular invasion and histologic grade: Implications for selection of surgical treatment for hepatocellular carcinoma. Liver Transpl. 2005;11(9):1086-92.

84.   Llovet JM, Bru C, Bruix J. Prognosis of hepatocellular carcinoma: the BCLC staging classification. Semin Liver Dis. 1999;19(3):329-38.

85.   Llovet JM, Ricci S, Mazzaferro V, Hilgard P, Gane E, Blanc JF, et al. Sorafenib in advanced hepatocellular carcinoma. N Engl J Med. 2008;359(4):378-90.

86.   Takaki H, Yamakado K, Tsurusaki M, Yasumoto T, Baba Y, Narimatsu Y, et al. Hepatic arterial infusion chemotherapy with fine-powder cisplatin and iodized-oil suspension in patients with intermediate-stage and advanced-stage (Barcelona Clinic Liver Cancer stage-B or stage-C) hepatocellular carcinoma: multicenter phase-II clinical study. Int J Clin Oncol.20(4):745-54.

87.   Dai Y, Li C, Wen TF, Yan LN. Comparison of liver resection and transplantation for Child-pugh A cirrhotic patient with very early hepatocellular carcinoma and portal hypertension. Pak J Med Sci. 2014;30(5):996-1000.

88.   Llovet JM, Fuster J, Bruix J. Intention-to-treat analysis of surgical treatment for early hepatocellular carcinoma: resection versus transplantation. Hepatology. 1999;30(6):1434-40.

89.   Otto G, Schuchmann M, Hoppe-Lotichius M, Heise M, Weinmann A, Hansen T, et al. How to decide about liver transplantation in patients with hepatocellular carcinoma: size and number of lesions or response to TACE? J Hepatol. 2013;59(2):279-84.

90.   Sala M, Llovet JM, Vilana R, Bianchi L, Sole M, Ayuso C, et al. Initial response to percutaneous ablation predicts survival in patients with hepatocellular carcinoma. Hepatology. 2004;40(6):1352-60.

91.   Mazzaferro V, Llovet JM, Miceli R, Bhoori S, Schiavo M, Mariani L, et al. Predicting survival after liver transplantation in patients with hepatocellular carcinoma beyond the Milan criteria: a retrospective, exploratory analysis. Lancet Oncol. 2009;10(1):35-43.

92.   Llovet JM, Bruix J. Systematic review of randomized trials for unresectable

hepatocellular carcinoma: Chemoembolization improves survival. Hepatology. 2003;37(2):429-42.

93.   Cabibbo G, Enea M, Attanasio M, Bruix J, Craxi A, Camma C. A meta-analysis of survival rates of untreated patients in randomized clinical trials of hepatocellular carcinoma. Hepatology. 2010;51(4):1274-83.

94.   Roxburgh P, Evans TR. Systemic therapy of hepatocellular carcinoma: are we making progress? Adv Ther. 2008;25(11):1089-104.

95.   Wong R, Frenette C. Updates in the management of hepatocellular carcinoma. Gastroenterol Hepatol. 2011;7(1):16-24.

96.   Allemann P, Demartines N, Bouzourene H, Tempia A, Halkic N. Long-term outcome after liver resection for hepatocellular carcinoma larger than 10 cm. World J Surg. 2013;37(2):452-8.

97.   Choi SH, Choi GH, Kim SU, Park JY, Joo DJ, Ju MK, et al. Role of surgical resection for multiple hepatocellular carcinomas. World J Gastroenterol. 2013;19(3):366-74.

98.   Liu PH, Lee YH, Hsu CY, Hsia CY, Huang YH, Chiou YY, et al. Surgical resection is better than transarterial chemoembolization for hepatocellular carcinoma beyond Milan criteria independent of performance status. J Gastrointest Surg. 2014;18(9):1623-31.

99.   Mancuso A. Management of hepatocellular carcinoma: Enlightening the gray zones. World J Hepatol. 2013;5(6):302-10.

100.   Mazzaferro V, Regalia E, Doci R, Andreola S, Pulvirenti A, Bozzetti F, et al. Liver transplantation for the treatment of small hepatocellular carcinomas in patients with cirrhosis. N Engl J Med. 1996;334(11):693-9.

101.   Figueras J, Jaurrieta E, Valls C, Benasco C, Rafecas A, Xiol X, et al. Survival after liver transplantation in cirrhotic patients with and without hepatocellular carcinoma: a comparative study. Hepatology. 1997;25(6):1485-9.

102.   Yao FY, Xiao L, Bass NM, Kerlan R, Ascher NL, Roberts JP. Liver transplantation for hepatocellular carcinoma: validation of the UCSF-expanded criteria based on preoperative imaging. Am J Transplant. 2007;7(11):2587-96.

103.   Kudo M, Izumi N, Kokudo N, Matsui O, Sakamoto M, Nakashima O, et al. Management of hepatocellular carcinoma in Japan: Consensus-Based Clinical Practice Guidelines proposed by the Japan Society of Hepatology (JSH) 2010 updated version. Dig Dis. 2011;29(3):339-64.

104.   Yao FY, Kerlan RK, Jr., Hirose R, Davern TJ, 3rd, Bass NM, Feng S, et al. Excellent outcome following down-staging of hepatocellular carcinoma prior to liver transplantation: an intention-to-treat analysis. Hepatology. 2008;48(3):819-27.

105.   Ahn CS, Moon DB, Lee SG, Hwang S, Kim KH, Ha TY, et al. Survival differences between Milan criteria after down-staging and De novo Milan in living donor liver transplantation for hepatocellular carcinoma. Hepatogastroenterology. 2014;61(129):187-91.

106.   Hameed B, Mehta N, Sapisochin G, Roberts JP, Yao FY. Alpha-fetoprotein level > 1000 ng/mL as an exclusion criterion for liver transplantation in patients with hepatocellular carcinoma meeting the Milan criteria. Liver Transpl. 2014;20(8):945-51.

107.   Crissien AM, Frenette C. Current management of hepatocellular carcinoma. Gastroenterol Hepatol. 2014;10(3):153-61.

108.   Marrero JA. Multidisciplinary management of hepatocellular carcinoma: where are we today? Semin Liver Dis. 2013;33 Suppl 1:S3-10.

109.   Genco C, Cabibbo G, Maida M, Brancatelli G, Galia M, Alessi N, et al. Treatment of hepatocellular carcinoma: present and future. Expert Rev Anticancer Ther. 2013;13(4):469-79.

110.   Meza-Junco J, Montano-Loza AJ, Liu DM, Sawyer MB, Bain VG, Ma M, et al. Locoregional radiological treatment for hepatocellular carcinoma; Which, when and how? Cancer Treat Rev. 2012;38(1):54-62.

111.   Maluccio M, Covey A. Recent progress in understanding, diagnosing, and treating hepatocellular carcinoma. CA Cancer J Clin. 2012;62(6):394-9.

112.   Zhang L, Hu P, Chen X, Bie P. Transarterial chemoembolization (TACE) plus sorafenib versus TACE for intermediate or advanced stage hepatocellular carcinoma: a meta-analysis. PLoS One. 2014;9(6):e100305.

113. Min JH, Lee MW, Cha DI, Jeon YH, Shin SW, Cho SK, et al. Radiofrequency ablation combined with chemoembolization for intermediate-sized (3-5 cm) hepatocellular carcinomas under dual guidance of biplane fluoroscopy and ultrasonography. Korean J Radiol. 2013;14(2):248-58.

114. Peng ZW, Zhang YJ, Chen MS, Xu L, Liang HH, Lin XJ, et al. Radiofrequency ablation with or without transcatheter arterial chemoembolization in the treatment of hepatocellular carcinoma: a prospective randomized trial. J Clin Oncol. 2013;31(4):426-32.

115. Llovet JM, Bruix J. Molecular targeted therapies in hepatocellular carcinoma. Hepatology. 2008;48(4):1312-27.

116. Ribatti D, Vacca A, Dammacco F. The role of the vascular phase in solid tumor growth: a historical review. Neoplasia. 1999;1(4):293-302.

117. Mignatti P, Rifkin DB. Biology and biochemistry of proteinases in tumor invasion. Physiol Rev. 1993;73(1):161-95.

118. McCuskey RS, Reilly FD. Hepatic microvasculature: dynamic structure and its regulation. Semin Liver Dis. 1993;13(1):1-12.

119. Mc Cuskey R. The hepatic microvascular system. In: Arias I, Boyer J, Fausto N, Jakoby W, Schachter D, Shafritz D, editors. The liver: biology and pathology. New York: Raven Press; 1994. p. 1089–106.

120. Harris AL. Hypoxia-a key regulatory factor in tumour growth. Nat Rev Cancer. 2002;2(1):38-47.

121. Semela D, Dufour JF. Angiogenesis and hepatocellular carcinoma. J Hepatol. 2004;41(5):864-80.

122. Kaseb AO, Hanbali A, Cotant M, Hassan MM, Wollner I, Philip PA. Vascular endothelial growth factor in the management of hepatocellular carcinoma: a review of literature. Cancer. 2009;115(21):4895-906.

123. van der Meel R, Symons MH, Kudernatsch R, Kok RJ, Schiffelers RM, Storm G, et al. The VEGF/Rho GTPase signalling pathway: a promising target for anti-angiogenic/anti-invasion therapy. Drug Discov Today. 2011;16(5-6):219-28.

124. Yamaguchi R, Yano H, Iemura A, Ogasawara S, Haramaki M, Kojiro M. Expression

of vascular endothelial growth factor in human hepatocellular carcinoma. Hepatology. 1998;28(1):68-77.

125. Zhou J, Tang ZY, Fan J, Wu ZQ, Li XM, Liu YK, et al. Expression of platelet-derived endothelial cell growth factor and vascular endothelial growth factor in hepatocellular carcinoma and portal vein tumor thrombus. J Cancer Res Clin Oncol. 2000;126(1):57-61.

126. Whittaker S, Marais R, Zhu AX. The role of signaling pathways in the development and treatment of hepatocellular carcinoma. Oncogene. 2010;29(36):4989-5005.

127. Trujillo CA, Nery AA, Alves JM, Martins AH, Ulrich H. Development of the anti-VEGF aptamer to a therapeutic agent for clinical ophthalmology. Clin Ophthalmol. 2007;1(4):393-402.

128. Giles RH, van Es JH, Clevers H. Caught up in a Wnt storm: Wnt signaling in cancer. Biochim Biophys Acta. 2003;1653(1):1-24.

129. Wehrli M, Dougan ST, Caldwell K, O'Keefe L, Schwartz S, Vaizel-Ohayon D, et al. arrow encodes an LDL-receptor-related protein essential for Wingless signalling. Nature. 2000;407(6803):527-30.

130. Clevers H. Wnt/beta-catenin signaling in development and disease. Cell. 2006;127(3):469-80.

131. Shtutman M, Zhurinsky J, Simcha I, Albanese C, D'Amico M, Pestell R, et al. The cyclin D1 gene is a target of the beta-catenin/LEF-1 pathway. Proc Natl Acad Sci U S A. 1999;96(10):5522-7.

132. Ihara A, Koizumi H, Hashizume R, Uchikoshi T. Expression of epithelial cadherin and alpha- and beta-catenins in nontumoral livers and hepatocellular carcinomas. Hepatology. 1996;23(6):1441-7.

133. Wong CM, Fan ST, Ng IO. beta-Catenin mutation and overexpression in hepatocellular carcinoma: clinicopathologic and prognostic significance. Cancer. 2001;92(1):136-45.

134. Takigawa Y, Brown AM. Wnt signaling in liver cancer. Curr Drug Targets. 2008;9(11):1013-24.

135. Yothaisong S, Dokduang H, Techasen A, Namwat N, Yongvanit P, Bhudhisawasdi

V, et al. Increased activation of PI3K/AKT signaling pathway is associated with cholangiocarcinoma metastasis and PI3K/mTOR inhibition presents a possible therapeutic strategy. Tumour Biol. 2013;34(6):3637-48.

136.   Hassan B, Akcakanat A, Holder AM, Meric-Bernstam F. Targeting the PI3-kinase/Akt/mTOR signaling pathway. Surg Oncol Clin N Am. 2013;22(4):641-64.

137.   Naing A, Aghajanian C, Raymond E, Olmos D, Schwartz G, Oelmann E, et al. Safety, tolerability, pharmacokinetics and pharmacodynamics of AZD8055 in advanced solid tumours and lymphoma. Br J Cancer. 2012;107(7):1093-9.

138.   Naing A. Overcoming resistance to mTOR inhibition for enhanced strategies in clinical trials. Expert Opin Investig Drugs. 2013;22(6):679-85.

139.   Zheng L, Yang W, Wu F, Wang C, Yu L, Tang L, et al. Prognostic significance of AMPK activation and therapeutic effects of metformin in hepatocellular carcinoma. Clin Cancer Res. 2013;19(19):5372-80.

140.   Lee CW, Wong LL, Tse EY, Liu HF, Leong VY, Lee JM, et al. AMPK promotes p53 acetylation via phosphorylation and inactivation of SIRT1 in liver cancer cells. Cancer Res. 2012;72(17):4394-404.

141.   Santoro A, Simonelli M, Rodriguez-Lope C, Zucali P, Camacho LH, Granito A, et al. A Phase-1b study of tivantinib (ARQ 197) in adult patients with hepatocellular carcinoma and cirrhosis. Br J Cancer. 2013;108(1):21-4.

142.   Trojan J, Zeuzem S. Tivantinib in hepatocellular carcinoma. Expert Opin Investig Drugs. 2013;22(1):141-7.

143.   Goyal L, Muzumdar MD, Zhu AX. Targeting the HGF/c-MET pathway in hepatocellular carcinoma. Clin Cancer Res. 2013;19(9):2310-8.

144.   Hasegawa R, Futakuchi M, Mizoguchi Y, Yamaguchi T, Shirai T, Ito N, et al. Studies of initiation and promotion of carcinogenesis by N-nitroso compounds. Cancer Lett. 1998;123(2):185-91.

145.   Oliveira PA, Colaco A, Chaves R, Guedes-Pinto H, De-La-Cruz PL, Lopes C. Chemical carcinogenesis. An Acad Bras Cienc. 2007;79(4):593-616.

146.   Trosko JE. The role of stem cells and gap junctional intercellular communication in

carcinogenesis. J Biochem Mol Biol. 2003;36(1):43-8.

147.   Player A, Barrett JC, Kawasaki ES. Laser capture microdissection, microarrays and the precise definition of a cancer cell. Expert Rev Mol Diagn. 2004;4(6):831-40.

148.   Klaunig JE, Kamendulis LM, Xu Y. Epigenetic mechanisms of chemical carcinogenesis. Hum Exp Toxicol. 2000;19(10):543-55.

149.   Gomes-Carneiro MR, Ribeiro-Pinto LF, Paumgartten FJ. [Environmental risk factors for gastric cancer: the toxicologist's standpoint]. Cad Saude Publica. 1997;13 Suppl 1:27-38.

150.   Berenblum I, Shubik P. The role of croton oil applications, associated with a single painting of a carcinogen, in tumour induction of the mouse's skin. Br J Cancer. 1947;1(4):379-82.

151.   Hanahan D, Weinberg RA. The hallmarks of cancer. Cell. 2000;100(1):57-70.

152.   Yuspa SH, Poirier MC. Chemical carcinogenesis: from animal models to molecular models in one decade. Adv Cancer Res. 1988;50:25-70.

153.   Lutz WK. A true threshold dose in chemical carcinogenesis cannot be defined for a population, irrespective of the mode of action. Hum Exp Toxicol. 2000;19(10):566-8.

154.   El-Ashmawy   NE,   El-Bahrawy   HA,   Shamloula   MM,   El-Feky   OA. Biochemical/metabolic changes associated with hepatocellular carcinoma development in mice. Tumour Biol. 2014;35(6):5459-66.

155.   Binato M, Kruel Schmidt M, Silveira Volkweis B, Behrend Silva Ribeiro G, Isabel Edelweiss M, Ricachenevsky Gurski R. Mouse model of diethylnitrosamine-induced gastric cancer. J Surg Res. 2008;148(2):152-7.

156.   Wang ZY, Agarwal R, Khan WA, Mukhtar H. Protection against benzo[a]pyrene- and N-nitrosodiethylamine-induced lung and forestomach tumorigenesis in A/J mice by water extracts of green tea and licorice. Carcinogenesis. 1992;13(8):1491-4.

157.   Gray R, Peto R, Brantom P, Grasso P. Chronic nitrosamine ingestion in 1040 rodents: the effect of the choice of nitrosamine, the species studied, and the age of starting exposure. Cancer Res. 1991;51:6470-91.

158.   Verna L, Whysner J, Williams GM. N-nitrosodiethylamine mechanistic data and risk

assessment: bioactivation, DNA-adduct formation, mutagenicity, and tumor initiation. Pharmacol Ther. 1996;71(1-2):57-81.

159.   Williams GM, Iatropoulos MJ, Jeffrey AM. Mechanistic basis for nonlinearities and thresholds in rat liver carcinogenesis by the DNA-reactive carcinogens 2-acetylaminofluorene and diethylnitrosamine. Toxicol Pathol. 2000;28(3):388-95.

160.   Teoh NC, Dan YY, Swisshelm K, Lehman S, Wright JH, Haque J, et al. Defective DNA strand break repair causes chromosomal instability and accelerates liver carcinogenesis in mice. Hepatology. 2008;47(6):2078-88.

161.   Qi Y, Chen X, Chan CY, Li D, Yuan C, Yu F, et al. Two-dimensional differential gel electrophoresis/analysis of diethylnitrosamine induced rat hepatocellular carcinoma. Int J Cancer. 2008;122(12):2682-8.

162.   Valko M, Rhodes CJ, Moncol J, Izakovic M, Mazur M. Free radicals, metals and antioxidants in oxidative stress-induced cancer. Chem Biol Interact. 2006;160(1):1-40.

163.   Stahl S, Ittrich C, Marx-Stoelting P, Kohle C, Altug-Teber O, Riess O, et al. Genotype-phenotype relationships in hepatocellular tumors from mice and man. Hepatology. 2005;42(2):353-61.

164.   Wang Q, Lin ZY, Feng XL. Alterations in metastatic properties of hepatocellular carcinoma cell following H-ras oncogene transfection. World J Gastroenterol. 2001;7(3):335-9.

165.   Calvisi DF, Ladu S, Gorden A, Farina M, Conner EA, Lee JS, et al. Ubiquitous activation of Ras and Jak/Stat pathways in human HCC. Gastroenterology. 2006;130(4):1117-28.

166.   Lee JS, Chu IS, Mikaelyan A, Calvisi DF, Heo J, Reddy JK, et al. Application of comparative functional genomics to identify best-fit mouse models to study human cancer. Nat Genet. 2004;36(12):1306-11.

167.   Rao KV, Vesselinovitch SD. Age- and sex-associated diethylnitrosamine dealkylation activity of the mouse liver and hepatocarcinogenesis. Cancer Res. 1973;33(7):1625-7.

168.   Vesselinovitch SD, Mihailovich N. Kinetics of diethylnitrosamine

hepatocarcinogenesis in the infant mouse. Cancer Res. 1983;43(9):4253-9.

169.   Nakatani T, Roy G, Fujimoto N, Asahara T, Ito A. Sex hormone dependency of diethylnitrosamine-induced liver tumors in mice and chemoprevention by leuprorelin. Jpn J Cancer Res. 2001;92(3):249-56.

170.   Buchmann A, Bauer-Hofmann R, Mahr J, Drinkwater NR, Luz A, Schwarz M. Mutational activation of the c-Ha-ras gene in liver tumors of different rodent strains: correlation with susceptibility to hepatocarcinogenesis. Proc Natl Acad Sci U S A. 1991;88(3):911-5.

171.   Bird AP, Wolffe AP. Methylation-induced repression--belts, braces, and chromatin. Cell. 1999;99(5):451-4.

172.   Park TJ, Kim JY, Oh SP, Kang SY, Kim BW, Wang HJ, et al. TIS21 negatively regulates hepatocarcinogenesis by disruption of cyclin B1-Forkhead box M1 regulation loop. Hepatology. 2008;47(5):1533-43.

173.   Hacker HJ, Mtiro H, Bannasch P, Vesselinovitch SD. Histochemical profile of mouse hepatocellular adenomas and carcinomas induced by a single dose of diethylnitrosamine. Cancer Res. 1991;51(7):1952-8.

174.   Vesselinovitch SD, Mihailovich N, Rao KV. Morphology and metastatic nature of induced hepatic nodular lesions in C57BL x C3H F1 mice. Cancer Res. 1978;38(7):2003-10.

175.   Frey S, Buchmann A, Bursch W, Schulte-Hermann R, Schwarz M. Suppression of apoptosis in C3H mouse liver tumors by activated Ha-ras oncogene. Carcinogenesis. 2000;21(2):161-6.

176.   Zimmers TA, Jin X, Gutierrez JC, Acosta C, McKillop IH, Pierce RH, et al. Effect of in vivo loss of GDF-15 on hepatocellular carcinogenesis. J Cancer Res Clin Oncol. 2008;134(7):753-9.

177.   Shiota G, Harada K, Ishida M, Tomie Y, Okubo M, Katayama S, et al. Inhibition of hepatocellular carcinoma by glycyrrhizin in diethylnitrosamine-treated mice. Carcinogenesis. 1999;20(1):59-63.

178.   Finnberg N, Stenius U, Hogberg J. Heterozygous p53-deficient (+/-) mice develop

fewer p53-negative preneoplastic focal liver lesions in response to treatment with diethylnitrosamine than do wild-type (+/+) mice. Cancer Lett. 2004;207(2):149-55.

179.   Waxman DJ, Azaroff L. Phenobarbital induction of cytochrome P-450 gene expression. Biochem J. 1992;281 (Pt 3):577-92.

180.   Imaoka S, Osada M, Minamiyama Y, Yukimura T, Toyokuni S, Takemura S, et al. Role of phenobarbital-inducible cytochrome P450s as a source of active oxygen species in DNA-oxidation. Cancer Lett. 2004;203(2):117-25.

181.   Watson RE, Goodman JI. Effects of phenobarbital on DNA methylation in GC-rich regions of hepatic DNA from mice that exhibit different levels of susceptibility to liver tumorigenesis. Toxicol Sci. 2002;68(1):51-8.

182.   Loeppen S, Schneider D, Gaunitz F, Gebhardt R, Kurek R, Buchmann A, et al. Overexpression of glutamine synthetase is associated with beta-catenin-mutations in mouse liver tumors during promotion of hepatocarcinogenesis by phenobarbital. Cancer Res. 2002;62(20):5685-8.

183.   Lee GH, Ooasa T, Osanai M. Mechanism of the paradoxical, inhibitory effect of phenobarbital on hepatocarcinogenesis initiated in infant B6C3F1 mice with diethylnitrosamine. Cancer Res. 1998;58(8):1665-9.

184.   Klaunig JE, Pereira MA, Ruch RJ, Weghorst CM. Dose-response relationship of diethylnitrosamine-initiated tumors in neonatal balb/c mice: effect of phenobarbital promotion. Toxicol Pathol. 1988;16(3):381-5.

185.   Goldsworthy TL, Fransson-Steen R. Quantitation of the cancer process in C57BL/6J, B6C3F1 and C3H/HeJ mice. Toxicol Pathol. 2002;30(1):97-105.

186.   Akhtar T, Sheikh N. An overview of thioacetamide-induced hepatotoxicity. Toxin Reviews. 2013;32(3):43-6.

187.   Ramaiah SK, Apte U, Mehendale HM. Cytochrome P4502E1 induction increases thioacetamide liver injury in diet-restricted rats. Drug Metab Dispos. 2001;29(8):1088-95.

188.   Kang JS, Wanibuchi H, Morimura K, Wongpoomchai R, Chusiri Y, Gonzalez FJ, et al. Role of CYP2E1 in thioacetamide-induced mouse hepatotoxicity. Toxicol Appl Pharmacol. 2008;228(3):295-300.

189.   Koen YM, Sarma D, Hajovsky H, Galeva NA, Williams TD, Staudinger JL, et al. Protein targets of thioacetamide metabolites in rat hepatocytes. Chem Res Toxicol. 2013;26(4):564-74.

190.   Akhtar T, Sheikh N. An overview of thioacetamide-induced hepatotoxicity. Toxin Reviews. 2013;32(3):43-6.

191.   Hajovsky H, Hu G, Koen Y, Sarma D, Cui W, Moore DS, et al. Metabolism and toxicity of thioacetamide and thioacetamide S-oxide in rat hepatocytes. Chem Res Toxicol. 2012;25(9):1955-63.

192.   Stankova P, Kucera O, Lotkova H, Rousar T, Endlicher R, Cervinkova Z. The toxic effect of thioacetamide on rat liver in vitro. Toxicol In Vitro. 2010;24(8):2097-103.

193.   Abou-Alfa GK, Schwartz L, Ricci S, Amadori D, Santoro A, Figer A, et al. Phase II study of sorafenib in patients with advanced hepatocellular carcinoma 2006.

194.   Cheng AL, Guan Z, Chen Z, Tsao CJ, Qin S, Kim JS, et al. Efficacy and safety of sorafenib in patients with advanced hepatocellular carcinoma according to baseline status: subset analyses of the phase III Sorafenib Asia-Pacific trial. Eur J Cancer. 2012;48(10):1452-65.

195.   Alexandrescu DT, McClure R, Farzanmehr H, Dasanu CA. Secondary erythrocytosis produced by the tyrosine kinase inhibitors sunitinib and sorafenib. J Clin Oncol. 2008;26(24):4047-8.

196.   Grindlay D, Reynolds T. The Aloe vera phenomenon: a review of the properties and modern uses of the leaf parenchyma gel. J Ethnopharmacol. 1986;16(2-3):117-51.

197.   Hamman JH. Composition and applications of Aloe vera leaf gel. Molecules. 2008;13(8):1599-616.

198.   Ajabnoor MA. Effect of aloes on blood glucose levels in normal and alloxan diabetic mice. J Ethnopharmacol. 1990;28(2):215-20.

199.   Ralph A, GJ P. Phytoprotectants. In: Garrow JS, James WPT, A R, editors. In Human Nutrition and Dietetics. Edinburgh: Churchill Livingstone; 2000:417–26.

200.   Ishii Y, Tanizawa H, Takino Y. Studies of aloe. III. Mechanism of cathartic effect. (2). Chem Pharm Bull (Tokyo). 1990;38(1):197-200.

201.   Cardenas C, Quesada AR, Medina MA. Evaluation of the anti-angiogenic effect of aloe-emodin. Cell Mol Life Sci. 2006;63(24):3083-9.

202.   Ulbricht C, Armstrong J, Basch E, Basch S, Bent S, Dacey C, et al. An evidence-based systematic review of Aloe vera by the natural standard research collaboration. J Herb Pharmacother. 2007;7(3-4):279-323.

203.   Beppu H, Koike T, Shimpo K, Chihara T, Hoshino M, Ida C, et al. Radical-scavenging effects of Aloe arborescens Miller on prevention of pancreatic islet B-cell destruction in rats. J Ethnopharmacol. 2003;89(1):37-45.

204.   Langmead L, Makins RJ, Rampton DS. Anti-inflammatory effects of aloe vera gel in human colorectal mucosa in vitro. Aliment Pharmacol Ther. 2004;19(5):521-7.

205.   Tanaka M, Misawa E, Ito Y, Habara N, Nomaguchi K, Yamada M, et al. Identification of five phytosterols from Aloe vera gel as anti-diabetic compounds. Biol Pharm Bull. 2006;29(7):1418-22.

206.   Pothuraju R, Sharma RK, Onteru SK, Singh S, Hussain SA. Hypoglycemic and Hypolipidemic Effects of Aloe vera Extract Preparations: A Review. Phytother Res. 2016;30(2):200-7.

207.   Venkatesh P, Mukherjee PK, Pal BC. Acridanone alkaloid in Baliospermum montanum-evaluation of its effect against anaphylaxis. Planta Med. 2011;77(17):1947-9.

208.   Ogura M, Koike K, Cordell GA, Farnsworth NR. Potential anticancer agents VIII. Constituents of Baliospermum montanum (Euphorbiaceae). Planta Med. 1978;33(2):128-43.

209.   Johnson M, Wesely E, Zahir Hussain M, Selvan N. In vivo and in vitro phytochemical and antibacterial efficacy of Baliospermum montanum(Willd.) Muell. Arg. Asian Pacific Journal of Tropical Medicine. 2010:894-7.

210.   Patil KS, Jalalpure SS, Wadekar RR. Effect of Baliospermum montanum Root Extract on Phagocytosis by Human Neutrophils. Indian J Pharm Sci. 2009;71(1):68-71.

211.   Mali RG, Wadekar RR. In Vitro Anthelmintic Activity of Baliospermum montanum Muell. Arg roots. Indian J Pharm Sci. 2008;70(1):131-3.

212.   Cai Y, Luo Q, Sun M, Corke H. Antioxidant activity and phenolic compounds of 112

traditional Chinese medicinal plants associated with anticancer. Life Sci. 2004;74(17):2157-84.

213. Sulaiman CT, Balachandran I. Total phenolics and total flavonoids in selected Indian medicinal plants. Indian J Pharm Sci. 2012;74(3):258-60.

214. Nandagaon VS, Kulkarni AR. In vitro antioxidant and cytotoxicity activity of Bacopa monnieri and Baliospermum Montanum Muell Arg. International Journal of Pharmaceutical Applications. 2013;4(3):63-7.

215. Han XZ, Gao S, Cheng YN, Sun YZ, Liu W, Tang LL, et al. Protective effect of naringenin-7-O-glucoside against oxidative stress induced by doxorubicin in H9c2 cardiomyocytes. Biosci Trends. 2012;6(1):19-25.

216. Ampasavate C, Okonogi S, Anuchapreeda S. Cytotoxicity of extracts from fruit plants against leukemic cell lines. African Journal of Pharmacy and Pharmacology. 2010;4(1):013-21.

217. Jayaraman J, Namasivayam N. Naringenin modulates circulatory lipid peroxidation, anti-oxidant status and hepatic alcohol metabolizing enzymes in rats with ethanol induced liver injury. Fundam Clin Pharmacol. 2011;25(6):682-9.

218. Du G, Jin L, Han X, Song Z, Zhang H, Liang W. Naringenin: a potential immunomodulator for inhibiting lung fibrosis and metastasis. Cancer Res. 2009;69(7):3205-12.

219. Li R, Li J, Hu C, Zhang L, Zhang Q. Immunomodulative effect of hesperidin on immunodepressed mice. Chinese Pharmacol Bull. 2007;23(2):169-72.

220. Mahendra P, Bisht S. Ferula asafoetida: Traditional uses and pharmacological activity. Pharmacogn Rev. 2012;6(12):141-6.

221. Takeoka G. Volatile Constituents of Asafoetida: ACS Symposium Series; 2001.

222. Hadavand Mirzaei H, Hasanloo T. Assessment of chemical composition of essential oil of Ferula assa-foetidaoleo-gum-resin from two different sites of Yazd province in center of Iran. Res J Pharmacogn. 2014;1(2):51-4.

223. Nabavi SM, Ebrahimzadeh MA, Nabavi SF, Eslami B, Dehpour AA. Antioxidant and antihaemolytic activities of Ferula foetida regel (Umbelliferae). Eur Rev Med Pharmacol Sci.

2011;15(2):157-64.

224.   Abu-Zaiton AS. Anti-diabetic activity of Ferula assafoetida extract in normal and alloxan-induced diabetic rats. Pak J Biol Sci. 2010;13(2):97-100.

225.   Iranshahy M, Iranshahi M. Traditional uses, phytochemistry and pharmacology of asafoetida (Ferula assa-foetida oleo-gum-resin)-a review. J Ethnopharmacol. 2011;134(1):1-10.

226.   Akaberi M, Iranshahy M, Iranshahi M. Review of the traditional uses, phytochemistry, pharmacology and toxicology of giant fennel (Ferula communis L. subsp. communis). Iran J Basic Med Sci. 2014;18(11):1050-62.

227.   Mallikarjuna GU, Dhanalakshmi S, Raisuddin S, Rao AR. Chemomodulatory influence of Ferula asafoetida on mammary epithelial differentiation, hepatic drug metabolizing enzymes, antioxidant profiles and N-methyl-N-nitrosourea-induced mammary carcinogenesis in rats. Breast Cancer Res Treat. 2003;81(1):1-10.

228.   Sukpondma Y, Rukachaisirikul V, Phongpaichit S. Antibacterial caged-tetraprenylated xanthones from the fruits of Garcinia hanburyi. Chem Pharm Bull (Tokyo). 2005;53(7):850-2.

229.   Han QB, Wang YL, Yang L, Tso TF, Qiao CF, Song JZ, et al. Cytotoxic polyprenylated xanthones from the resin of Garcinia hanburyi. Chem Pharm Bull (Tokyo). 2006;54(2):265-7.

230.   Zhang HZ, Kasibhatla S, Wang Y, Herich J, Guastella J, Tseng B, et al. Discovery, characterization and SAR of gambogic acid as a potent apoptosis inducer by a HTS assay. Bioorg Med Chem. 2004;12(2):309-17.

231.   Wu ZQ, Guo QL, You QD, Zhao L, Gu HY. Gambogic acid inhibits proliferation of human lung carcinoma SPC-A1 cells in vivo and in vitro and represses telomerase activity and telomerase reverse transcriptase mRNA expression in the cells. Biol Pharm Bull. 2004;27(11):1769-74.

232.   Guo QL, Lin SS, You QD, Gu HY, Yu J, Zhao L, et al. Inhibition of human telomerase reverse transcriptase gene expression by gambogic acid in human hepatoma SMMC-7721 cells. Life Sci. 2006;78(11):1238-45.

233. Zhao Q, Yang Y, Yu J, You QD, Zeng S, Gu HY, et al. Posttranscriptional regulation of the telomerase hTERT by gambogic acid in human gastric carcinoma 823 cells. Cancer Lett. 2008;262(2):223-31.

234. Wang T, Wei J, Qian X, Ding Y, Yu L, Liu B. Gambogic acid, a potent inhibitor of survivin, reverses docetaxel resistance in gastric cancer cells. Cancer Lett. 2008;262(2):214-22.

235. Tewtrakul S, Hase K, Kadota S, Namba T, Komatsu K, Tanaka K. Fruit oil composition of Piper chaba Hunt., P. longum L. and P. nigrum L. J Essent Oil Res. 2000;12:603–8.

236. Morikawa T, Matsuda H, Yamaguchi I, Pongpiriyadacha Y, Yoshikawa M. New amides and gastroprotective constituents from the fruit of Piper chaba. Planta Med. 2004;70(2):152-9.

237. Matsuda H, Ninomiya K, Morikawa T, Yasuda D, Yamaguchi I, Yoshikawa M. Protective effects of amide constituents from the fruit of Piper chaba on D-galactosamine/TNF-alpha-induced cell death in mouse hepatocytes. Bioorg Med Chem Lett. 2008;18(6):2038-42.

238. Matsuda H, Ninomiya K, Morikawa T, Yasuda D, Yamaguchi I, Yoshikawa M. Hepatoprotective amide constituents from the fruit of Piper chaba: Structural requirements, mode of action, and new amides. Bioorg Med Chem. 2009;17(20):7313-23.

239. Ahmad N, Fazal H, Abbasi BH, Farooq S, Ali M, Khan MA. Biological role of Piper nigrum L. (Black pepper): A review Asian Pacific Journal of Tropical Biomedicine. 2012;2(3):S1945-S53.

240. Szallasi A. Piperine: researchers discover new flavor in an ancient spice. Trends Pharmacol Sci. 2005;26(9):437-9.

241. Bezerra DP, Pessoa C, de Moraes MO, Saker-Neto N, Silveira ER, Costa-Lotufo LV. Overview of the therapeutic potential of piplartine (piperlongumine). Eur J Pharm Sci. 2013;48(3):453-63.

242. Selvendiran K, Banu SM, Sakthisekaran D. Protective effect of piperine on benzo(a)pyrene-induced lung carcinogenesis in Swiss albino mice. Clin Chim Acta.

2004;350(1-2):73-8.

243.   Lee W, Kim KY, Yu SN, Kim SH, Chun SS, Ji JH, et al. Pipernonaline from Piper longum Linn. induces ROS-mediated apoptosis in human prostate cancer PC-3 cells. Biochem Biophys Res Commun. 2013;430(1):406-12.

244.   Aggarwal BB, Shishodia S. Molecular targets of dietary agents for prevention and therapy of cancer. Biochem Pharmacol. 2006;71(10):1397-421.

245.   Okumura Y, Narukawa M, Iwasaki Y, Ishikawa A, Matsuda H, Yoshikawa M, et al. Activation of TRPV1 and TRPA1 by black pepper components. Biosci Biotechnol Biochem. 2010;74(5):1068-72.

246.   Sriwiriyajan S, Ninpesh T, Sukpondma Y, Nasomyon T, Graidist P. Cytotoxicity Screening of Plants of Genus Piper in Breast Cancer Cell Lines. Tropical Journal of Pharmaceutical Research. 2014;13(6).

247.   Semwal RB, Semwal DK, Combrinck S, Viljoen AM. Gingerols and shogaols: Important nutraceutical principles from ginger. Phytochemistry. 2015;117:554-68.

248.   Zick SM, Djuric Z, Ruffin MT, Litzinger AJ, Normolle DP, Alrawi S, et al. Pharmacokinetics of 6-gingerol, 8-gingerol, 10-gingerol, and 6-shogaol and conjugate metabolites in healthy human subjects. Cancer Epidemiol Biomarkers Prev. 2008;17(8):1930-6.

249.   Li F, Nitteranon V, Tang X, Liang J, Zhang G, Parkin KL, et al. In vitro antioxidant and anti-inflammatory activities of 1-dehydro-[6]-gingerdione, 6-shogaol, 6-dehydroshogaol and hexahydrocurcumin. Food Chem. 2012;135(2):332-7.

250.   Pan MH, Hsieh MC, Kuo JM, Lai CS, Wu H, Sang S, et al. 6-Shogaol induces apoptosis in human colorectal carcinoma cells via ROS production, caspase activation, and GADD 153 expression. Mol Nutr Food Res. 2008;52(5):527-37.

251.   Liu Q, Peng YB, Zhou P, Qi LW, Zhang M, Gao N, et al. 6-Shogaol induces apoptosis in human leukemia cells through a process involving caspase-mediated cleavage of eIF2alpha. Mol Cancer. 2013;12(1):135.

252.   Kim MO, Lee MH, Oi N, Kim SH, Bae KB, Huang Z, et al. [6]-shogaol inhibits growth and induces apoptosis of non-small cell lung cancer cells by directly regulating

Akt1/2. Carcinogenesis. 2014;35(3):683-91.

253. Chen CY, Liu TZ, Liu YW, Tseng WC, Liu RH, Lu FJ, et al. 6-shogaol (alkanone from ginger) induces apoptotic cell death of human hepatoma p53 mutant Mahlavu subline via an oxidative stress-mediated caspase-dependent mechanism. J Agric Food Chem. 2007;55(3):948-54.

254. Ishiguro K, Ando T, Maeda O, Ohmiya N, Niwa Y, Kadomatsu K, et al. Ginger ingredients reduce viability of gastric cancer cells via distinct mechanisms. Biochem Biophys Res Commun. 2007;362(1):218-23.

255. Saftlas AF, Olson DR, Franks AL, Atrash HK, Pokras R. Epidemiology of preeclampsia and eclampsia in the United States, 1979-1986. Am J Obstet Gynecol. 1990;163(2):460-5.

256. Mostello D, Catlin TK, Roman L, Holcomb WL, Jr., Leet T. Preeclampsia in the parous woman: who is at risk? Am J Obstet Gynecol. 2002;187(2):425-9.

257. American College of Obstetricians & Gynecologists and Task Force on Hypertension in Pregnancy. Hypertension in pregnancy. Report of the American College of Obstetricians and Gynecologists' Task Force on Hypertension in Pregnancy. Obstet Gynecol. 2013;122(5):1122-31.

258. MacKay AP, Berg CJ, Atrash HK. Pregnancy-related mortality from preeclampsia and eclampsia. Obstet Gynecol. 2001;97(4):533-8.

259. Srebro DP, Vuckovic S, Vujovic KS, Prostran M. Anti-hyperalgesic effect of systemic magnesium sulfate in carrageenan-induced inflammatory pain in rats: influence of the nitric oxide pathway. Magnes Res. 2014;27(2):77-85.

260. Srebro D, Vuckovic S, Prostran M. Inhibition of neuronal and inducible nitric oxide synthase does not affect the analgesic effects of NMDA antagonists in visceral inflammatory pain. Acta Neurobiol Exp (Wars). 2016;76(2):110-16.

261. Wolf FI, Maier JA, Nasulewicz A, Feillet-Coudray C, Simonacci M, Mazur A, et al. Magnesium and neoplasia: from carcinogenesis to tumor growth and progression or treatment. Arch Biochem Biophys. 2007;458(1):24-32.

262. Szewczyk B, Poleszak E, Sowa-Kucma M, Siwek M, Dudek D, Ryszewska-

Pokrasniewicz B, et al. Antidepressant activity of zinc and magnesium in view of the current hypotheses of antidepressant action. Pharmacol Rep. 2008;60(5):588-9.

263.   Grober U, Schmidt J, Kisters K. Magnesium in Prevention and Therapy. Nutrients. 2015;7(9):8199-226.

264.   Wee A. Fine needle aspiration biopsy of the liver: Algorithmic approach and current issues in the diagnosis of hepatocellular carcinoma. Cytojournal. 2005;2:7.

265.   รุ่งระวี เต็มศิริฤกษ์กุล. เบญจอำมฤตตำรับยารักษามะเร็งตับ

266.   Yossathera K, Worakunphanich W, Teerachaisakul M, Stienrut P. Traditional thai medicine formula benja amarit in liver cancer patients: a safety and auality of life. Journal of Thai Traditional&Alternative Medicine. 2017;15(3).

267.   Suboj P, Babykutty S, Valiyaparambil Gopi DR, Nair RS, Srinivas P, Gopala S. Aloe emodin inhibits colon cancer cell migration/angiogenesis by downregulating MMP-2/9, RhoB and VEGF via reduced DNA binding activity of NF-kappaB. Eur J Pharm Sci. 2012;45(5):581-91.

268.   Pan Q, Pan H, Lou H, Xu Y, Tian L. Inhibition of the angiogenesis and growth of Aloin in human colorectal cancer in vitro and in vivo. Cancer Cell Int. 2013;13(1):69.

269.   Weng CJ, Chou CP, Ho CT, Yen GC. Molecular mechanism inhibiting human hepatocarcinoma cell invasion by 6-shogaol and 6-gingerol. Mol Nutr Food Res. 2012;56(8):1304-14.

270.   Kim EC, Min JK, Kim TY, Lee SJ, Yang HO, Han S, et al. [6]-Gingerol, a pungent ingredient of ginger, inhibits angiogenesis in vitro and in vivo. Biochem Biophys Res Commun. 2005;335(2):300-8.

271.   Rhode J, Fogoros S, Zick S, Wahl H, Griffith KA, Huang J, et al. Ginger inhibits cell growth and modulates angiogenic factors in ovarian cancer cells. BMC Complement Altern Med. 2007;7:44.

272.   Raj L, Ide T, Gurkar AU, Foley M, Schenone M, Li X, et al. Selective killing of cancer cells by a small molecule targeting the stress response to ROS. Nature. 2011;475(7355):231-4.

273.   Doucette CD, Hilchie AL, Liwski R, Hoskin DW. Piperine, a dietary phytochemical,

inhibits angiogenesis. J Nutr Biochem. 2013;24(1):231-9.

274.   Guo QL, You QD, Wu ZQ, Yuan ST, Zhao L. General gambogic acids inhibited growth of human hepatoma SMMC-7721 cells in vitro and in nude mice. Acta Pharmacol Sin. 2004;25(6):769-74.

275.   Chang X, Zhao J, Tian F, Jiang Y, Lu J, Ma J, et al. Aloe-emodin suppresses esophageal cancer cell TE1 proliferation by inhibiting AKT and ERK phosphorylation. Oncol Lett. 2016;12(3):2232-8.

276.   Chen HC, Hsieh WT, Chang WC, Chung JG. Aloe-emodin induced in vitro G2/M arrest of cell cycle in human promyelocytic leukemia HL-60 cells. Food Chem Toxicol. 2004;42(8):1251-7.

277.   Kim KH, Lee HJ, Jeong SJ, Lee HJ, Lee EO, Kim HS, et al. Galbanic acid isolated from Ferula assafoetida exerts in vivo anti-tumor activity in association with anti-angiogenesis and anti-proliferation. Pharm Res. 2011;28(3):597-609.

278.   Lee SH, Cekanova M, Baek SJ. Multiple mechanisms are involved in 6-gingerol-induced cell growth arrest and apoptosis in human colorectal cancer cells. Mol Carcinog. 2008;47(3):197-208.

279.   Choi JS, Ryu J, Bae WY, Park A, Nam S, Kim JE, et al. Zingerone Suppresses Tumor Development through Decreasing Cyclin D1 Expression and Inducing Mitotic Arrest. Int J Mol Sci. 2018;19(9).

280.   Jyothi D, Vanathi P, Mangala Gowri P, Rama Subba Rao V, Madhusudana Rao J, Sreedhar AS. Diferuloylmethane augments the cytotoxic effects of piplartine isolated from Piper chaba. Toxicol In Vitro. 2009;23(6):1085-91.

281.   Ouyang DY, Zeng LH, Pan H, Xu LH, Wang Y, Liu KP, et al. Piperine inhibits the proliferation of human prostate cancer cells via induction of cell cycle arrest and autophagy. Food Chem Toxicol. 2013;60:424-30.

282.   Fofaria NM, Kim SH, Srivastava SK. Piperine causes G1 phase cell cycle arrest and apoptosis in melanoma cells through checkpoint kinase-1 activation. PLoS One. 2014;9(5):e94298.

283.   Lai LH, Fu QH, Liu Y, Jiang K, Guo QM, Chen QY, et al. Piperine suppresses tumor

growth and metastasis in vitro and in vivo in a 4T1 murine breast cancer model. Acta Pharmacol Sin. 2012;33(4):523-30.

284.   Yaffe PB, Power Coombs MR, Doucette CD, Walsh M, Hoskin DW. Piperine, an alkaloid from black pepper, inhibits growth of human colon cancer cells via G1 arrest and apoptosis triggered by endoplasmic reticulum stress. Mol Carcinog. 2015;54(10):1070-85.

285.   Kakarala M, Brenner DE, Korkaya H, Cheng C, Tazi K, Ginestier C, et al. Targeting breast stem cells with the cancer preventive compounds curcumin and piperine. Breast Cancer Res Treat. 2010;122(3):777-85.

286.   Nie F, Zhang X, Qi Q, Yang L, Yang Y, Liu W, et al. Reactive oxygen species accumulation contributes to gambogic acid-induced apoptosis in human hepatoma SMMC-7721 cells. Toxicology. 2009;260(1-3):60-7.

287.   Arcella A, Oliva MA, Staffieri S, Sanchez M, Madonna M, Riozzi B, et al. Effects of aloe emodin on U87MG glioblastoma cell growth: In vitro and in vivo study. Environ Toxicol. 2018;33(11):1160-7.

288.   Cherian AM, Snima KS, Kamath CR, Nair SV, Lakshmanan VK. Effect of Baliospermum montanum nanomedicine apoptosis induction and anti-migration of prostate cancer cells. Biomed Pharmacother. 2015;71:201-9.

289.   Oh BS, Shin EA, Jung JH, Jung DB, Kim B, Shim BS, et al. Apoptotic Effect of Galbanic Acid via Activation of Caspases and Inhibition of Mcl-1 in H460 Non-Small Lung Carcinoma Cells. Phytother Res. 2015;29(6):844-9.

290.   Ren J, Xu Y, Huang Q, Yang J, Yang M, Hu K, et al. Chabamide induces cell cycle arrest and apoptosis by the Akt/MAPK pathway and inhibition of P-glycoprotein in K562/ADR cells. Anticancer Drugs. 2015;26(5):498-507.

291.   de Souza Grinevicius VM, Kviecinski MR, Santos Mota NS, Ourique F, Porfirio Will Castro LS, Andreguetti RR, et al. Piper nigrum ethanolic extract rich in piperamides causes ROS overproduction, oxidative damage in DNA leading to cell cycle arrest and apoptosis in cancer cells. J Ethnopharmacol. 2016;189:139-47.

292.   Das A, Miller R, Lee P, Holden CA, Lindhorst SM, Jaboin J, et al. A novel component from citrus, ginger, and mushroom family exhibits antitumor activity on human

meningioma cells through suppressing the Wnt/beta-catenin signaling pathway. Tumour Biol. 2015;36(9):7027-34.

293. หมออาสา แพทย์แผนไทย. มหัศจรรย์เบญจอำมฤตย์ สุดยอดยาต้านมะเร็งตับแห่งยุค: ปัญญาชน; 2014.

294. ทองสุข สมบูรณ์. ๙ ยามหัศจรรย์ เบญจอำมฤตย์ ต้านมะเร็ง: มีดอกมีผล; 2014.

295. Nakano M, Tanaka M, Kuromatsu R, Nagamatsu H, Tajiri N, Satani M, et al. Sorafenib for the treatment of advanced hepatocellular carcinoma with extrahepatic metastasis: a prospective multicenter cohort study. Cancer Med. 2015;4(12):1836-43.

296. Kuroda D, Hayashi H, Nitta H, Imai K, Abe S, Hashimoto D, et al. Successful treatment for sorafenib-induced liver dysfunction: a report of case with liver biopsy. Surg Case Rep. 2016;2(1):4.
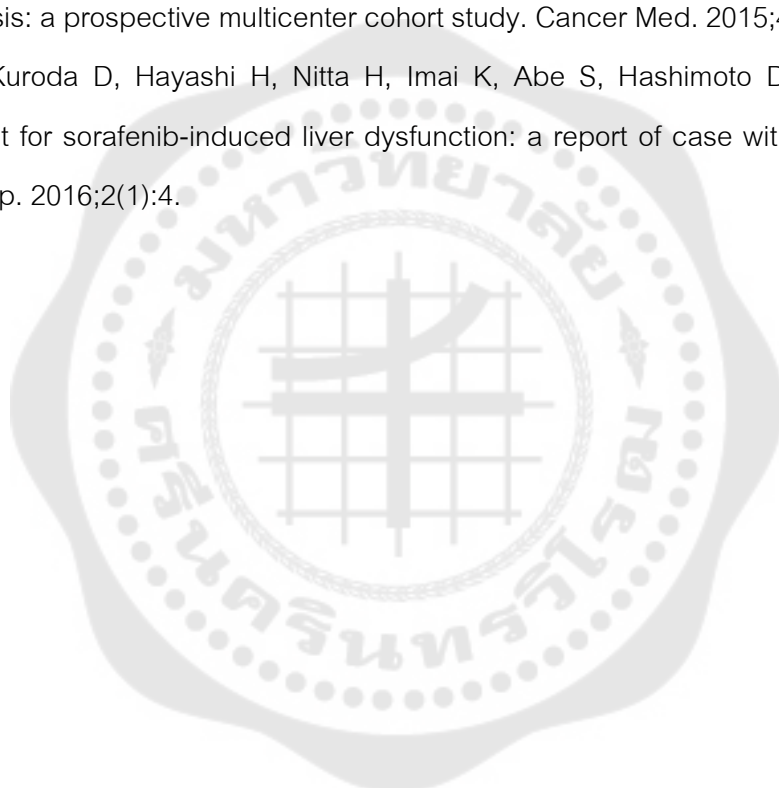
VITA

NAME	Mr.Nattpawit Kaewnoonual
DATE OF BIRTH	12 May 1981
PLACE OF BIRTH	Songkhla
INSTITUTIONS ATTENDED	2004 B.Sc. (Biomedical Science), Rangsit University
	2008 M.Sc. (Medical Science), Thammasat University,
	2019 Ph.D. (Biomedical Science), Srinakharinwirot University,
HOME ADDRESS	218/128 Ratchadapisek Rd., Huaikwang, Huaikwang, Bangkok 10310
PUBLICATION	1. Chiamchanya C, Kaewnoonual N, Visutakul P, Manochantr S, Chaiya J. Comparative study of the effects of three semen preparation media on semen analysis, DNA damage and protamine deficiency, and the correlation between DNA integrity and sperm parameters. Asian J Androl. 2010;12(2):271-7
	2. Poonkhum R, Rodniem S, Kaewnoonual N, Nilbu-nga C, Pradidarcheep W. Relationship between Mast Cells and Hepatic Myofibroblasts Induced Cirrhosis Rats. J Med Assoc Thai 100: 10, 2016